

**ENSEMBLE SIZE EFFECT IN CATALYSIS BY PLATINUM-COPPER SILICA
SUPPORTED BIMETALLIC CATALYSTS**

by

Dmitry Kazachkin

Master of Science, Chemistry, Novosibirsk State University, 2000

Submitted to the Graduate Faculty of

The School of Engineering in partial fulfillment

of the requirements for the degree of

Master of Science

University of Pittsburgh

2006

UNIVERSITY OF PITTSBURGH
SCHOOL OF ENGINEERING

This thesis was presented

by

Dmitry Kazachkin

It was defended on

January 23rd, 2006

and approved by

Götz Vesper, Assistant Professor, Department of Chemical and Petroleum Engineering

Radisav D. Vidic, Professor, Department of Civil and Environmental Engineering

Thesis Advisor: J. Karl Johnson, Professor, Department of Chemical and Petroleum Engineering

ENSEMBLE SIZE EFFECT IN CATALYSIS BY PLATINUM-COPPER SILICA
SUPPORTED BIMETALLIC CATALYSTS

Dmitry Kazachkin, M. S.

University of Pittsburgh, 2006

The present study is of great importance both from industrial application side and from fundamental point of view. The work considers ecologically significant industrial processes - utilization of chlorinated hydrocarbons. Particularly, 1,2-dichloroethane utilization is chosen as a model reaction to study the kinetics of hydrogenation process in fixed batch flow reactor over Pt-Cu silica supported bimetallic catalysts. The fundamental part of the study includes correlation search between kinetics performance and electronic-structural properties of Pt-Cu bimetallic catalyst. Establishing correlation between electronic-structural properties and performance in chemical reactions are of prime significance for understanding of chemical nature of particular chemical systems. The understanding means the ability to govern the process that is of huge interest for industrial applications.

The kinetic performance is determined directly by testing the selected catalyst in fixed bed reactor. The main characteristics derived from kinetics testing that are interesting for current study - selectivity and activity. The product of interest for presented process is ethylene, C₂H₄. The electronic-structural properties were derived mainly from the infrared-red (FTIR) study of

carbon monoxide (CO) test molecule. The correlation between electronic-structural properties and kinetics performance are related to freshly pretreated catalyst.

It was established that the selectivity toward C_2H_4 is a strong function of Cu/Pt atomic ratio that depends on the size of Pt ensembles: the smaller the size of Pt ensembles the higher selectivity toward C_2H_4 . Activity slightly decreases as Cu/Pt ratio is increasing. The observed kinetics performance is rationalized based on knowledge derived from FTIR study and knowledge from previously published works.

Structural sensitivity of C-Cl bond cleavage reaction is established for 1,2-dichloroethane hydrodechlorination. Elementary step of C-Cl bond cleavage is require 2-6 platinum atoms. Besides, the role of Cu as a main component responsible for C_2H_4 formation is shown experimentally. The structural dependence is rationalized in terms of ensemble size effect.

The mechanism of 1,2-dichloroethane hydrodechlorination reaction for highly selective catalysts is explained in terms of independent role of Pt and Cu.

Keywords: Bimetallic Catalysts, Platinum-Copper Silica Supported Catalysts (Pt-Cu/SiO₂), 1,2-dichloroethan (1,2-DCE), Hydrodechlorination

TABLE OF CONTENTS

LIST OF TABLES	vii
LIST OF FIGURES	viii
GLOSSARY	xi
ACKNOWLEDGEMENTS	xii
1.0 INTRODUCTION	1
1.1 IMPORTANCE OF THE WORK	1
1.2 THE GOAL AND SCOPE OF THE WORK	2
2.0 EQUIPMENT AND EXPERIMENTAL SETUP	4
2.1 EQUIPMENT	4
2.2 CALIBRATION	7
2.3 PRECAUTION: EXPERIMENTAL CONCERNS AND SAFETY ISSUES	11
3.0 LIGAND AND ENSEMBLE SIZE EFFECT IN CATALYSIS BY PLATINUM-COPPER CONVENTIONAL SILICA SUPPORTED BIMETALLIC CATALYSTS: 1,2-DICHLOROETHANE HYDRODECHLORINATION REACTION.....	13
3.1 INTRODUCTION	13
3.2 EXPERIMENTAL PROCEDURE	14
3.3 RESULTS	21
3.4 DISCUSSION	44
3.5 SUMMARY	51
4.0 ENSEMBLE SIZE EFFECT: MODEL CATALYST APPROACH	53

4.1 INTRODUCTION	53
4.2 EXPERIMENTAL PROCEDURE	54
4.3 RESULTS	59
4.4 DISCUSSION	71
4.5 SUMMARY	75
5.0 STRUCTURAL SENSITIVITY OF C-CL BOND CLEAVAGE. ROLE OF COPPER.	78
5.1 INTRODUCTION	78
5.2 EXPERIMENTAL PROCEDURE	79
5.3 RESULTS	82
5.4 DISCUSSION	85
5.5 SUMMARY	87
6.0 EXECUTIVE CONCLUSIONS	88
7.0 RECOMMENDATIONS FOR FUTURE WORK	91
APPENDICES	93
APPENDIX A	93
APPENDIX B	97
APPENDIX C	99
BIBLIOGRAPHY	101

LIST OF TABLES

Table 1. Characteristic features of ^{12}CO adsorption over bimetallic PtCu/SiO₂ catalysts reduced at 220 and 500 °C.....24

Table 2. Initial/final kinetics performance of PtCu catalysts subjected to different pretreatments.....36

LIST OF FIGURES

Figure 1.	Generalized scheme of experimental approach. Independent studies were performed to establish correlation between electronic-structural properties and kinetics performance of the catalyst.	3
Figure 2.	Analysis System: HP 5890 GC with FID was governed by computer allowing automatic analysis of experimental data.	5
Figure 3.	Calculated dispersion of Pt based on volume of CO chemisorbed.....	22
Figure 4.	Carbon monoxide adsorption over Pt/SiO ₂ catalyst reduced at 220 and 500 °C.....	25
Figure 5.	Carbon monoxide adsorption over PtCu1/SiO ₂ catalyst reduced at 220 and 500 °C	26
Figure 6.	Carbon monoxide adsorption over PtCu2/SiO ₂ catalyst reduced at 220 and 500 °C	28
Figure 7.	Carbon monoxide adsorption over PtCu3/SiO ₂ catalyst reduced at 220 and 500 °C	29
Figure 8.	Carbon monoxide adsorption over PtCu4/SiO ₂ catalyst reduced at 220 and 500 °C	30
Figure 9.	Carbon monoxide adsorption over PtCu5/SiO ₂ catalyst reduced at 220 and 500 °C	31
Figure 10.	Carbon monoxide adsorption over PtCu6/SiO ₂ catalyst reduced at 220 and 500 °C	32
Figure 11.	Singleton frequencies for samples with varying Cu/Pt ratio reduced at 220 or at 500 °C	33
Figure 12.	Calculated dipole-dipole coupling for samples with varying Cu/Pt ratio reduced at 220 or at 500 °C	34
Figure 13.	On stream performance for Pt/SiO ₂ catalyst reduced at 220 and 500 °C	35
Figure 14.	On stream performance for Cu/SiO ₂ catalyst reduced at 220 and 500 °C	36

Figure 15.	On stream performance for PtCu1/SiO ₂ catalyst reduced at 220 and 500 °C.....	37
Figure 16.	On stream performance for PtCu2/SiO ₂ catalyst reduced at 220 and 500 °C.....	38
Figure 17.	On stream performance for PtCu3/SiO ₂ catalyst reduced at 220 and 500 °C.....	39
Figure 18.	On stream performance for PtCu4/SiO ₂ catalyst reduced at 220 and 500 °C.....	40
Figure 19.	On stream performance for PtCu5/SiO ₂ catalyst reduced at 220 and 500 °C.....	41
Figure 20.	On stream performance for PtCu6/SiO ₂ catalyst reduced at 220 and 500 °C.....	42
Figure 21.	Specific activities at steady-state conditions for catalysts with different Cu/Pt ratio reduced at 220 and 500 °C	43
Figure 22.	Schematic procedure of spin-coating technique sequencing for preparation of Pt and PtCu1/SiO ₂ /Si(100) model catalyst.....	55
Figure 23.	Effect of reduction temperature on reducibility of Pt in Pt/SiO ₂ /Si(100) model catalyst sample prepared from H ₂ PtCl ₆	59
Figure 24.	Effect of reduction temperature on reducibility of Cu in Cu/SiO ₂ /Si(100) model catalyst sample prepared from CuCl ₂	60
Figure 25.	Effect of reduction temperature on reducibility of Pt and Cu in PtCu1/SiO ₂ /Si(100) model catalyst sample prepared from H ₂ PtCl ₆ and CuCl ₂	61
Figure 26.	Effect of reduction temperature on average size of Pt particles in monometallic Pt/SiO ₂ /Si(100) model catalyst. Results of AFM Imaging.	64
Figure 27.	Effect of reduction temperature on average size of Pt particles in monometallic PtCu1/SiO ₂ /Si(100) model catalyst. Results of AFM Imaging.	65
Figure 28.	Variation of average height and lateral length as function of reduction temperature for Pt/SiO ₂ /Si(100) and PtCu1/SiO ₂ /Si(100) model catalysts.	66
Figure 29.	Pt/SiO ₂ /Si(100) reduced at 220 °C: A. HDCl of 1,2-DCE B. Hydrogenation of C ₂ H ₄	67
Figure 30.	Pt/SiO ₂ /Si(100) reduced at 500 °C: A. HDCl of 1,2-DCE B. Hydrogenation of C ₂ H ₄	68
Figure 31.	PtCu1/SiO ₂ /Si(100) reduced at 220 °C: A. HDCl of 1,2-DCE B. Hydrogenation of C ₂ H ₄	70

Figure 32.	PtCu1/SiO ₂ /Si(100) reduced at 500 °C: A. HDCl of 1,2-DCE B. Hydrogenation of C ₂ H ₄	71
Figure 33.	Comparison of initial selectivity performance for conventional and model catalysts reduced at 220 and 500 °C.....	72
Figure 34.	Kinetics testing of Pt/SiO ₂ conventional catalyst diluted with SiO ₂ in reaction of 1,2-dichloroethane hydrodechlorination.	73
Figure 35.	Kinetics testing of Pt/SiO ₂ conventional catalyst reduced at 650 °C for 20 h in reaction of 1,2-dichloroethane hydrodechlorination.	74
Figure 36.	Structure of Pt/SiO ₂ /Pt(100) model catalyst: silica (SiO ₂) layer has imperfect structure with exposed silicon (Si) layers and supported Pt particles.....	76
Figure 37.	Comparative adsorption of π - and di- σ -bonded C ₂ H ₄ over Pt(111) and Pt ₃ Si(110) surfaces	77
Figure 38.	Kinetics performance of C/Pt/SiO ₂ catalyst with different dispersion of Pt.....	82
Figure 39.	Dependence of selectivity toward monochloroethane (C ₂ H ₅ Cl) upon dispersion of Pt in C/Pt/SiO ₂ catalyst.	83
Figure 40.	Dependence of turn over frequency (TOF) on effective size of Pt ensemble.....	84
Figure 41.	Adsorption of methyl chloride on small Pt ensemble.....	86

GLOSSARY

1,2-DCE: 1,2-Dichloroethane ($C_2H_4Cl_2$)

MCE: Monochloroethane (C_2H_5Cl)

HDCI: Hydrodechlorination

SPM: Surface Probe Microscopy

AFM: Atomic Force Microscopy

FTIR: Fourier-Transform Infrared Spectroscopy

GC: Gas Chromatography

FID: Flame Ionization Detector

TEM: Transmission Electron Microscopy

TPR: Temperature Programmed Reduction

TPD: Temperature Programmed Desorption

XPS: X-ray Photoelectron Spectroscopy

ACKNOWLEDGEMENTS

First of all, I would like to say thank you to research advisor of this work Dr. Julie L. d'Itri. Her non-ordinary manner to teach allowed me to gain many important qualities of engineer and scientist. I would like to appreciate her support and desire to help in difficult times. Besides, I would like to acknowledge my co-advisor and project coordinator Dr. Vladimir I. Kovalchuk for fruitful discussion and advice on experimental realization of many parts of the work.

I appreciate the participation of Chairman of Chemical Engineering Department Dr. Robert Enick and Graduate Student Coordinator Dr. William Federspiel in making final defense possible. Besides, I will never find the precious words to express my gratitude and thankfulness to thesis committee members Dr. Götz Vesper, Dr. Dadisav Vidic, and current thesis advisor Dr. Karl Johnson.

The help of all the students, visiting scholars and research fellows who gave me either a piece of advice or even their hands is acknowledged greatly. Especially, I would like to say thank you to Dr. Victor Borovkov for fruitful discussion of results, graduate student Vladimir Pushkarev and to Dr. David R. Luebke for helping on equipment installment, to Dr. Sergei Smirnov and his graduate student Pavel Tokmakov (NMSU) for helping me to collect AFM data. Besides, I would like to acknowledge the help of technical staff of the University of Pittsburgh: Bob Greer (Glass Shop), Tom Gasmire, Dennis Sicher, Jeff Sicher (Chemistry Machine Shop), Dave Emala (Electronics Shop), and of course Ron Bartlett and Bob Maniet (Chemical Engineering Technical

Staff). Their input in this work is truly significant and without their help this work would not be possible.

I would like to say thank to all professors who taught me for past years - without their devotion and to the Academy my life would be less colorful and lively. The fund of knowledge that I got here is tremendous. And I hope to have a chance to share that knowledge with other people and apply it to make our life better.

The financial support of granting organization DOE and Dow Chemical is appreciated.

This dissertation is dedicated to my wife, who supported and encouraged me all ten years we are together and brought me a strong son. Her love made my life and work more blazing and meaningful.

Thank all of you!

1.0 INTRODUCTION

1.1 IMPORTANCE OF THE WORK

There is an ongoing demand for safe and efficient methods to dispose chlorinated hydrocarbons ^{1,2}. Of particular importance is technology to dispose of 1,2-dichloroethane (1,2-DCE). This chemical is widely used as a solvent and is used in large quantities for vinyl chloride production, a feedstock for polyvinyl chloride production ³. In 1996 the amount of “byproduct” 1,2-DCE was more than 82 thousand tons and at least 580 tons were released into the environment ⁴. The yearly increasing demands of Environmental Protection agency as well as increase of rotation of chlorinated hydrocarbons on industrial scale makes environmental engineers to search for new ways of chlorinated hydrocarbons disposal. Currently there are several different approaches known.

Incineration of wastes containing chlorinated compounds has been used for decades. Though, being highly effective method for destruction of original chlorinated hydrocarbons ⁵, it was reported that incineration leads to high emission level ⁶, and generates toxic chemicals such as dioxins ⁷, phosgene ⁸.

Hydrodechlorination (HDCI) is alternative method to dispose chlorinated compounds in which chlorine-containing hydrocarbons are converted to alkanes over catalyst formed of Group

VIII metal ^{9, 10}. As well, hydrogen-assisted dechlorination (HAD) has been used to convert chlorine-containing hydrocarbons to olefins over catalyst formed of Group VIII metal with addition of metal of Group IB ¹¹⁻¹⁷.

The HDCI and HAD catalysts have activity of the same order at steady-state conditions, while sole Group IB supported metals have activity of two order of magnitude less than typical HDCI and HAD catalyst with 100% selectivity to olefins ¹⁵. The selectivity for the HDCI and HAD catalytic processes strongly depends on the catalyst nature. The possible explanation for such catalytic performance might be electronic modification of one metal with another, due to alloy formation, or it might be ensemble size effect due to simple dilution of one metal with another ^{15, 16, 18}.

1.2 THE GOAL AND SCOPE OF THE WORK

To explain the catalytic performance of Pt-Cu bimetallic catalyst in comparison with catalytic performance of Pt and Cu monometallic catalyst the following hypothesis was proposed in our group: Alloying between Pt and Cu leads to mutual modification of metal properties. That modification can be either electronic or structural. The change of kinetics performance is associated with modification.

To explore the hypothesis series experiments for designed. The main objective of the work was establishing what kind of modification is responsible for unique catalytic properties of bimetallic catalysts in comparison with monometallic.

Figure 1 explains briefly the experimental approach used to establish factors influencing the kinetics performance of bimetallic catalyst.

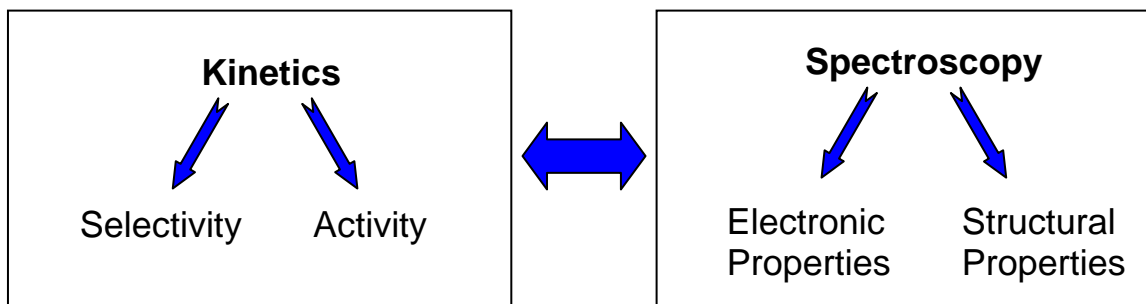


Figure 1. Generalized scheme of experimental approach. Independent studies were performed to establish correlation between electronic-structural properties and kinetics performance of the catalyst.

The work presented will be organized according to the following scheme. In Chapter 2 the equipment used in this study and its calibration will be described. Chapter 3 will consider the set of experimental procedures and findings directed to establishing correlation between kinetics performance and electronic-structural properties. In Chapter 4 the attempt to get direct evidence on ensemble size effect by using a model catalyst approach will be presented. Chapter 5 will be devoted to detailed investigation of influence of “pure” ensemble size effect on sensitivity of C-Cl bond cleavage and elucidation of role of copper.

2.0 EQUIPMENT AND EXPERIMENTAL SETUP

2.1 EQUIPMENT

The work presented in this thesis was done with application of a wide variety of experimental techniques: kinetics investigation with GC analysis, infrared spectroscopic investigation, and volumetric adsorption techniques. The design and calibration of equipment for this study is of particular importance, as soon as the results obtained directly depends on accurate and accurate realization of experimental approach. In this chapter we will consider design of selected equipment pieces. The details of experimental procedures will be considered in the beginning of corresponding sections.

2.1.1 Kinetics System

All kinetics experiments were conducted in a stainless-steel flow reaction system operated in a differential regime. The general reaction system scheme was in details described before ¹⁹. The only difference was the absence of heating tape on lines conduction reactants, as soon as it was detected in test reaction (Dr. Alex Kudryashev) that uncontrolled lines heating gives non-zero conversion (~2%) even in the absence of catalyst. The reactor consisted of a quartz tube (10 mm i.d.) in which the catalyst was supported on a quartz frit. The pretreatment

gases and gaseous reactants were metered by mass flow controllers (5850E, Brooks) and were mixed prior entering the reactor. The 1,2-dichloroethane was metered into the system by flowing He through a saturator containing the liquid reactant at $0(\pm 1)$ °C. The saturator temperature was maintained by a recirculating cooling system (RTE-111, Neslab). A blank (without catalyst or with support only) experiment always preceded the kinetics testing.

The sample temperature was controlled to ± 1 °C using a temperature controller (CN2011, Omega) connected to K-type thermocouple (Omega) placed in a quartz pocket that was in direct contact with the catalyst bed. The reaction products were analyzed by on-line GC (HP 5890). Hydrogen and hydrogen chloride were not quantified: all calculations of kinetics performance are based on the carbon balance. The GC was equipped with 3 m 60/80 Porapak Q packed column (Supelco) and flame ionization detector (FID) with a detection limit of <0.2 ppm for all hydrochlorocarbons and hydrocarbons involved in this study. The analytical part of reaction system is sketched on Figure 2.

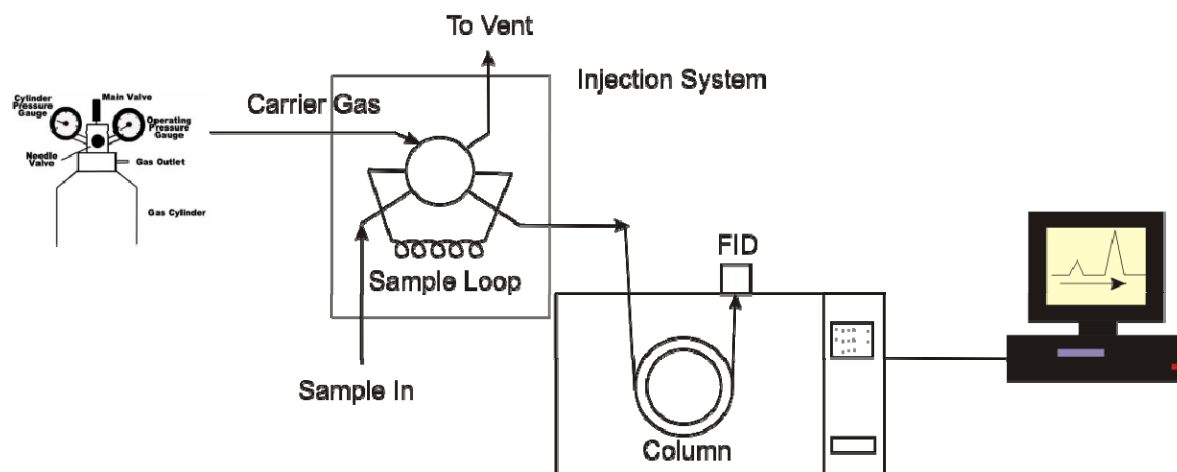


Figure 2. Analysis System: HP 5890 GC with FID was governed by computer allowing automatic analysis of experimental data.

2.1.2 FTIR System

The infrared spectra were recorded using a Research Series II FTIR spectrometer (Mattson) equipped with a liquid N₂ cooled MCT detector (Judson Technologies). The spectra were measured in the range of 400 to 4000 cm⁻¹ with resolution of 2 cm⁻¹. For each spectrum 64 scans were collected and averaged. Samples for FTIR study were prepared in the following way. First, the powdered catalyst was pressed at 800 atm. for 1 min into a pellet with density of 20-30 mg cm⁻². Then the catalyst pellet was placed into the quartz sample-holder of a vacuum IR-cell (0.5 l, 12 cm optical path) with NaCl windows. The *in-situ* cell operated in the temperature range from 20 to 500 °C, and it was equipped with grease-free glass stopcocks (Ace Glass, Inc.) connected to gas inlet/outlet ports and a vacuum port with a turbo-molecular pump (Leibold, 2000 l sec⁻¹).

2.1.3 Volumetric Adsorption System

Volumetric adsorption system ASAP 2010 (Accelerated Surface Area and Porosimetry System) from Micromeritics Company was used for volumetric chemisorption measurements. The system was computer governed and completely automatic, demanding only sample loading and creating appropriate pretreatment policy. Chemisorption measurements utilize the principle of specific adsorption. For our system carbon monoxide (CO) was used as an adsorbate molecule with adsorption policy from manufacture (35 °C). Carbon monoxide was used as an adsorbate due to specificity of CO interaction with the surface of Pt⁰ only for catalyst in reduced state: Cu⁰ or SiO₂ are unable to chemisorb CO at 35 °C.

Chemisorption measurements of CO “irreversibly” adsorbed were used for calculating the dispersion of Pt atoms (that is the same as the fraction of Pt atoms exposed to the surface). To define the volume of CO bound to the surface “irreversibly” two consecutive measurements with steadily increasing CO pressure were performed. The first measurement gave the total volume of CO both “irreversibly” and reversibly adsorbed to the catalyst surface. After evacuation of the sample the second measurement was performed and it gave information on reversibly adsorbed CO volume. The volume of “irreversibly” adsorbed or chemisorbed CO was calculated as a difference between first and second measurements. From known CO volume adsorbed per gram of catalyst the total number of chemisorption sites (Pt atoms) was calculated. And from the known Pt weight loading the dispersion of Pt atoms was calculated.

2.2 CALIBRATION

The calibration procedure was of prime concern in doing all quantitative measurements for this work. Each piece of equipment that could give rise to errors in quantitative measurement was thoroughly checked after installation and later inspected on a regular basis or when any suspicious results were noted.

2.2.1 Temperature Controllers and Thermocouples

Calibration and check-up of thermocouples were done by following the requirements of manufacture. The temperature controllers were calibrated at manufacture site when assembled.

To calibrate the thermocouple (J – Iron / Constantan or K – chromel/alumel type) the NIST approved thermometer was placed along with the thermocouple into the oven and the temperature was steadily increased to higher values. Both temperature readings from the thermometer and thermocouple were traced at the same time. To provide additional assurance, several different thermocouples attached to different temperature controllers were used. The low temperatures range was checked by placing a thermocouple (K-type) into liquid N₂. In this study all thermocouple readings had an error of less than ± 1 °C and no further calibrations were performed.

Temperature controllers were adjusted in such manner in order to keep temperature constant and avoid temperature under- and over-shooting at temperature ramps. Unfortunately, downhill ramps during the pretreatment steps gave undershooting of temperature as much as 10 °C that is 1-5% on the whole scale (reaction temperature 200 °C). The undershooting of temperature during the pretreatment steps is not critical for the purpose of our experiment: before the reaction was started the temperature was allowed to equilibrate around 200 °C.

2.2.2 Mass-Flow Controllers

Calibration of mass-flow controllers (Brooks 5850E, MFC) as a rule was performed on a regular basis (once in a three month period), besides additional checkups were performed from time to time (once in a week). Calibration a-values ($a \cdot x + b$, $b \sim 0$) for MFC-calibration curves did not change significantly between calibrations. Moreover, linear correlation was found to be extremely good (with $R > 0.995$).

Reference device for measuring flows was conditioned bubble flow-meter. The time was measured with a stopwatch. For each MFC flow setting at least three points were collected. Total 4-5 setting points were collected in a whole range of available flows on a percentile scale (5-80%). The desired flow corresponding to experimental conditions was adjusted by calculation through linear form equation ($a \cdot x + b$, $b \sim 0$) by setting desired percentile (x) value to desired range. All flows corresponding to experimental conditions were double checked at the setting point (x).

2.2.3 Infrared System

FTIR calibration was as rule a matter of performance. Regular checkups and alignments were performed once the deterioration of performance was observed. The checkup included the deviation of observed wavenumbers from standard positions: polystyrene (for rough evaluation, 4 cm^{-1}) or carbon monoxide (CO) and carbon dioxide (CO₂) rotational structures (fine evaluation, 0.25 cm^{-1}). During the whole 3 years of work no deviation for wavenumbers was found.

In case of quantitative measurements of gas of interest (HCl, CO, and etc.) the calibration of FTIR cell was performed. For this purpose the desired pressure of gas was injected into FTIR system and absorption value of reference band (f.g., for HCl 2843 cm^{-1}) was measured. Absorption as a function of absolute pressure was plotted. From this data complex extension coefficient for particular band was calculated ($\epsilon \cdot l [\text{Torr}^{-1}]$).

2.2.4 GC FID Calibration

The calibration of FID GC detector was of prime importance for quantitative measurements in kinetics study. Calibration was done on the regular basis usually along with calibration of MFC or as needed (FID cleaning, lines modification). First, the desired column (Porapak Q, 60/80, 12 ft form Supelco) was calibrated with a mixture of expected products to determine approximate the retention times (min). On the second stage the temperature program on the column was adjusted to minimize the time of analysis. And finally FID response was calibrated with respect to available compounds (C_2H_4 , C_2H_5Cl , $C_2H_4Cl_2$). The FID for the rest of compounds (C_2H_6) was estimated based on relative heat of combustion (as it was shown later this approximation gave errors of less than 2%).

The calibration of FID response to particular compound was done by flowing a gas mixture of this compound though the sample-loop (at constant T) along with a diluent gas (He). The concentration of the compound was adjusted by variation of relative flows. The calibration curve represented the dependence of integrated area under the peak on concentration (parts per million, ppm) of the compound in a calibration mixture. The response factor (RF) represented the a-value for straight line approximation ($a \cdot x + b$, $b \sim 0$), with x-concentration (ppm). A perfectly straight line (usually with $R > 0.999$) in a wide range of flows evidenced of the absence of any significant flow-resistance (pressure change) inside the kinetics system.

2.3 PRECAUTION: EXPERIMENTAL CONCERNS AND SAFETY ISSUES

In this section some notion of the importance of experimental realization will be given. The author sincerely believes that these precautions will allow avoiding critical mistakes for starting experimenter-students. I will try to follow troubleshooting manner sequence in the following paragraphs.

First, I would like to note that any strange behavior (either irreproducible or that is in contradiction with previously published data) is an evidence of probable mistakes in realization of the experiment. The first part to start troubleshooting one's system is a detection part. The second is MFC or pressure gadgets. And finally the last (but very important part) is leak tracking. Every new connection or modification must be considered as a potential leak source!

For GC analysis the variation of any parameter either for column temperature program or a flow of a carrier gas must be considered as an absolutely new analysis condition and calibration must be done again. Besides, prolonged use of a FID detector without cleaning may cause significant variation of RF factors (more than 10%). It is of high importance to clean FID detector and recalibrate it after that on a regular basis.

For FTIR system the first reason of signal change is variation in the amount of light passing through the sample. It is as a rule the IR-cell windows aging due to interaction with moisture from air. Cleaning with alcohol and polisher might help to improve transparency; otherwise new windows must be attached. The other reason might be de-alignment of mirrors, beam-splitter,

detector or light source. In this case automatic alignment must be tried in the first turn. If it does not help – cubic mirror or detector alignment might help. It is not advised to start with alignment of parabolic mirrors! No signal is, as a rule, associated with the light-source failure (check cooling water) or detector failure (check liquid N₂ level).

Moreover, vacuum is also of extreme importance for good results. To prevent failure of turbo pumps regular cleaning of the ceramic bearing must be performed. Mechanical pumps should be maintained in good condition by regular 6-8 month (or as needed) oil replacement. Oil filter must be placed to prevent oil coming to vacuum system. IR-cell or vacuum connection might be a source of the leaks. Regular cut off of particular parts of the system and pressure monitoring might allow discovering the leak source. Otherwise, mass-spectrometer might be used to find out the leak source with He as a probe gas. Or for glass system regular checking with Tesla device might help to find the leaks.

To conclude, the work with extremely dangerous explosive gases as H₂ at high pressures must be of prime concern. Besides, such poisons as 1,2-dichloroethane and CO must be treated properly. Follow materials safety data sheets (MSDS) precautions. Check and secure all cylinders. Check all lines for leaks. Work under the hood and use safety glasses.

**3.0 LIGAND AND ENSEMBLE SIZE EFFECT IN CATALYSIS BY PLATINUM-COPPER CONVENTIONAL SILICA SUPPORTED BIMETALLIC CATALYSTS:
1,2-DICHLOROETHANE HYDRODECHLORINATION REACTION**

3.1 INTRODUCTION

As it was already mentioned in a general introduction section the prime objective of this work was establishing a correlation between electronic-structural properties and kinetics performance. Reaction of 1,2-dichloroethane elimination on a bimetallic catalysts was chosen due to several important reasons. Its selectivity pattern on bimetallic catalyst allows assuming either ligand effect and/or ensemble size effect due to alloying between platinum and copper. This experimental work was designed in such a manner as to answer the question what is the prime factor that defines kinetics performance.

3.2 EXPERIMENTAL PROCEDURE

3.2.1 Catalysts Preparation

Silica powder* (Aldrich, 99+%, 60-100 mesh, $300 \text{ m}^2 \text{ g}^{-1}$, 150 \AA) was used as the catalyst support. The silica was air-calcined at $500 \text{ }^\circ\text{C}$ for 12 h before impregnation with metal salts. The monometallic Pt and the bimetallic Pt-Cu catalysts were prepared from a 0.1 N HCl aqueous solution of $\text{H}_2\text{PtCl}_6 \cdot 6 \text{ H}_2\text{O}$ (Alfa, 99.9%) and 0.1 N HCl aqueous solution $\text{CuCl}_2 \cdot 2 \text{ H}_2\text{O}$ (MCB Manufacturing Chemist, 99.5%). The concentrations of the metals in the impregnating solutions were adjusted to obtain the desired loading of each metal. The SiO_2 powder was added to the solution containing the dissolved metal precursors at ambient conditions while stirring continuously, and then the mixture was stirred for 12 h. The impregnated SiO_2 was isolated from the solution by filtration and dried at ambient conditions for 24 h. Subsequently, it was dried for 12 h at $100 \text{ }^\circ\text{C}$ under a static vacuum ($\sim 25 \text{ Torr}$). As soon as all SiO_2 samples are humectants, the water was absorbed from the air. To “stabilize” the H_2O balance and as a result the aging phenomena connected with increase of metal crystallites after reduction step²⁰ we added H_2O into the jars with samples on 1/5 mass basis (1 g of water/5 g of sample). During this procedure, the dark-brown color of samples immediately turned into light-green with a tint of yellow; this is

* The experimental procedure outlined for catalysts preparation was developed by Professor V. Kovalchuk.

the evidence of formation of chlorinated Pt and Cu aqua-complexes. Sample with the following weight loadings of each metal were prepared for the current research study: 2.7%Pt, 2.8Pt%0.9%Cu, 2.7Pt%1.8%Cu, 2.7Pt%2.7%Cu, 2.7Pt%3.5%Cu, 2.7%Pt4.2%Cu, 2.6Pt%5.1%Cu, and 0.5%Cu. The nomenclature used henceforth for the bimetallic samples is PtCuX, where X denotes the atomic ratio Cu/Pt (from 1 to 6).

3.2.2 Temperature Programmed Desorption (TPD) and Reduction (TPR)

The TRP and TPR experiments were performed *in situ* FTIR system. The following samples were tested: Pt, PCu1, PtCu3, PtCu6 and Cu. For each experiment a sample pellet of 0.02-0.05 g was placed into the sample holder of the FTIR cell. The objective of the TPD experiments was to check for the species released during the drying step. The sample was evacuated (10^{-6} Torr) at room temperature for 2 h before the TPD experiment. The TPD experiment was performed in a closed IR-cell evacuated to pressure of 10^{-6} Torr. The temperature was continuously increasing from 20 to 130 °C at ramp of 4 °C min⁻¹. Once the temperature reached 130 °C, the sample was hold for 1 h, after that, the vacuum port was opened, and the sample was evacuated for 0.5 h at 130 °C. Later, this sample was used in TPR experiments. To summarize results briefly, TPD showed release of H₂O at 70 °C and release of HCl started at 100-110 °C for all samples except the Cu monometallic sample. The Cu monometallic sample showed release of HCl at 120 °C. The temperature ascription of the beginning of HCl release can not be accurate because the HCl detection limit for a given IR-cell geometry depends on the sample mass and total metal chlorides loading. The most important fact here is that we have detectable release of HCl and H₂O, which is typical for our catalytic systems and leads to the formation of hydroxychlorides²¹.

TPR experiments were performed to check reducibility of the Pt-Cu catalyst. Two types of TPD experiments were done. First type, sample from TPD experiment after being dried at 130 °C for 1.5 h under vacuum was cooled to room temperature and 600 Torr of H₂ (99.99%, PennOxygen) were injected into FTIR cell. Then the heating started at a ramp of 4 °C min⁻¹ and the temperature was increasing continuously up to 500 °C. These types of TPR experiments showed that the reduction of Pt samples started around 85 °C and above 150 °C no significant increase of HCl concentration was detected. Water formation was observed during the whole run: the water release might be due to reduction of hydroxychloride species as well as due to desorption of water chemically bonded to hydroxy-groups of silica. Moreover, formation CO was detected at 250 °C and CH₄ formation was observed starting around 300 °C for Pt sample and all bimetallic samples tested. That is probably due to decomposition of carbonate species with following hydrogenation of CO and CO₂ to CH₄. Monometallic Cu sample showed traces of HCl after the temperature reached 180 °C. The IR-TPR profile had two different slopes in the 18-221 and at 221-280 °C regions. According to literature data they correspond to reduction of CuCl₂ to CuCl and CuCl to Cu^{22, 23}. Though, according to thermodynamic calculation the complete reduction of CuCl to Cu does not happen due to equilibrium. Water release was observed through the whole run as in the case of Pt samples. Release of CO was observed around 280 °C. The TPR of PtCu1, PtCu3 and PtCu6 bimetallic samples showed release of HCl around 130 °C. Two slopes were observed for bimetallic samples: 130-150 and 150-212 °C. At higher temperature no increase of HCl concentration in a gas phase was observed. At 250 °C traces of CO were detected in a gas phase. Both Cu and PtCu6 sample formed no CH₄.

The second type of TPR experiment was performed according to the following policy. First, the sample was dried at 130 °C for 1.5 h and then reduced at 220 °C for 2 h in flowing

10% H_2 /Ar. After reduction at 220 °C the temperature was lowered to 200 °C and the sample was evacuated for 0.5 h. Up to this point the procedure was absolutely the same as the pretreatment procedure used before FTIR study of CO adsorption. Then, still keeping temperature at 200 °C, 600 Torr of H_2 was injected into the IR-cell and temperature started to increase at 4 °C min^{-1} up to 500 °C. During the heating, the gas phase in the IR-cell was monitored periodically and spectra were collected at different temperatures. To summarize results briefly, the reduction at 220 °C in 10% H_2 /Ar does not allow the reduction of metal chlorides completely. The monometallic Pt sample showed formation of H_2O and traces of HCl after temperatures reached 300 °C, along with CH_4 formation. Though, in comparison with bimetallic samples and the monometallic Cu sample gave the least amount of HCl per mass of catalyst. Bimetallic PtCu samples and monometallic Cu sample, gave 6 times more of HCl per gram of sample loaded than monometallic Pt samples. Water and CO were formed as well. The TPR experiments done on the samples reduced at 500 °C for 2 h in flowing 10% H_2 /Ar showed no formation of HCl.

Thus, TPR study showed that significant amount of Cl present in bimetallic PtCu and monometallic samples after reduction at 220 °C. According to literature data it might be bulk chloride and oxychloride species²¹. Moreover, some of the metals are in the carbonated form. Reduction at 500 °C eliminates the Cl and O completely and leads to decomposition of carbonates.

3.2.3 Volumetric Adsorption Study

The samples were characterized by CO chemisorptions measurements using a volumetric sorption analyzer (Micromeritics, ASAP 2010). The results were used to calculate the fraction of exposed Pt atoms for each catalyst, as described elsewhere in Section 2.1.3. According to our FTIR data after reduction at 500 °C adsorption of CO was observed both on Pt and Cu. For reduction of 500 °C we assumed the ratio between CO/Cu and CO/Pt is proportional to respective absolute intensities of CO after evacuation for 15 min. Dispersion of Pt was calculated after subtraction of CO/Cu.

3.2.4 FTIR Study

The standard pretreatment of the catalyst before the FTIR experiment consisted of several steps. Initially the catalyst sample was dried under vacuum (10^{-6} Torr) while heating at 5 °C min^{-1} from room temperature to 130 °C and then holding at 130 °C for 1.5 h. Afterwards a 30 cc min^{-1} 10% H_2/Ar (Airgas, 99.99%) flow was introduced into the cell, and the catalyst was heated at 5 °C min^{-1} from 130 to 220 °C. The catalyst was held for 2 h at 220 °C. Subsequently the temperature was lowered at 5 °C min^{-1} to 200 °C while flowing the 10% H_2/Ar mixture at 30 cc min^{-1} . The system was evacuated for 0.5 h at 200 °C. Then the pellet was cooled to room temperature (0.5 h) still under vacuum (10^{-6} Torr). After the pretreatment the catalyst was characterized by FTIR using CO as a probe molecule.

To begin, 10 Torr of ^{12}CO was introduced into the cell for 15 min. Then the spectrum was recorded. After that the cell was evacuated for 15 min, and another spectrum was recorded. Next, the dipole-dipole coupling shifts and the singleton frequencies for $^{13}\text{C}^{18}\text{O}$ adsorbed on Pt were

determined by a modified isotopic dilution method²⁴ using mixtures of ^{12}CO (Praxair, 99.99+%) and $^{13}\text{C}^{18}\text{O}$ (Isotec, 99+% ^{13}C , 95+% ^{18}O). The small amount of $^{13}\text{C}^{18}\text{O}$ was used to exclude frequency overlap with ^{12}CO . Initially, a $^{12}\text{CO}:$ $^{13}\text{C}^{18}\text{O}$ isotopic mixture with 1:1 ratio at total pressure of 10 Torr was introduced into the IR-cell with the sample having pre-adsorbed ^{12}CO . The system was allowed to equilibrate for 15 min. The continuous monitoring of IR-intensities of ^{12}CO and $^{13}\text{C}^{18}\text{O}$ showed that exchange between gas phase and adsorbed carbon monoxide molecules was close to the equilibrium after 5 min: only a slight increase of intensity was observed after 15 min with no change in the position of the corresponding ^{12}CO and $^{13}\text{C}^{18}\text{O}$ bands. Then, the spectrum in the presence of the $^{12}\text{CO}:$ $^{13}\text{C}^{18}\text{O}$ isotopic mixture in the gas phase was recorded. The cell was evacuated to 10^{-6} Torr for 15 min at ambient temperature, and the spectrum was recorded again. Afterwards a new isotopic mixture with a different $^{12}\text{CO}:$ $^{13}\text{C}^{18}\text{O}$ ratio was introduced into the cell. The procedure was conducted with different $^{12}\text{CO}:$ $^{13}\text{C}^{18}\text{O}$ ratios: 9:1, 8:3, 7:2, 6:4, and 1:9. The exact ratio was calculated for every mixture as the ratio of the partial pressure of the corresponding isotopic analogues. The following assumptions were used in calculation of $^{13}\text{C}^{18}\text{O}$ singleton frequency and dipole-dipole coupling shifts. First, we assumed the same $^{12}\text{CO}:$ $^{13}\text{C}^{18}\text{O}$ ratio in the gas phase and at the surface of metallic particles independent of preabsorbed gases, as soon as the volume of injected CO was at least 1000 times higher than the volume of CO hold by the sample. Second, we approximated the singleton frequency for $^{13}\text{C}^{18}\text{O}$ by extrapolation of $\nu(^{13}\text{C}^{18}\text{O})$ as a $f(^{13}\text{C}^{18}\text{O})$ to zero coverage. Third, the difference between ^{12}CO and $^{13}\text{C}^{18}\text{O}$ in a gas phase was set to 100 cm^{-1} for calculation of the frequency of $^{13}\text{C}^{18}\text{O}$ on the surface, assuming pure $^{13}\text{C}^{18}\text{O}$ in a gas phase.

After completion of the FTIR study of CO adsorption on the sample reduced at $220\text{ }^{\circ}\text{C}$, the sample was heated in $10\%\text{H}_2/\text{Ar}$ (30 cc min^{-1}) at $5\text{ }^{\circ}\text{C min}^{-1}$ from 20 to $500\text{ }^{\circ}\text{C}$ and then held at

500 °C for 2 h. The pellet was cooled at 5 °C min⁻¹ to 200 °C while flowing 10%H₂/Ar mixture (30 cc min⁻¹), that sample was evacuated at 200 °C for 0.5 h to remove gas phase and adsorbed species, and cooled to ambient temperature at which the same series of FTIR experiments were performed as for the catalyst reduced at 220 °C.

3.2.5 Kinetics Study

The kinetics experiments were conducted in a stainless-steel flow reaction system operated in a differential regime as was described in Section 2.1.1. The amount of the catalyst used in an experiment ranged between 50-300 mg so that the steady-state conversion was in the range 1.5-3 %. The catalyst temperature was controlled to ±1 °C using a temperature controller (CN2011, Omega) connected to a K-type thermocouple (Omega) placed in a quartz pocket that was in direct contact with the catalyst bed. The reaction products were analyzed by on-line GC (HP 5890). The GC was equipped with 3 m 60/80 Porapak Q packed column (Supelco) and flame ionization detector with a detection limit of <0.2 ppm for all chlorocarbons and hydrocarbons involved in this study.

The catalyst pretreatment for the kinetics and volumetric sorption studies was, in general, the same as for the FTIR study. First, the sample was loaded into reactor and heated in He (30 cc min⁻¹, PraxAir, 99.999%) from room temperature to 130 °C at 5 °C min⁻¹, and then it was held at 130 °C for 1.5 h while flowing He (30 cc min⁻¹). Second, the He flow was switched to 10%H₂/Ar (30 cc min⁻¹), and the temperature was increased either to 220 or 500 °C at 5 °C min⁻¹. The catalyst sample was held for 2 h while flowing 10%H₂/Ar (30 cc min⁻¹). Third, the temperature was decreased at 5 °C min⁻¹ from either 220 or 500 °C to 200 °C, and 10%H₂/Ar (30 cc min⁻¹)

was switched to He (30 cc min⁻¹). Finally, the system was purged for 0.5 h with He at 200 °C, and the reaction was started.

The reaction was conducted at 200 °C and at atmospheric pressure. The reaction mixture consisted of 7000 ppm of 1,2-dichloroethane (Fisher Scientific, 99.8+%), 36000 ppm H₂, and the balance He. The total flow-rate was 41 cc min⁻¹. The reaction was run for 40 or more hours until steady-state performance with respect to activity was obtained. For this investigation, steady-state selectivity was defined as a change less than 0.2% in 10 h. For each kinetics experiment a new sample of catalyst was loaded into reactor.

3.3 RESULTS

3.3.1 Temperature Programmed Desorption (TPD) and Reduction (TPR)

The results of TPD and TPR experiments are summarized here. First, TPD experiments showed formation of HCl during the drying step and water release. This is a sign that chlorides convert partially to oxychlorides during the drying step²¹. The results of TPR experiments for both monometallic Pt and Cu samples are in good agreement with the literature data^{21-23, 25}. The TPR1 experiments showed that bimetallic catalysts start to react with H₂ at a temperature of 130 °C that is intermediate to those for monometallic Pt (85 °C) and Cu (180 °C) catalysts. One might speculate that formation of mixed Pt and Cu oxychlorides takes place in bimetallic samples. The TPR2 experiments showed that reduction at 220 °C is not enough to eliminate Cl

and O ions completely. While the reduction at 500 °C leads to elimination of virtually all Cl and O anions.

3.3.2 Volumetric Adsorption Study

The results of CO chemisorption measurements showed that the monometallic Pt samples reduced either at 220 or 500 °C had the highest dispersion values. When the reduction temperature was 220 °C, the Pt sample had a dispersion of 27.0% (Figure 3). When the same sample was reduced at 500 °C, the dispersion was 26.7%.

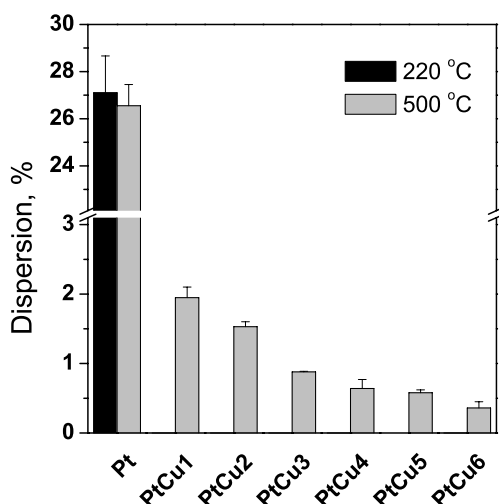


Figure 3. Calculated dispersion of Pt based on volume of CO chemisorbed. Adsorption at 35 °C. CO:Pt ratio was set to 1.

In contrast to the results for the monometallic Pt samples, for the bimetallic Pt-Cu samples, the total volume of CO adsorbed was much higher after reduction at 500 °C than after reduction at 220 °C. According to chemisorption measurements, for all samples reduced at 220 °C the total volume of chemisorbed CO was essentially zero. Though, according to FTIR results – significant amount of CO was chemisorbed over Pt. In turn, for all samples reduced at 500 °C the total

volume of CO adsorbed was much greater than zero. A significant decrease of Pt dispersion was observed for the PtCu1 sample in comparison with the monometallic Pt sample. The catalysts with Cu/Pt ratios of 1, 2, 3, 4, 5, and 6 had a dispersion of 1.95, 1.53, 0.88, 0.64, 0.58, and 0.36%, respectively (Figure 3). In general, the decrease of Pt dispersion was 1.1-1.7 times upon increase of Cu/Pt ratio by 1.

Catalysts showed the same trend with respect to CO chemisorption as in published works^{15, 26}: an increase in the Cu/Pt ratio resulted in a decrease in the number of exposed Pt atoms. The most significant decrease of dispersion was observed for PtCu1 sample in comparison with Pt sample. Reduction at 500 °C resulted in an increase in the number of exposed Pt atoms in the bimetallic catalysts, while monometallic Pt sample manifested slight segregation after reduction at 500 °C (Figure 3).

3.3.3 Results of FTIR Study

The general characteristic features of CO adsorption on PtCu bimetallic samples are summarized in Table 1. The reader is encouraged to apply the information in that table while reading “*Results of FTIR Study*” section.

Pt. Adsorption of 10 Torr CO over Pt sample reduced at 220 °C was accompanied by appearance of two bands in the spectrum - 2077 and 1835 cm⁻¹ (Figure 4 A). The red shift and intensity decrease were observed for both bands after removal of CO from the gas phase; the bands shifted to 2070 and 1815 cm⁻¹, respectively.

Table 1. Characteristic features of ^{12}CO adsorption over bimetallic PtCu/SiO₂ catalysts reduced at 220 and 500 °C.

220 °C						
	$^{12}\text{CO}/\text{Cu}$			$^{12}\text{CO}/\text{Pt}$		
	ν, cm^{-1}	$I_{\text{abs}}, \text{Abs. cm}^{-2} \text{g}^{-1} \text{cat}$	$I_{\text{int},2}, \text{Abs. cm}^{-2} \text{g}^{-1} \text{cat}$ cm^{-1}	ν, cm^{-1}	$I_{\text{abs}}, \text{Abs. cm}^{-2} \text{g}^{-1} \text{cat}$	$I_{\text{int},2}, \text{Abs. cm}^{-2} \text{g}^{-1} \text{cat}$ cm^{-1}
Pt	---	---	---	2077/2069	95.1/87.0	3664/3674
PtCu1	2137/2131	5.4/0.1	170/1	2037/2048	2.8/3.3	221/222
PtCu2	2137/2131	4.5/0.1	139/1	2031/2044	1.6/1.7	112/109
PtCu3	2139/2129	4.6/0.1	151/2	2029/2042	1.5/1.7	95/97
PtCu4	2141/2131	3.9/0.0	130/1	2029/2042	1.0/1.1	70/70
PtCu5	2143/2125	5.0/0.1	173/1	2029/2040	1.6/1.5	130/97
PtCu6	2144/-----	3.9/0.0	130/0	2030/2040	1.2/1.1	99/71
500 °C						
Pt	---	---	---	2075/2071	43.2/39.3	2222/2156
PtCu1	2125/2123	5.5/1.6	134/34	2051/2052	4.3/6.6	309/431
PtCu2	2129/2127	4.2/0.7	111/15	2050/2052	3.1/5.5	183/298
PtCu3	2123/2123	7.3/2.5	214/66	2038/2043	2.2/5.2	120/303
PtCu4	2127/2129	9.1/1.8	317/46	2038/2044	2.8/5.3	273/272
PtCu5	2125/2129	9.3/1.9	324/49	2036/2042	2.8/5.0	265/251
PtCu6	2125/2129	10.2/2.0	340/47	2038/2042	2.5/4.5	278/228

After adsorption of 10 Torr CO over Pt monometallic sample reduced at 500 °C the bands at 2075 and 1760 cm^{-1} were observed. The first band decreased in intensity and shifted to 2071 cm^{-1} after evacuation; while the second band developed no significant change either in intensity or position (Figure 4 B).

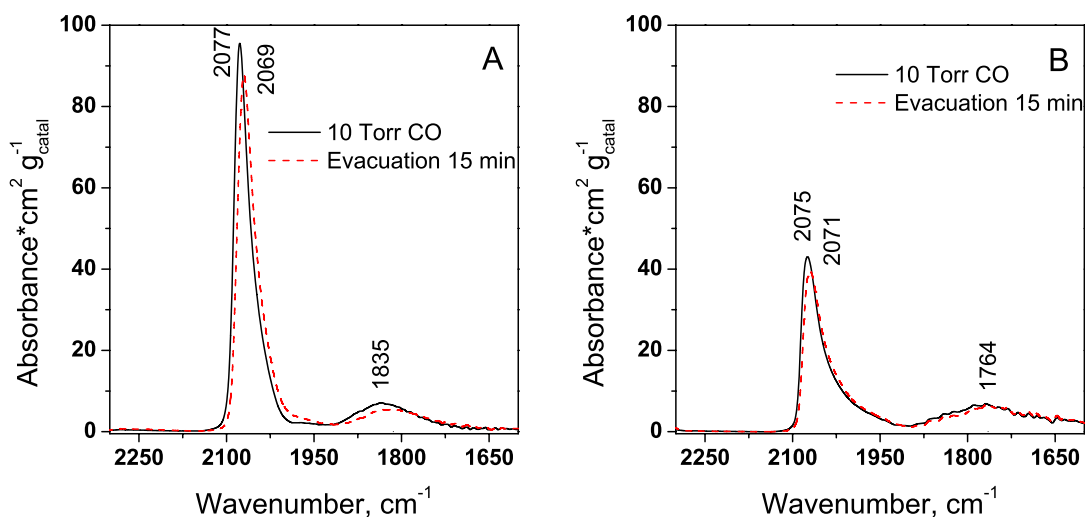


Figure 4. Carbon monoxide adsorption over Pt/SiO₂ catalyst reduced at 220 (A) and 500 °C (B): — 10 Torr CO, ···· Evacuation 15 min.

According to literature data the band 2070-2075 cm⁻¹ can be ascribed to linear form of CO adsorbed on exposed Pt atoms^{15, 27-31}. While the band 1760-1840 was ascribed to multi-bond (bridged and three-fold) of CO/Pt^{28,29}.

PtCu1. Investigation of CO adsorption on the PtCu1 sample reduced at 220 °C revealed two bands at 2136 and 2037 cm⁻¹ when 10 Torr CO was present in the gas phase. Upon evacuation, the band at 2136 cm⁻¹ significantly decreased in intensity and shifted to 2131 cm⁻¹. While the band at 2037 cm⁻¹ shifted to 2049 cm⁻¹ with insignificant increase in absolute intensity (Figure 5 A).

The PtCu1 sample reduced at 500 °C showed three bands at 2125 cm⁻¹ and 2051 cm⁻¹, and a band at 1750 cm⁻¹. Intensity of the first band decreased when CO was removed from the FTIR cell and band shifted to 2123 cm⁻¹, while the second band gained some intensity and shifted to 2052 cm⁻¹ (Figure 5 B).

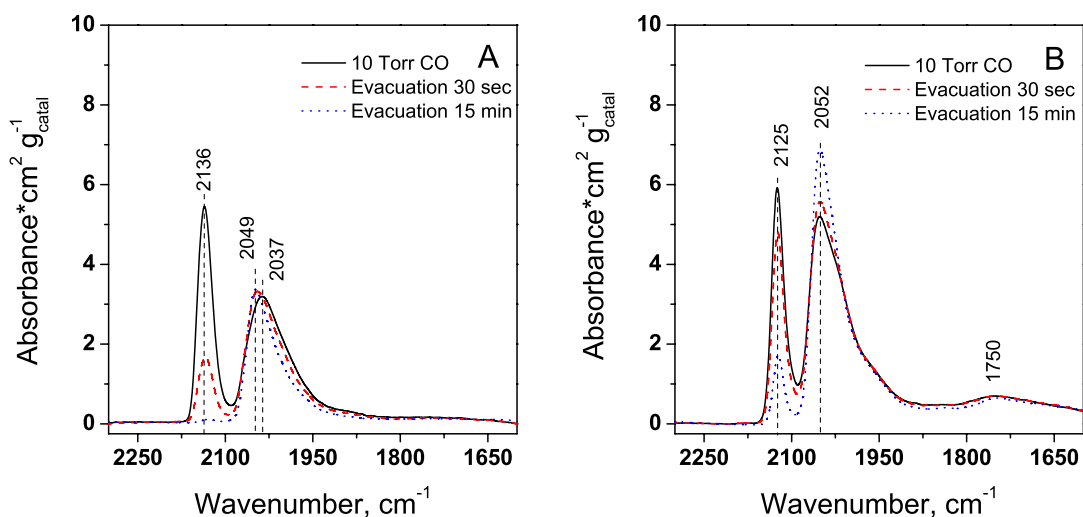


Figure 5. Carbon monoxide adsorption over PtCu1/SiO₂ catalyst reduced at 220 (A) and 500 °C (B):

— 10 Torr CO, --- Evacuation 30 sec, Evacuation 15 min.

Band 2030-2050 cm⁻¹ can be assigned to linear form of CO adsorbed over Pt atoms embedded into Cu matrix³²⁻³⁵. The difference in frequency for LCO/Pt (2070 cm⁻¹) and LCO/Pt-Cu (2040 cm⁻¹) is due to lower dipole-dipole coupling³⁶. The band 1750 cm⁻¹ as in the case of pure platinum can be ascribed to multi-bond CO/Pt species^{28,29}. The band at 2120-2140 cm⁻¹ can be ascribed to CO/Cu. The assignment of CO/Cu⁰ and CO/Cu¹⁺, CO/Cu²⁺ band is rather complicated question: the frequency of CO on Cu depends on the type support, roughness of the Cu surface, and degree of reduction^{37,38}. The assignment is usually made by checking the stability of the 2120-2140 cm⁻¹ band to evacuation. The CO/Cu⁰ ($\Delta H = 19.7 \text{ kJ mol}^{-1}$ ³⁷) and CO/Cu²⁺ ($\Delta H = 29.3 \text{ kJ mol}^{-1}$ ³⁷) are unstable in the absence of CO in a gas phase at ambient temperature. While CO/Cu¹⁺ is more stable and longer evacuation is needed to remove CO from Cu¹⁺ ($\Delta H = 50-115 \text{ kJ mol}^{-1}$ ^{37,39}).

The data presented in this research study can be used to assign the 2137 cm^{-1} band either to CO/Cu^0 or to CO/Cu^{2+} , but according to literature data, the frequency of CO/Cu^{2+} for SiO_2 supported samples develop at 2180-2215 cm^{-1} , depending on coordination^{37, 38}. Thus, we assign the band at 2137 cm^{-1} to CO/Cu^0 . The asymmetric band can be fitted by a minimum of two gaussian peaks with maxima at 2142-2150 cm^{-1} and 2125-2132 cm^{-1} . It is therefore reasonable to assume that we have two different types of CO/Cu^0 . Perhaps, the first band at 2142-2150 cm^{-1} is due to CO adsorbed at Cu^0 resting over partially reduced Cu moieties that still contain Cl and O ligands. While the band at 2125-2132 cm^{-1} is due to CO/Cu^0 , where Cu forms the top layer in a multilayer covered Pt particles.

The stable band 2125 cm^{-1} that appears after reduction at 500 °C can be assigned to CO adsorbed over Cu atoms either embedded into Pt matrix or sitting at the surface of Pt. It has been shown theoretically for a cluster model⁴⁰ that for Cu atoms adsorbed over Pt surface there is concerted $\text{Cu}(\text{s,p}) \rightarrow \text{Pt}$ and $\text{Pt} \rightarrow \text{Cu}(\text{d})$ electron transfer takes place that is accompanied by and $\text{Cu}(\text{s,p}) \rightarrow \text{Cu}(\text{d})$ electron rehybridization. Thus, electronically modified surface Cu atoms are able to bind CO much strongly in comparison with surface of bulk Cu due to donation of electron density from d-orbitals to $2\pi^*$ -orbital of CO. It was shown experimentally by XPS and UP spectroscopy that for monolayer of Cu over Pt foil a core-level binding shift of -0.5 eV is observed and this shift lead to increase of bond strength for CO-Cu bond⁴¹.

PtCu2. Room temperature adsorption of 10 Torr CO on *PtCu2* sample reduced at 220 °C allowed to distinguish two bands at 2137 and 2031 cm^{-1} . Evacuation for 15 min resulted in a red

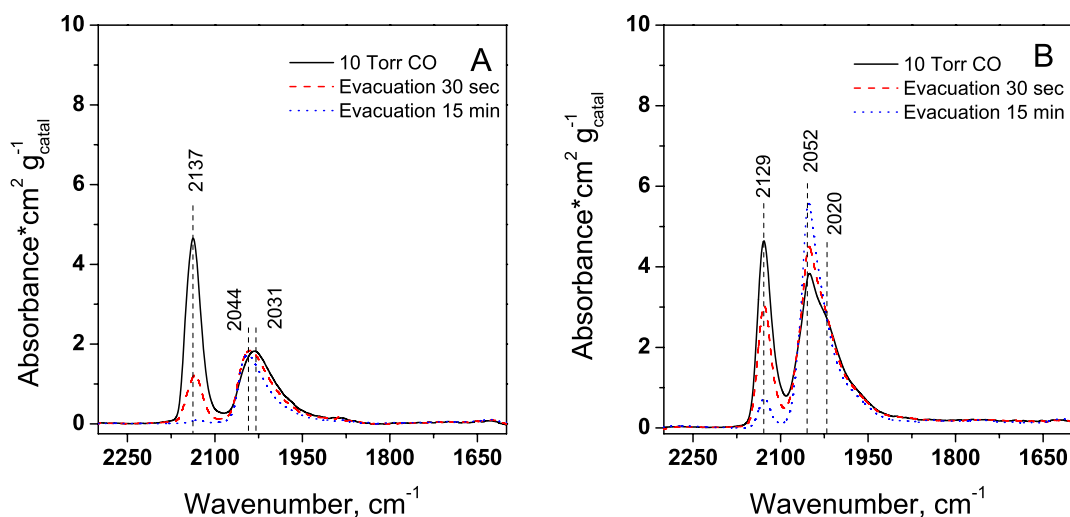


Figure 6. Carbon monoxide adsorption over PtCu₂/SiO₂ catalyst reduced at 220 (A) and 500 °C (B): — 10 Torr CO, --- Evacuation 30 sec, Evacuation 15 min.

shift to 2131 cm⁻¹ with significant decrease of intensity for the first band, and blue shift and insignificant increase of absolute intensity for the second band to 2044 cm⁻¹ (Figure 6 A).

When the PtCu₂ sample was reduced at 500 °C bands at 2129 and 2050 cm⁻¹ appeared after injection of 10 Torr CO into FTIR vacuum cell. Room temperature evacuation caused decrease of intensity and shift to 2127 cm⁻¹ for the first band. For the second band considerable increase of intensity and shift to 2052 cm⁻¹ were observed. For this sample, a distinct shoulder for at 2020 cm⁻¹ was observed for 2050 cm⁻¹ band. Note that for the PtCu₁ sample reduced at 500 °C it was less pronounced (Figure 6 B).

The band 2020 cm⁻¹ is ascribed by some authors to the bridged form of CO between Pt and Cu³⁶. On the other hand the same band is observed for monometallic Cu samples and opinions on the nature of the band differ. One group of authors ascribe the 2000-2020 cm⁻¹ band to bridged CO adsorbed over Cu^{37,39}. While, in work⁴² more stable band 2018 cm⁻¹ was observed

along with less stable band 2045 cm^{-1} ; by variation of CO pressure it was shown the presence of isosteric point between two bands. Thus, authors concluded that isosteric point is due to transition between mono- and dicarbonyl species. In our research, by variation of partial pressure and adsorption of labeled molecules we were able to reproduce the results of work ⁴²: we observed three bands at CO elevated pressures 2050 , 2030 and 2020 cm^{-1} . Band 2050 cm^{-1} appeared after 2020 cm^{-1} developed in the spectrum.

PtCu3. Adsorption of 10 Torr CO on PtCu3 sample reduced at $220\text{ }^{\circ}\text{C}$ was accompanied by development of two bands at 2139 and 2029 cm^{-1} . The first band was asymmetric and after a short time evacuation time it was clear that it is a composite of two sub-bands at 2149 and 2132 cm^{-1} . Prolonged evacuation at ambient temperature led to disappearance of both subbands. The second band 2029 cm^{-1} was stable under vacuum conditions and shifted to 2042 cm^{-1} with insignificant absolute intensity gain (Figure 7A).

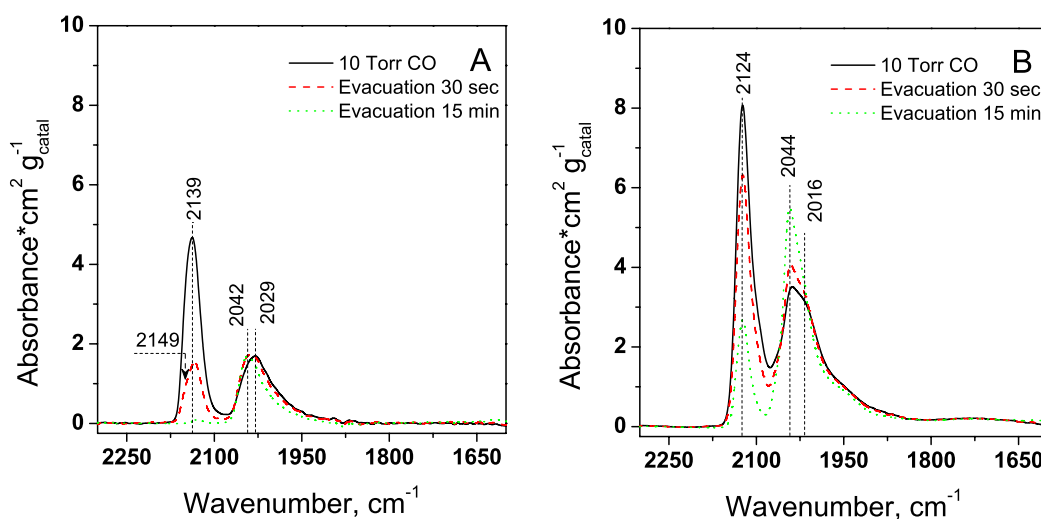


Figure 7. Carbon monoxide adsorption over PtCu3/SiO₂ catalyst reduced at 220 (A) and $500\text{ }^{\circ}\text{C}$ (B): — 10 Torr CO, --- Evacuation 30 sec, Evacuation 15 min.

PtCu₃ reduced at 500 °C showed two bands 15 min of 10 Torr CO adsorption – 2124 and 2038 cm⁻¹ with shoulder at 2016 cm⁻¹. When evacuating the intensity of the band 2124 cm⁻¹ was slowly decreasing with no change in position. After evacuation of CO shoulder 2016 cm⁻¹ also steadily disappeared. In turn the band 2038 cm⁻¹ shifted to 2044 cm⁻¹ and its intensity increased from the gas phase by almost two times in comparison with the same band in excess of CO in a gas phase (Figure 7 B).

PtCu₄. The same set of bands as for the PtCu₃ sample reduced at 220 °C was developing after addition of 10 Torr CO to PtCu₄ sample reduced at 220 °C – bands at 2140 and 2029 cm⁻¹ were observed. The band 2140 cm⁻¹ was formed of two bands 2149 and 2134 cm⁻¹.

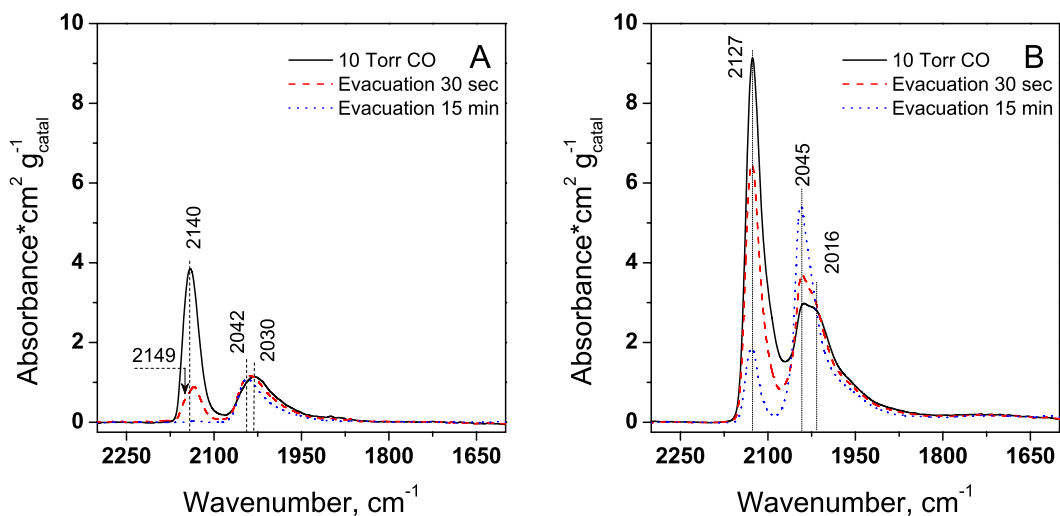


Figure 8. Carbon monoxide adsorption over PtCu₄/SiO₂ catalyst reduced at 220 (A) and 500 °C (B): — 10 Torr CO, --- Evacuation 30 sec, Evacuation 15 min.

Both composite bands were unstable under vacuum conditions and disappeared after evacuation for 15 min. Band 2029 cm⁻¹ did not change in intensity and shifted to 2042 cm⁻¹ after evacuation for 15 min (Figure 8A).

After the PtCu₄ sample was reduced at 500 °C bands at 2127 and 2038 cm⁻¹ appeared in the spectrum of 10 Torr CO adsorbed. The band 2038 cm⁻¹ had a shoulder at 2016 cm⁻¹. Evacuation caused intensity decrease of the 2126 cm⁻¹ band with a blue shift to 2129 cm⁻¹. While the band 2038 cm⁻¹ shifted to 2044 cm⁻¹ and its intensity increased 1.9 times (Figure 8B).

PtCu5. When the PtCu₅ sample reduced at 500 °C was exposed to 10 Torr CO at ambient temperature two bands at 2142 and 2029 cm⁻¹ developed in the spectrum. The first band is a composite of two bands 2149 and 2133 cm⁻¹ and it disappeared after evacuation for 15 min. While the second band was stable to evacuation and shifted to 2040 cm⁻¹ with a decrease in intensity by a factor of 0.9 (Figure 9A).

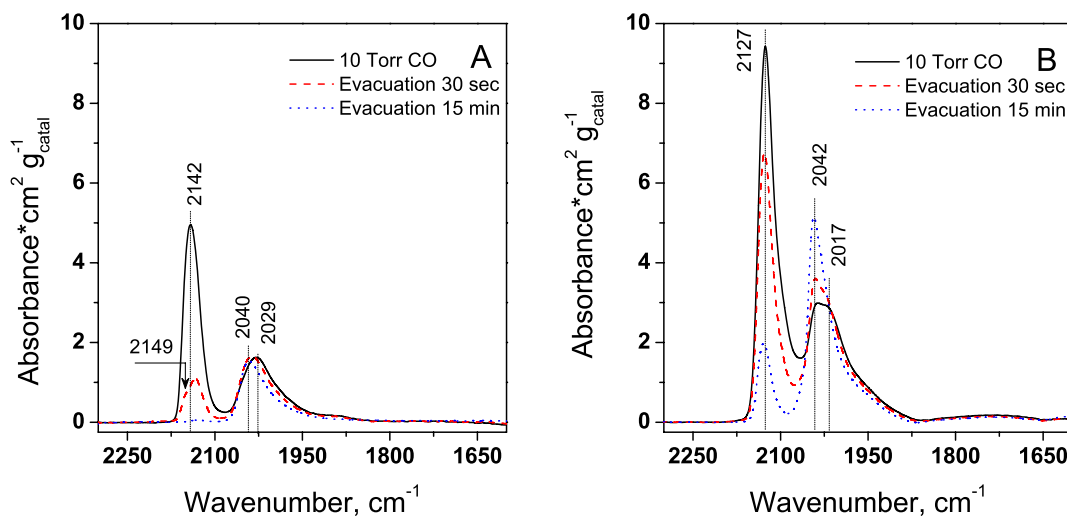


Figure 9. Carbon monoxide adsorption over PtCu₅/SiO₂ catalyst reduced at 220 (A) and 500 °C (B): — 10 Torr CO, --- Evacuation 30 sec, Evacuation 15 min.

After reduction at 500 °C PtCu₅ exposed to 10 Torr CO developed bands at 2127 and 2036 cm⁻¹. The second band had a shoulder at 2017 cm⁻¹. Evacuation for 15 min caused a factor of 6

decrease in the intensity of the first band with a blue shift to 2129 cm^{-1} . The band at 2036 cm^{-1} shifted to 2042 cm^{-1} with an intensity increase of 1.8 times (Figure 9 B).

PtCu6. Reduction of the PtCu6 sample at $220\text{ }^{\circ}\text{C}$ followed by adsorption of 10 Torr CO gave rise to 2143 and 2030 cm^{-1} bands. The first band, as in the previous cases, was a composite of the two subbands at 2149 and 2132 cm^{-1} . When system was evacuated for 15 min at ambient temperature the composite 2143 cm^{-1} band disappeared completely, while the second band 2030 cm^{-1} blue shifted to 2043 cm^{-1} with decrease of intensity 1.1 times (Figure 10A).

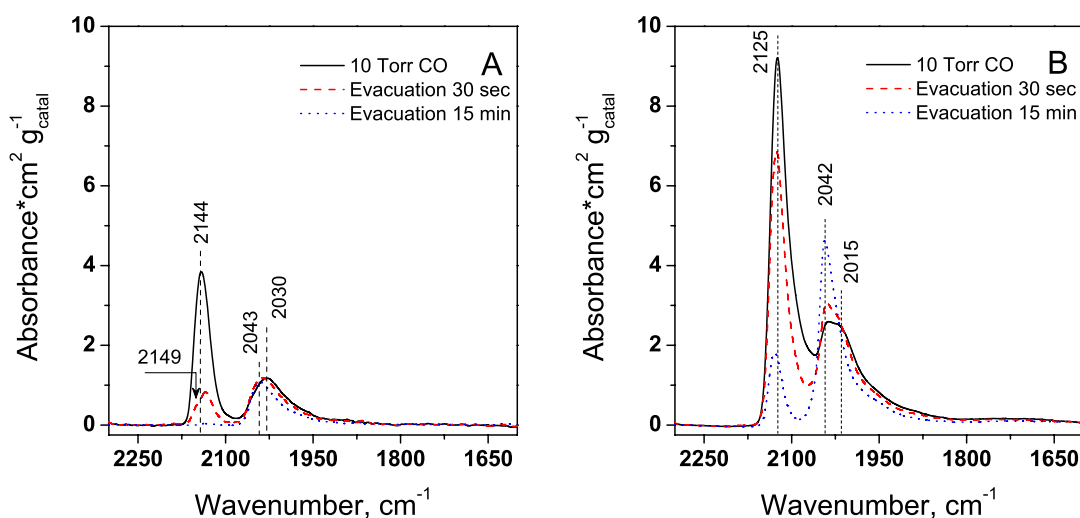


Figure 10. Carbon monoxide adsorption over PtCu6/SiO₂ catalyst reduced at 220 (A) and 500 °C (B): — 10 Torr CO, --- Evacuation 30 sec, Evacuation 15 min.

Reduction of the PtCu6 sample at $500\text{ }^{\circ}\text{C}$ and followed by adsorption of 10 Torr CO resulted in two bands developing at 2125 and 2038 cm^{-1} . The second band had a shoulder at 2015 cm^{-1} . The first band was unstable under vacuum conditions and slowly decreased in intensity with a slight blue shift to 2127 cm^{-1} . The shoulder of the second band disappeared after

prolonged evacuation, while the band by itself gained 1.8 times intensity increase and was blue shifted to 2042 cm^{-1} (Figure 10 B).

Isotopic Dilution Study. The Figure 11 represents the corresponding singleton frequencies of $L^{13}\text{C}^{18}\text{O}/\text{Pt}$ as a function of reduction temperature and Cu/Pt ratio. No pronounced dependence on the Cu/Pt ratio for samples reduced at 220 °C can be revealed. The higher $\nu_s(^{13}\text{C}^{18}\text{O})$ for all bimetallic samples in comparison with monometallic Pt sample is due to the depth reduction: some anion ligands (Cl and O) are still present in the sample reduced at 220 °C and Cu containing samples are more difficult to reduce.

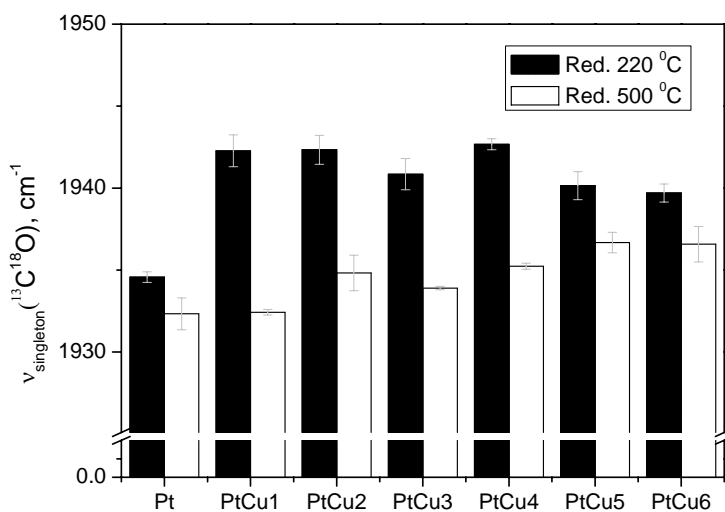


Figure 11. Singleton frequencies for samples with varying Cu/Pt ratio reduced at 220 (solid back bar) or at 500 °C (empty bar).

Some increase of $\nu_s(^{13}\text{C}^{18}\text{O})$ with increase of the Cu/Pt ratio for samples reduced at 500 °C is observed. This effect is especially clear for Pt and PtCu6 samples (Figure 11). The overall increase of $\nu_s(^{13}\text{C}^{18}\text{O})$ assumes the decrease of back donation from Pt(d) orbitals to $2\pi^*$ -orbital of CO.

Finally, Figure 12 introduces the calculated dipole-dipole shifts for $^{13}\text{C}^{18}\text{O}$ adsorbed on Pt ensembles. An obvious decrease in the dipole-dipole coupling is observed for samples with high Cu/Pt content. The reduction at high temperature leads to significant increase of dipole-dipole interaction for samples with fixed Cu/Pt ratio. For sample reduced at 220 °C with Cu/Pt ratio 2 and higher the dipole-dipole coupling was essentially zero. While all samples independent of Cu/Pt ratio and reduced at 500 °C showed significant dipole-dipole coupling shifts. For the Pt, PtCu1, and PtCu2 samples reduced at 500 °C negative slope of 0.5 for dipole-dipole coupling is observed. For the sample with higher Cu/Pt ratio deviation from linear law is clear.

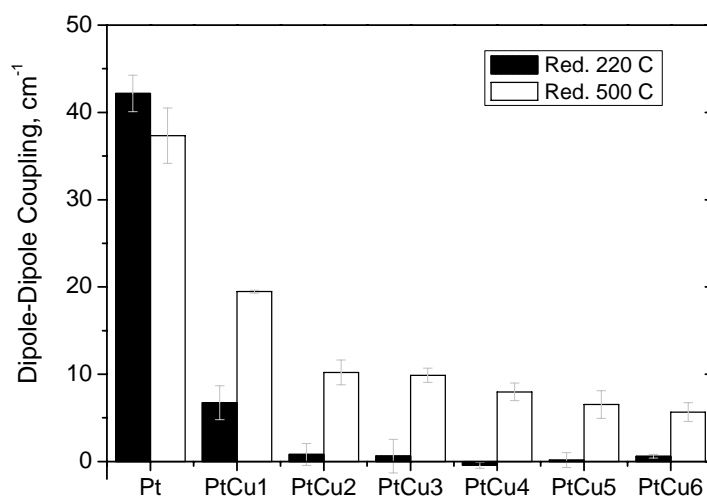


Figure 12. Calculated dipole-dipole coupling for samples with varying Cu/Pt ratio reduced at 220 (solid black bar) or at 500 °C (empty bar).

3.3.4 Kinetics Study

When the reaction between H_2 and 1,2-DCE was catalyzed by Pt/SiO₂ reduced at 220 °C (Figure 13A) or at 500 °C (Figure 13B), the steady-state C₂H₆ selectivity was 90-93% (Table 2). Slight change in selectivity was observed during the time of reaction. The only other product

formed was C_2H_5Cl . Initially, the conversion was $\sim 10-20\%$, and then it decreased to 2-4% during the time on stream.

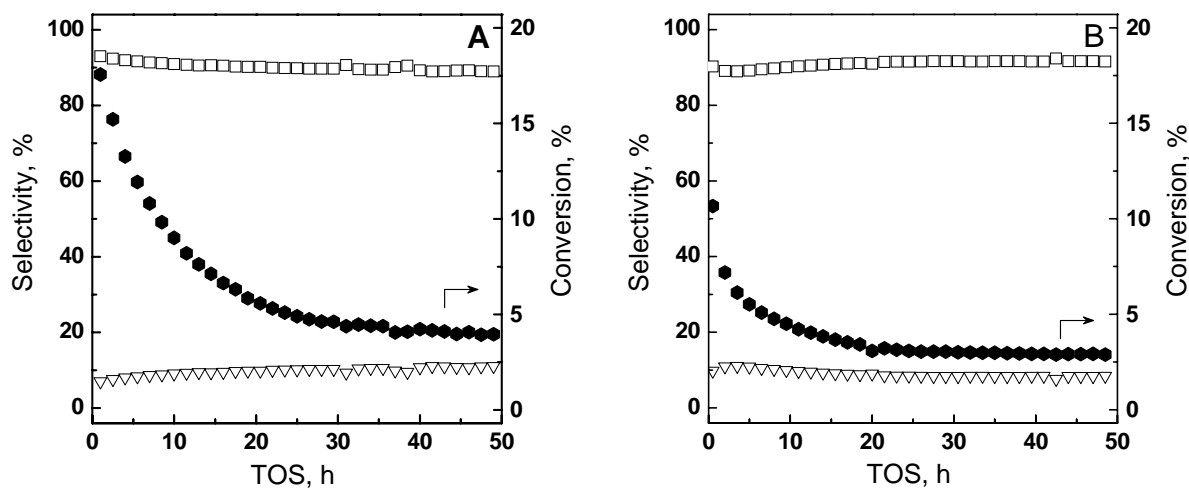


Figure 13. On stream performance for Pt/SiO_2 catalyst reduced at 220 (A) and 500 °C (B): \square - Ethane, ∇ - Monochloroethane, \bullet - Conversion

A monometallic Cu/SiO_2 sample reduced at 220 °C showed 100% selectivity toward C_2H_4 and extremely low activity in comparison with Pt/SiO_2 : the conversion of Cu/SiO_2 was 0.008% at the beginning of reaction. The conversion was increasing continuously and reached 0.016% after 50 h time on stream (Figure 14 A). The Cu/SiO_2 sample reduced at 500 °C was still 100% selective toward C_2H_4 (Figure 14B), but had higher initial activity:

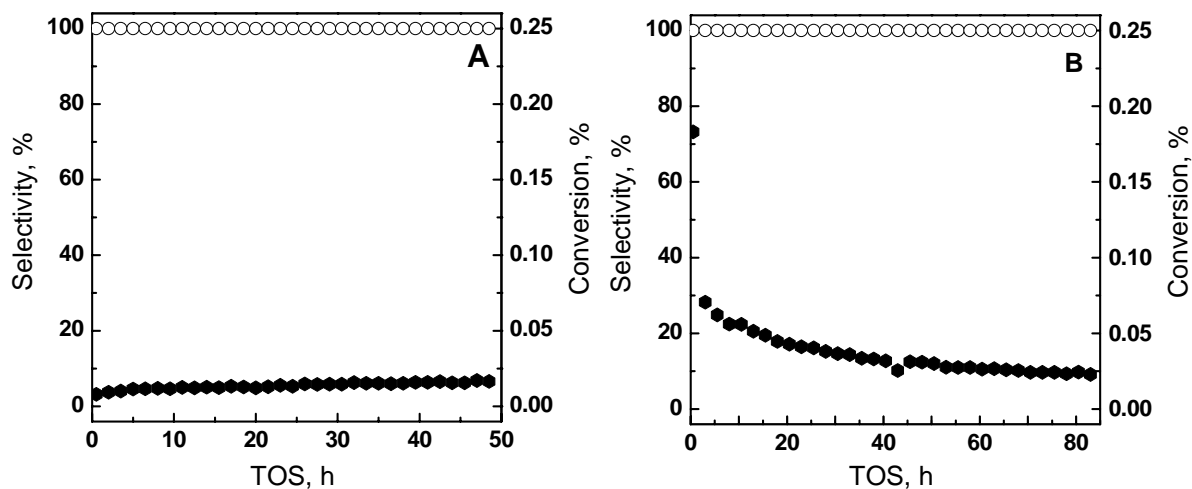


Figure 14. On stream performance for the Cu/SiO₂ catalyst reduced at 220 (A) and 500 °C (B): ○ -Ethylene, ● – Conversion

the initial conversion was 0.18% and decreased abruptly during the first 3 h to 0.07%. The following decrease of activity was more continuous; after 80 h on stream the conversion was equal to 0.025%.

Table 2. Initial/final kinetics performance* of PtCu catalysts subjected to different pretreatments.

	220 °C			500 °C		
	C ₂ H ₄	C ₂ H ₆	C ₂ H ₅ Cl	C ₂ H ₄	C ₂ H ₆	C ₂ H ₅ Cl
Pt	0/0	93/89	7/11	0/0	90/92	10/8
PtCu1	54/55	46/45	0/0	0/3	95/93	5/4
PtCu2	89/77	11/23	0/0	6/42	94/58	0/0
PtCu3	98/95	2/5	0/0	20/85	80/15	0/0
PtCu4	99/96	1/4	0/0	15/98	85/2	0/0
PtCu5	100/95	0/5	0/0	38/97	62/3	0/0
PtCu6	100/96	0/4	0/0	85/97	15/3	0/0
Cu	100/100	0/0	0/0	100/100	0/0	0/0

* Final – at 40 h on stream. Reaction conditions: 7000 ppm 1,2-C₂H₄Cl₂: 35000 ppm H₂, balance He, 41 cc min⁻¹, 200 °C.

The kinetics performance of the bimetallic samples with varying Cu/Pt ratios and reduced at either 220 or 500 °C was different from the behavior observed for the monometallic catalysts. They were as active as monometallic Pt sample, but had higher selectivity toward C₂H₄.

Reducing the PtCu1 at 220 °C resulted in the formation of C₂H₄ from 1,2-DCE and H₂ (Table 2). The initial selectivity toward C₂H₄ for the PtCu1 catalyst was 54%, and the initial conversion was 1.7%. After 40 h time on stream, the selectivity of 55% was obtained for PtCu1 reduced at 220 °C catalyst and the conversion decreased to 1.6% (Figure 15 A).

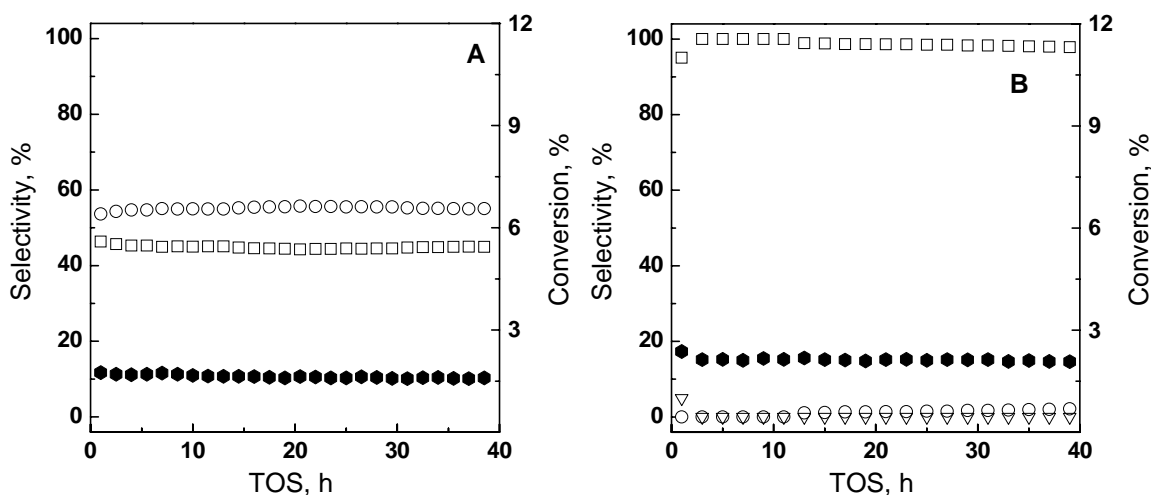


Figure 15. On stream performance for the PtCu1/SiO₂ catalyst reduced at 220 (A) and 500 °C (B): ○ -Ethylene, □ - Ethane, ▽ - Monochloroethane, ● - Conversion

Reducing the PtCu1 at 500 °C resulted in C₂H₆ as the major product rather than C₂H₄ (Figure 15B). For the PtCu1 catalyst the initial selectivity toward C₂H₆ was 95% and the initial conversion was 2.4%. There was also 5% of MCE formed. After first 2h MCE disappeared from reaction products and for next 8 h the C₂H₆ was the only product. But after 10 h on stream traces of C₂H₄ appeared along with C₂H₆. After 50 h on stream the selectivity toward C₂H₄ increased to

2.7%. During the whole run conversion was decreasing slowly: after 50 h on stream conversion reached 2.0%. The PtCu1 catalyst reduced at 500 °C was the only bimetallic catalyst that formed MCE.

The PtCu2 catalysts reduced at 220 °C showed higher selectivity toward C₂H₄ in comparison with the PtCu1 sample reduced at the same temperature (Figure 16 A). For the PtCu2 sample reduced at 220 °C the initial C₂H₄ selectivity was 89% at a conversion level of 1.9%. The only other product was C₂H₆. The selectivity decreased the entire reaction time: after 65 h time on stream the selectivity toward C₂H₄ decreased to 77% at a conversion of 1.6%.

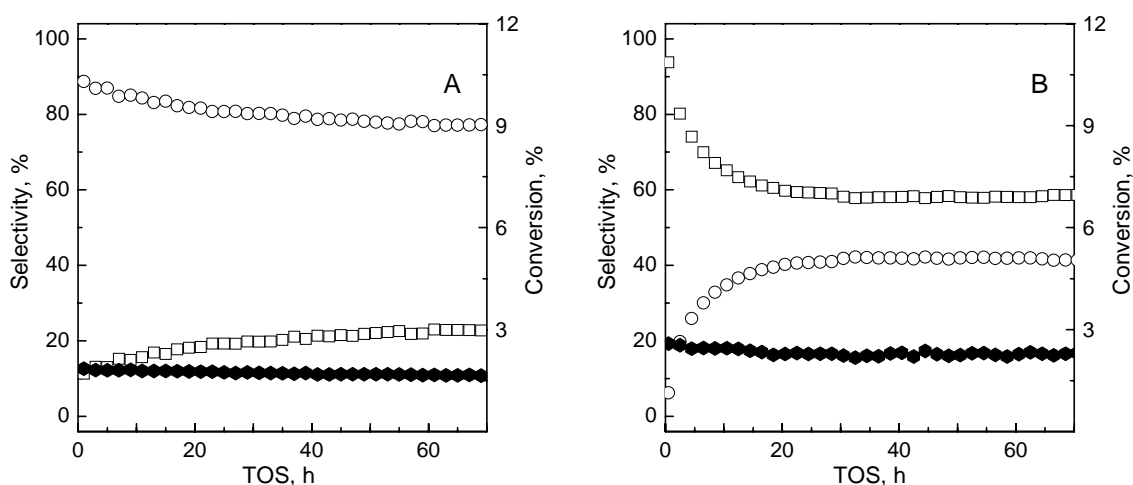


Figure 16. On stream performance for PtCu₂/SiO₂ catalyst reduced at 220 (A) and 500 °C (B): ○ - Ethylene, □ - Ethane, ● - Conversion

When the PtCu₂ sample was reduced at 500 °C, the selectivity toward C₂H₄ was significantly lower than for the same sample reduced at 220 °C. The PtCu₂ sample had an initial selectivity toward C₂H₄ of 7% at a conversion of 2.6%. With time on stream the selectivity toward C₂H₄ steadily increased. It reached 40% after 20 h while conversion decreased by 0.3%.

After 20 h of TOS, the selectivity and conversion stayed at the same level up to the end of the reaction at 70 h (Figure 16 B).

The PtCu₃ sample reduced at 220 °C had an initial selectivity toward C₂H₄ of 100% at a conversion of 2.5%. After 20 h the selectivity decreased to 95% and the conversion for the PtCu₃ decreased to 2.4%. The rest of the run the selectivity and conversion stayed at the same level (Figure 17 A).

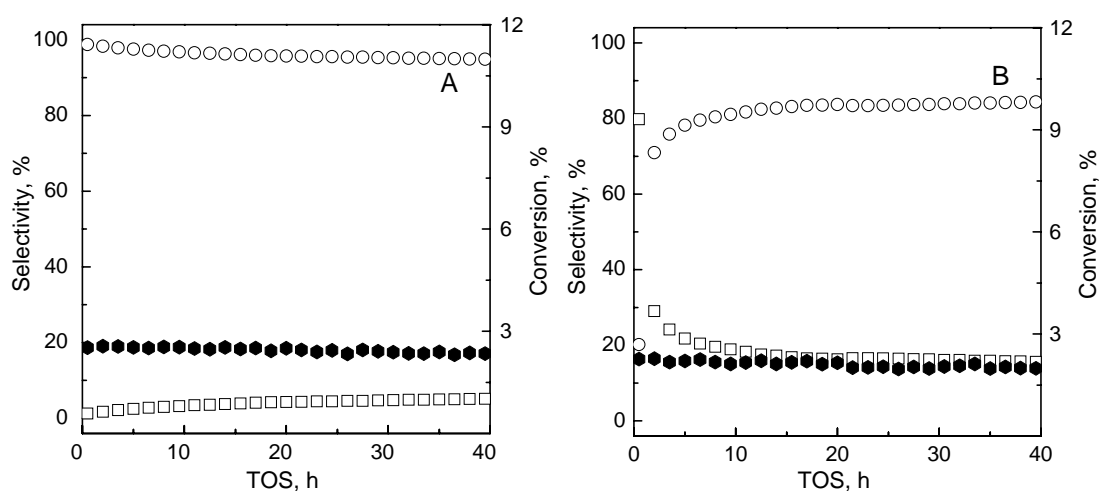


Figure 17. On stream performance for PtCu₃/SiO₂ catalyst reduced at 220 (A) and 500 °C (B): ○ -Ethylene, □ - Ethane, ● – Conversion

After reduction of the PtCu₃ sample at 500 °C the selectivity toward C₂H₄ was lower in comparison with same samples reduce at 220 °C. Initially the PtCu₃ was 20% selective toward C₂H₄ at a conversion of 2.3%. After 10 h, a steady-state selectivity of 84% was reached. The sample slowly deactivated, the conversion was 2.0% for the PtCu₃ after 40 h on stream (Figure 17 B).

When the PtCu₄ catalyst reduced at 220 °C was tested in the reaction of hydrogen assisted chlorine elimination, the initial selectivity toward C₂H₄ was 99% at a conversion of 2.1%. After 20 h on stream the selectivity toward C₂H₄ was 96% at a 2.0% conversion (Figure 18 A). In the following time on stream selectivity did not change, though conversion slowly decreased and after 40 h it was 1.9%.

However, when the PtCu₄ catalyst was reduced at 500 °C, the initial selectivity toward C₂H₄ was only 15% at a conversion of 2.9% (Figure 18 B). After 15 h on stream the selectivity reached 97% and the conversion decreased to 1.5%. After 30 h the selectivity was 98%, which is exactly the same level as for the PtCu₄ sample reduced at 220 °C.

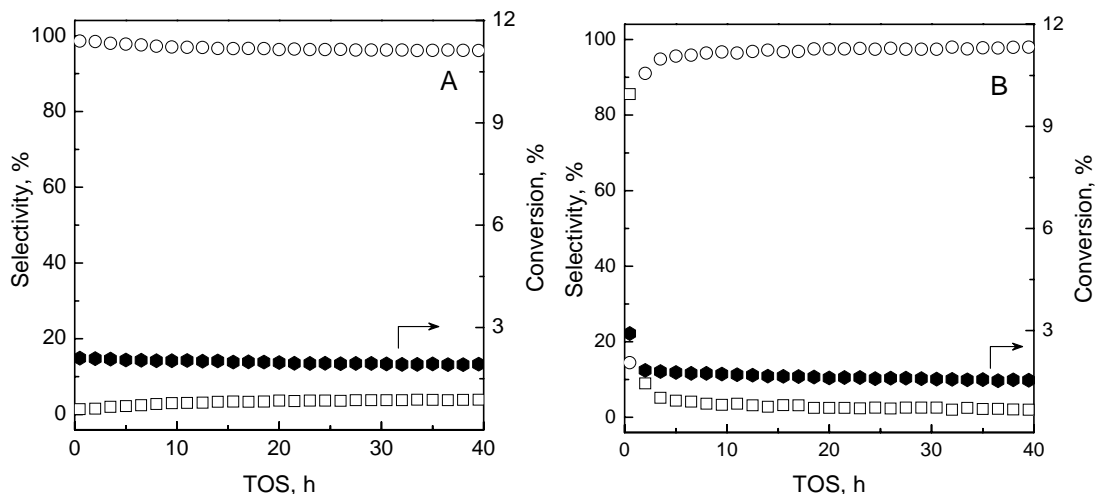


Figure 18. On stream performance for PtCu₄/SiO₂ catalyst reduced at 220 (A) and 500 °C (B): ○ -Ethylene, □ - Ethane, ● - Conversion

The PtCu₅ sample reduced at 220 °C had a selectivity of 100% toward C₂H₄ at a conversion of 2.6%. During the first 10 h the selectivity decreased to 95% and the conversion

slightly increased to 3.1%. The next 30 h on stream were characterized by the same conversion and selectivity levels (Figure 19 A).

Reduction of PtCu5 sample at 500 °C brought out low initial selectivity toward C₂H₄ (Figure 19B). The selectivity at the beginning of reaction was 38% at a conversion of 1.7%. The selectivity changed impetuously and it reached 94% after 10 h on stream. While during the same time the conversion dropped to 1.6%. The rest of the run was denoted only by slight increase of conversion to 96% with no significant change in selectivity.

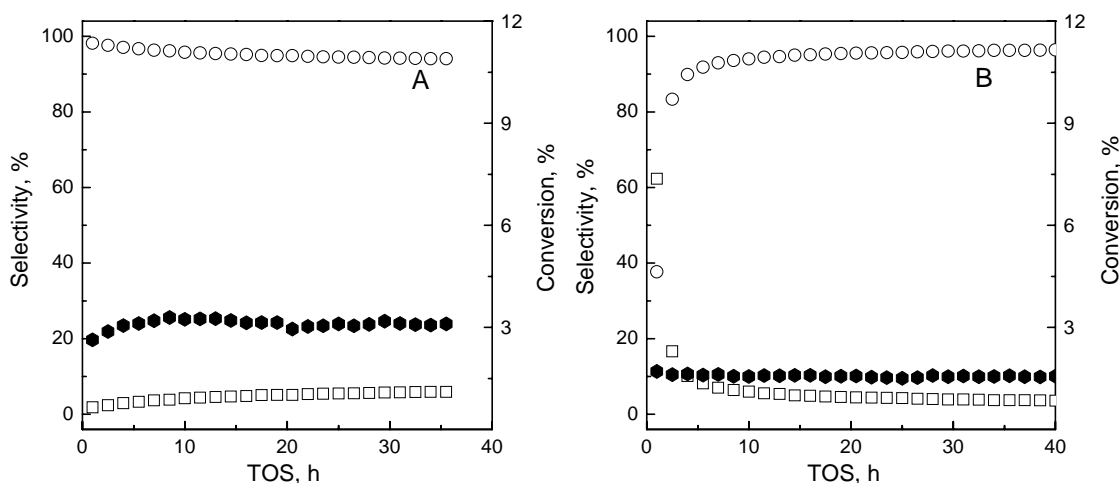


Figure 19. On stream performance for PtCu5/SiO₂ catalyst reduced at 220 (A) and 500 °C (B): ○ -Ethylene, □ - Ethane, ● – Conversion

The catalyst with a Cu/Pt ratio of 6 and reduced at 220 °C showed an initial selectivity toward C₂H₄ of 100% at a conversion of 1.2% (Figure 20A). In 12 h the selectivity decreased to 96%, while the conversion increased to 2.5%. In the following time on stream selectivity did not change, though conversion steadily decreased and became equal to 2.1% after 70 h on stream. The PtCu6 catalyst reduced at 500 °C formed C₂H₄ with initial selectivity of 85% at a conversion

of 1.7%. After 10 h on stream selectivity reached its steady state value of 97% and did not change in the following 40 h. In turn, conversion slowly decreased through whole run and reached 1.5% after 50 h on stream (Figure 20B).

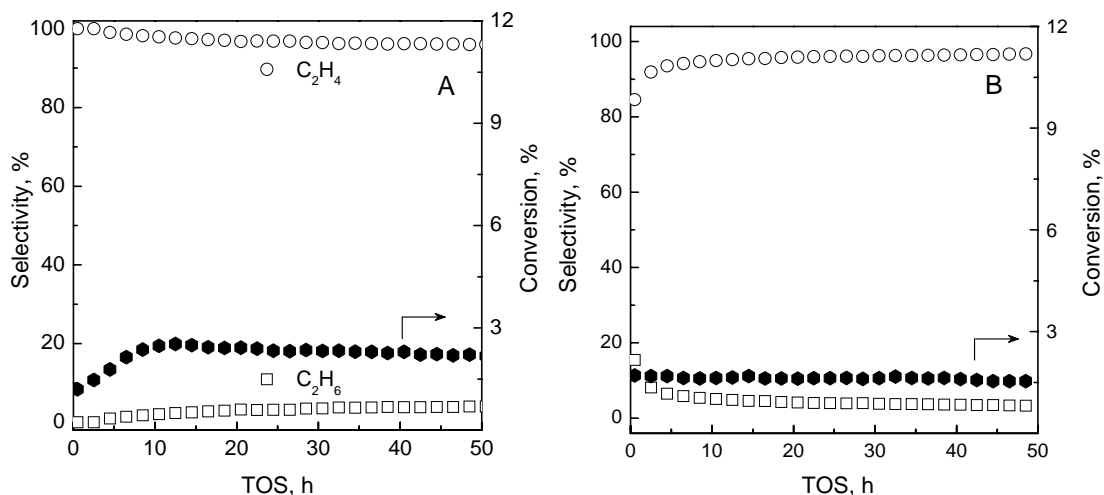


Figure 20. On stream performance for PtCu6/SiO₂ catalyst reduced at 220 (A) and 500 °C (B): ○ -Ethylene, □ - Ethane, ● - Conversion

Summarize here the general trends that were observed during the kinetics study for the Pt-Cu samples with different Cu/Pt ratio. Analysis of the catalytic activity showed that steady-state activity for a catalyst reduced either at 220 or 500 °C was roughly the same (Figure 21). The catalytic activity with respect to mass and Pt loading of the catalyst drops ~2.5 times for the Pt and PtCu1 samples. For all bimetallic catalyst independent of Cu/Pt ratio, the specific catalytic activity with respect to Pt loading and mass of the catalyst stayed at the same level (Figure 21 I and II). While specific catalytic activity with respect to Cu loading dropped with an increase of the Cu/Pt ratio (Figure 21 III). The well documented increase in selectivity toward C₂H₄ was

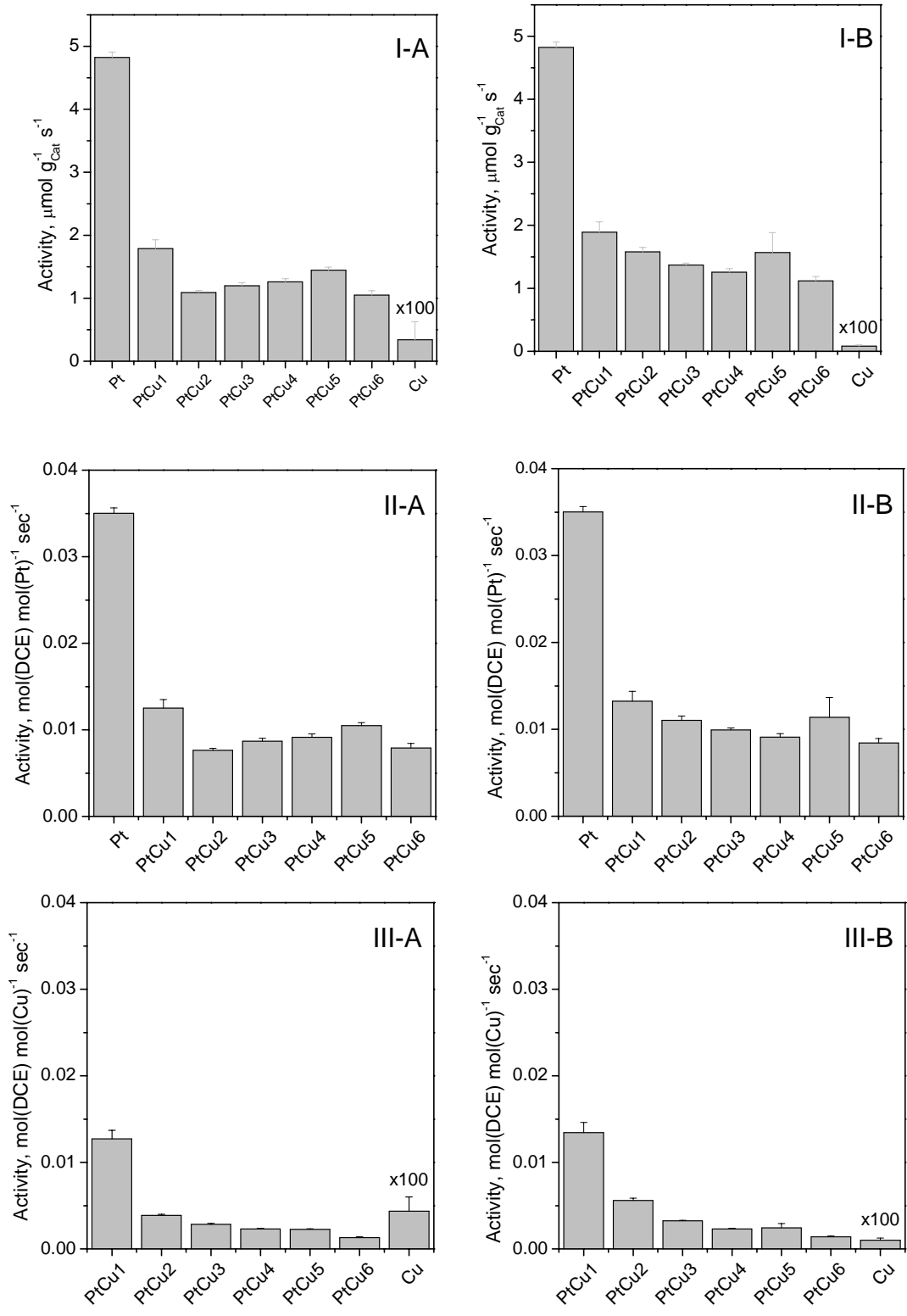


Figure 21. Specific activities at steady-state conditions for catalysts with different Cu/Pt ratio reduced at 220 (A) and 500 °C (B): I. Catalyst weight II. Pt loading III. Cu loading

when the ratio Cu/Pt was increasing^{15, 18, 26, 32}. And finally, to best of our knowledge, there is no publication that states the significant drop of initial selectivity toward C₂H₄ in 1,2-DCE hydrogen-assisted dechlorination reaction as function of reduction temperature.

3.4 DISCUSSION

The Pt and Cu form continuous series of solutions independent of relative content with and only a few ordered structures are known of PtCu₃, PtCu, and Pt₃Cu^{43, 44}. The free surface energy of Pt ($\gamma_{vs}=2,20 \text{ kJ m}^{-2}$) exceeds that for Cu ($\gamma_{vs}=1,57 \text{ kJ m}^{-2}$)⁴⁵. Besides, the PtCu alloy formation is a slightly exothermic process $\sim 10 \text{ kJ mol}^{-1}$ ⁴⁶. The differences in surface energy and exothermicity of alloy formation favor growth of Cu islands in monolayer first (2D-growth), and only then formation of 3D structures on the surface of Pt particles^{46, 47}.

The experimental data provides strong evidence that the surface Pt moieties are enriched with Cu. According to volumetric adsorption analysis the volume of adsorbed CO was essentially zero for PtCu1 and samples with higher Cu/Pt ratio reduced at 220 °C (Figure 3). FTIR data of CO adsorbed support the assumption about enrichment of Pt with Cu. One evidence is the absence of multibound form of CO ($1750\text{-}1860 \text{ cm}^{-1}$) adsorbed on Pt for PtCu1 sample reduced at 220 °C (Figure 5A). Moreover, the integral intensity of the linear form of ¹²CO adsorbed on Pt in the PtCu1 sample is 26 times less than for monometallic Pt sample reduced at 220 °C (Figure 4A and Figure 5A). Thus, the dilution of Pt with Cu drastically reduced the number of exposed Pt atoms.

The formation of bulk alloys for catalysts prepared from chlorides and reduced at 220 °C is rather questionable⁴⁴. The most probable outcome of the 220 °C reduction step is a formation of Pt particles covered with Cu (“eggshell” structure). To explain the mechanism of surface alloy formation, consider first what surface species we have after consecutive catalyst pretreatment steps.

The TPD data provide evidence for the formation of Pt and Cu oxychlorides formation after the drying step. In turn, from TPR data it might be concluded we have mixed Pt-Cu oxychloride structures. After H₂ is introduced into the reaction volume at 130 °C we have reduction of Pt chlorides with formation of metallic Pt⁰ (with some bulk bound chlorine left). The metallic Pt provides a center for H₂ activation and hydrogen spillover reduces neighboring Cu oxychloride moieties, assuming that some of the Cu oxychlorides species are mobile. It was shown for Al₂O₃ and SiO₂ that CuCl is mobile at 233 °C²³ and it is reasonable, given that melting point of CuCl is only 430 °C^{48, 49}. Migration of CuCl to Pt particle is accompanied by HCl release and migration of Cu atoms to the surface of Pt particles. Once formation of the first Cu layer is close to the end, the second layer of Cu starts to grow. Complete blockage of Pt by Cu is not favorable, because H forms a stronger bond with Pt⁵⁰⁻⁵² with than with Cu^{53, 54}. Thus, at the end of reduction at 220 °C we have bimetallic Pt-Cu particles, the surfaces of which are enriched in Cu. Both chemisorption and FTIR data supports this mechanism for the formation of bimetallic particles: i. The integral intensity of LCO/Pt for samples reduced at 220 °C stays roughly the same for all bimetallic samples with different Cu/Pt ratio – which means close dispersion of Pt for all bimetallic samples (remember that the Pt loading is fixed); ii. The integral intensity of CO/Cu also stays at the same level, independent of the Cu/Pt ratio (possible only for fixed Cu dispersion, given that we vary the Cu loading); iii. Evacuation of CO from gas phase

causes noticeable blue-shift of *LCO*/Pt, providing the evidence of strong donation of electron density to $2\pi^*$ -orbital of *LCO*/Pt orbital from 5σ -orbital of CO/Cu.

Reduction at 500 °C leads to reconstruction of the surface of bimetallic particles. By analysing the chemisorption data it is easy to notice significant increase in the volume of CO adsorbed for samples reduced at 500 °C (Figure 3). Surface reconstruction is also supported by increase of intensity of the band of *LCO*/Pt (Table 1) for samples reduced at 500 °C in comparison with samples reduced at 220 °C as a result of exposed Pt atoms increase. At the same time strong intensity-redistribution⁵⁵ for samples reduced at 500 °C evidences formation of extended surface Pt-Cu. Analysis of absolute and integral intensities of chemisorbed *LCO*/Pt for samples reduced at 500 °C tells us about the slight decrease of exposed Pt atoms with increase of Cu/Pt ratio. After reduction at 500 °C the exposition of Pt atoms is realized by segregation of Cu from the surface of Pt particles. The increase of intensity of CO/Cu at excess of CO on a gas phase for samples reduced at 500 °C does not contradict to Cu segregation phenomena owing to the intensity-redistribution effect⁵⁵ and stabilization of CO over Cu atoms at the surface of Pt. Thus, reconstruction of Pt-Cu bimetallic particles is accompanied by segregation of Cu and baring the Pt surface with partial embedment of Cu atoms into the surface of Pt particles. The forces that lead to increase of concentration of surface Pt atoms are segregation of Cu⁴⁵, exothermicity of the Pt-Cu alloy formation⁴⁶, and strong interaction of Pt with H₂⁵⁰⁻⁵⁴.

An analysis of electronic modification (ligand effect) by comparing the ¹³C¹⁸O singleton frequencies for samples with different Cu/Pt atomic ratios tells us that electronic modification of Pt with Cu for samples reduced at 220 °C is rather obscure (Figure 11). The singleton frequency of ¹³C¹⁸O on the Pt samples reduced either at 220 or 500 °C is of the same range and differs by 2 cm⁻¹ providing more evidence that the Pt is almost completely reduced even at 220 °C, bulk

chlorine may input into higher singleton frequencies for monometallic Pt samples reduced at different temperature. For all bimetallic samples reduced at 220 °C the singleton frequency shows no pronounced tendency to change with variation of the Cu/Pt ratio. Reduction at 500 °C leads to a decrease in the singleton frequency of $L^{13}C^{18}O/Pt$ for samples with given Cu/Pt ratio, which is probably connected to removal of residual oxygen and chlorine anions.

The singleton frequency of $L^{13}C^{18}O/Pt$ for samples reduced at 500 °C shows a tendency to increase with increase of Cu content assuming slight donation of electron from Pt to Cu. Here we have apparent contradiction to work ⁴⁰, where author reported a slight negative charge over Pt atoms that form adsorption centers for Cu atoms. This contradiction can be explained by the overall decrease of CO adsorption over catalyst sample (Figure 3), particularly due to the decrease of exposed Pt atoms and as result, a decrease of electron density on bimetallic particles (Table 1). On the other hand, one can not exclude the possibility that some anions (Cl or O) remain, even after reduction at 500 °C. The presence of anions will reduce the electron density at Pt atoms.

The analysis of dipole-dipole of $L(CO)/Pt$ interaction by modified isotopic dilution method shows strong dilution effect of Pt with Cu (Figure 12). This effect was described in previous works ^{33-35, 56} for similar bimetallic systems. For the Cu/Pt sample with a ratio of 1

the dipole-dipole coupling was decreased by a factor of eight compared with monometallic Pt sample. And, as soon as, dipole-dipole coupling connected to the size of Pt ensembles, the decrease of Pt islands is another direct evidence of Cu concentration on the surface of Pt particles. The PtCu₂ sample and sample with higher Cu/Pt ratio reduced at 220 °C show essentially zero dipole-dipole coupling. This means that for samples with high loading of Cu the size of Pt islands is negligible in comparison with Pt monometallic samples. We report here that

not only the Cu/Pt ratio, but also the pretreatment temperature can influence the dipole-dipole coupling magnitude. From Figure 19 one can conclude that reduction at 500 °C causes an increase of size of the Pt islands. This information supports surface reconstruction of Pt-Cu bimetallic particles. The dipole-dipole coupling decreases monotonically as well intensity of $L^{12}\text{CO}/\text{Pt}$ (Table 1) for samples with high Cu/Pt ratio (3 and higher) reduced at 500 °C, assuming that the concentration of Cu left on the surface of Pt particles after segregation correlates with Cu loading less strong than for transition from Pt monometallic to PtCu1 sample.

Analysing the kinetics performance of 1,2-DCE hydrogen assisted dechlorination reaction one can notice the increase of selectivity as Cu/Pt becomes higher and for PtCu3 sample reduced at 220 °C it is already close to 100% as for pure monometallic Cu sample. The increase of selectivity with increase of Cu was discussed in works ^{15, 26}. Slight decrease of selectivity for sample with high Cu content after some time on stream is probably due to some reconstruction equilibration of bimetallic particles the surface with exposition of Pt atoms.

The decrease of selectivity toward C_2H_4 with time on stream contradicts the results of works ^{15, 57} for PtCu carbon supported catalyst, where the increase of selectivity observed with time on stream was rationalized in terms of alloy formation between Pt and Cu. The explanation for decrease of selectivity toward C_2H_4 can be reverse effect – demixing of Pt and Cu supported on silica. That assumes that for silica we have originally Pt and Cu bimetallic particles perfectly formed for reaction of hydrogen-assisted dechlorination selective to olefins. We believe that differences in selectivity performance for PtCu/SiO₂ and PtCu/C catalysts are due to Pt particle formation becoming more enriched with Cu in case of SiO₂ support. One explanation of the higher enrichment of Pt with Cu for the SiO₂ support is chromatographic effect ²¹: differences in the distribution of surface concentration of given metals along the pores of the support due to

diffusion limitation (D), porosity (ρ) and adsorption strength ($C_{\text{sol.}}/C_{\text{surf.}}$). The chromatographic effect can be eliminated by increasing of impregnation time. Thus, for silica that has higher porosity in comparison with carbon this effect can be originally much less. Moreover, the addition of water that was made during the catalyst storage reduces the chromatographic effect for SiO_2 . Authors of work²⁰ showed that first, more “wet”-storage silica supported PtCu catalyst catalysts have lower dispersion and, second, lower adsorption properties with respect to H_2 . The later fact was explained by enrichment of Pt with Cu.

The reconstruction of the bimetallic due to reduction at $500\text{ }^\circ\text{C}$ lead to initial selectivity much less than for samples reduced at $220\text{ }^\circ\text{C}$ (Table 2). Form the fact that with TOS increase selectivity increases for all samples reduced at $500\text{ }^\circ\text{C}$ and reaches almost the same values as for samples reduced at $220\text{ }^\circ\text{C}$ (except PtCu1 sample that after reduction at $500\text{ }^\circ\text{C}$ had a maximum C_2H_4 selectivity of 3%), one might assume that the reconstruction of bimetallic particles is reversible. The difference in final selectivity after prolonged exposure to reaction mixture is only due to Cu that was occluded into the bulk of Pt particles.

If we compare steady-state selectivity toward C_2H_4 for PtCu2 sample reduced at $500\text{ }^\circ\text{C}$ (42%) with PtCu1 reduced at $220\text{ }^\circ\text{C}$ (55%) and also PtCu3 reduced at $500\text{ }^\circ\text{C}$ (85%) with PtCu2 $220\text{ }^\circ\text{C}$ (77%), we might notice that these samples have similar selectivity. While the PtCu1 sample reduced at $500\text{ }^\circ\text{C}$ has 0% initial selectivity and 3% selectivity after 50 h on stream, *i.e.* the PtCu1 sample selectivity performance resembles that for Pt monometallic sample. From this we can deduce that for the PtCu1 sample after reduction at $500\text{ }^\circ\text{C}$ surface Cu atoms diffuse into the bulk of Pt particles and form alloy with the surface enriched in Pt.

With time on stream the selectivity of all catalyst reduced at $500\text{ }^\circ\text{C}$ tends to the selectivity of catalyst reduced at $220\text{ }^\circ\text{C}$, one might conclude that reconstruction of PtCu bimetallic particles

is reversible. The principle that brings the particles back to the “initial” state is the same as in the case of pretreatment reduction procedure. The 1,2-DCE decomposed at the surface of Cu with formation of C_2H_4 and Cu chlorides. The later moieties pose some mobility and travel to the extended Pt particles, where they are reduced to Cu^0 and able to participate in the next C-Cl bond cleavage cycle. The “eggshell” structure, with the Pt in the core, is recovered under reaction conditions.

About constant steady-state activity with respect to the mass of the catalyst and total Pt loading for bimetallic samples (Figure 10-I and II), correlates with the FTIR data that provide roughly constant intensity for LCO/Pt form (Table 1). In turn, the specific activity with respect to Cu steadily decreases with increase of Cu loading (Figure 21 III). The conclusion that can be made – activity of the catalysts primarily depends on the number of exposed Pt atoms. The specific steady-state activity with respect to Cu loading decreases steadily with Cu/Pt ratio increase. The most probable explanation for this phenomenon might be the decrease of Cu dispersion with increased Cu loading is increasing. The “eggshell” model fits this interpretation very well. And the results of FTIR investigation support this interpretation: IR intensity for 10 Torr CO/Cu for samples with different Cu/Pt ratio reduced at 220 °C stays nearly the same 4-5 (Table 1). For samples reduced at 500 °C this statement needs more thorough investigation, because CO/Cu intensity has no direct proportionality with number of CO/Cu centers due to strong “screening effect”⁵⁵. Finally, the match of selectivity and activity performance for bimetallic catalyst tells us that the optimal Cu/Pt ratio for conversion of 1,2-DCE to C_2H_4 is 3: 98% of C_2H_4 formation and minimal loading of Cu.

The correlation between dipole-dipole coupling and initial selectivity performance was found for bimetallic catalyst: the higher the dipole-dipole coupling the lower the selectivity

toward C_2H_4 (see Table 1 and Figure 12). Strong dipole-dipole coupling implies extended Pt ensembles. Thus, the “bigger” is the Pt ensembles the lower selectivity toward C_2H_4 . This fact can be reasonably interpreted considering the mechanism of interaction of 1,2-DCE and C_2H_4 with Pt and Cu, presented at the beginning of discussion section.

3.5 SUMMARY

The kinetics study of 1,2- $C_2H_4Cl_2$ dechlorination and FTIR investigation of CO isotopic molecules adsorption over bimetallic Pt-Cu silica supported catalyst was performed to understand the prime factors that define high selectivity in reaction of hydrogen-assisted dechlorination of 1,2- $C_2H_4Cl_2$ to C_2H_4 . The kinetics study was carried out to track the selectivity and activity changes upon variation of Cu/Pt atomic ratio and reduction temperature in bimetallic catalysts. While, the FTIR investigation were performed to address to alloy formation, ensemble size, and electronic modification effects.

The mechanism of bimetallic particle formation and reconstruction was proposed. Low temperature reduction (220 °C) leads to formation of “eggshell” Pt-Cu structures in which the Cu atoms form the outer multilayer shell around the Pt core. Reduction at elevated temperatures (500 °C) leads to reconstruction of Pt-Cu bimetallic particles: one fraction of the Cu diffuse into the Pt with formation of disordered bulk alloy, while the rest of the Cu segregates into bigger Cu aggregates. The reconstruction process due to reduction at elevated temperatures is partially reversible under dechlorination condition and brings “eggshell” structure back according to the same mechanism as during pretreatment step at low-temperature reduction.

No electronic modification of Pt with Cu can be detected for samples after low-temperature reduction (220 °C): the presence of residual O and Cl masks this effect. After high-temperature reduction (500 °C) slight modification of Pt with Cu is observed: increase of Cu results in decrease of electronic density at Pt atoms. Moreover, the Cu atoms at the surface of PtCu bimetallic particles are able to stabilize CO at room temperature, that is a sign of inter and intra-redistribution of electron density between Pt and Cu.

Kinetics data analysis shows that Pt loading (“dispersion”) defines overall steady-state activity of PtCu silica supported bimetallic catalysts. For fixed Pt loading the increase of Cu loading is changing the selectivity. And finally, the selectivity performance correlates with the size of Pt ensembles: the more extended Pt ensembles favor C₂H₆ formation. This correlation can be rationalized by individual mechanism of interaction of 1,2-DCE with Pt and Cu.

4.0 ENSEMBLE SIZE EFFECT: MODEL CATALYST APPROACH

4.1 INTRODUCTION

In the Section 3.0 we have shown that the dipole-dipole coupling value correlates strongly with the selectivity of the hydrodechlorination reaction. The magnitude of dipole-dipole coupling correlates with the size of Pt ensembles, it was induced that the smaller the size of Pt ensembles the higher selectivity toward C₂H₄.

The dipole-dipole coupling is an indirect evidence of the ensemble size effect. It correlates strongly with the size of the Pt ensembles (Θ_{CO}):

$$v = v_{\text{singleton}} \sqrt{1 + \frac{\Theta_{CO} \alpha_v U}{1 + \Theta_{CO} \alpha_e U}}$$

under the assumption of constant polarization α_v and α_e , and constant surface sum function U (see Appendix A for more details).

To assure oneself and provide the community with the direct evidence on ensemble size effect the model catalyst approach was chosen⁵⁸⁻⁶⁰. Model catalyst has several significant advantages over the conventional supported catalysts. First, being a flat plate of Si(100) with oxidized layer of SiO₂ these catalysts represent ideal systems for controlled support of metals from corresponding salt solutions⁶⁰. Second, these catalysts have no diffusion limitation due to highly exposed surface and almost complete absence of porous structure. That makes them

convenient systems for kinetics testing, though low specific (per mass) activity makes problematic the achievement of significant conversion levels. And finally all active centers usually associated with metallic particles are exposed to the surface making possible characterization with surface probe techniques (XPS, AFM, LEIS, etc.). An experienced experimentalist could easily evaluate the precious advantages of model catalytic systems over conventional catalyst: they allow doing spectroscopic characterization and kinetics essentially on the same particles! That is indeed an important virtue if ones want to establish correlation between kinetics performance and electronic-structural properties.

4.2 EXPERIMENTAL PROCEDURE

4.2.1 Catalysts Preparation[†]

Two catalyst Pt/SiO₂/Si(100) and PtCu1/SiO₂/Si(100) were prepared by spin-coating technique Figure 22. First, the silicon single crystal plate with exposed (100) plane was calcined at 750 °C for 24 h to oxidize the surface of single crystal and produce 50 nm SiO₂ layer with exposed siloxanes groups. On the second stage, calcined Si-wafers were cleaned in a H₂O₂/NH₄OH (3:2) solution at 65 °C, and then the surface was hydroxylated by boiling in distilled water for 30 min.

[†] Catalysts for this study were prepared by graduate student Vladimir Pushkarev

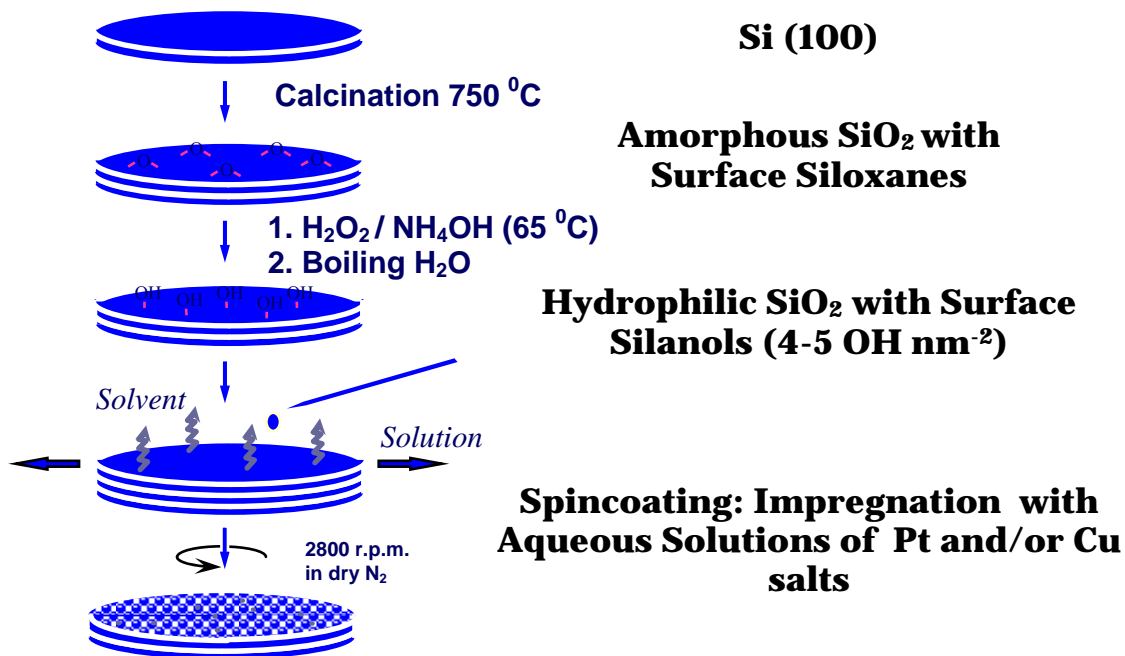


Figure 22. Schematic procedure of spin-coating technique sequencing for preparation of Pt and PtCu₁/SiO₂/Si(100) model catalyst

Subsequently, these model supports were spin-coated in a nitrogen atmosphere at 2800 rpm with an aqueous solution containing H₂PtCl₆ · 6 H₂O (Alfa, 99.9%) and 0.1 N HCl aqueous solution CuCl₂ · 2 H₂O (MCB Manufacturing Chemist, 99.5%), with varying Pt/Cu atomic ratios. The concentrations of the precursor solutions were adjusted to result in a total (Pt + Cu) metal loading of roughly 6 at/nm². After spin-coating the samples were dried in flowing nitrogen at 130 °C for 1.5 h.

4.2.2 XPS Study[‡]

XPS spectra were measured on a VG Escalab 200 MK spectrometer equipped with an aluminum anode (Al K_{α} = 1486.6 eV) operating at 510 W with a background pressure of $2 \cdot 10^{-9}$ mbar and a hemispherical analyzer connected to a five-channel detector. Measurements were carried out with 20 eV pass energy, 0.1 eV step, and 0.1 s dwelling time. Charging was typically around 0.5 eV. Energy correction was performed using the Si 2p peak of SiO₂ at 103.3 eV as a reference. The spectrometer was equipped with a transfer chamber (pressure $5 \cdot 10^{-5}$ mbar) that allows the reduction of the samples under H₂ at elevated temperatures (220 and 500 °C) before the XPS analysis.

4.2.3 AFM Investigation[§]

Atomic force microscopy (AFM) was performed using a Solver P47 base and SMENA head. The preferred tip was a non-contact gold-coated NSG 11 (NT-MDT) with a force constant of 5 N/m and a resonant frequency of 190 kHz. All measurements were performed in the noncontact (tapping) mode at ambient conditions (25 °C in air).

4.2.4 Kinetics Study

Reaction System. The reaction system was essentially similar to that described early (see Section 2.1.1 for details), except that the custom-made sample loop that was significantly increased (from 0.5 up to 5 ml) to improve the FID signal response. That modification was

[‡] XPS data were collected by Vladimir Pushkarev

[§] AFM data were collected by Armando Borgna and Pavel Tokmakov

required due to low conversion levels as a result of the extremely small specific surface area of a studied Me supported on SiO₂/Si(100) wafers.

The amount of the catalyst used in an experiment ranged between 1.5-2.5 g so that the steady-state conversion was in the range 0.005-0.02 %. The catalyst temperature was controlled to ± 1 °C using a temperature controller (CN2011, Omega) connected to a K-type thermocouple (Omega) placed in a quartz pocket that was in direct contact with the catalyst bed. The reaction products were analyzed by on-line GC (HP 5890). The GC was equipped with 3 m 60/80 Porapak Q packed column (Supelco) and flame ionization detector with a detection limit of <0.2 ppm for all chlorocarbons and hydrocarbons involved in this study.

The catalyst pretreatment procedure was absolutely the same as those for the conventional catalyst (Section 3.2.5). To remind reader briefly: first, the sample was dried in He (30 cc min⁻¹, PraxAir, 99.999%) from room temperature to 130 °C at 5 °C min⁻¹, and then it was held at 130 °C for 1.5 h while flowing He (30 cc min⁻¹). Second, the He flow was switched to 10%H₂/Ar (30 cc min⁻¹), and the temperature was increased to 220 at 5 °C min⁻¹. The catalyst sample was held for 2 h while flowing 10%H₂/Ar (30 cc min⁻¹). Third, the temperature was decreased at 5 °C min⁻¹ from either 220 or 500 °C to 200 °C, and 10%H₂/Ar (30 cc min⁻¹) was switched to He (30 cc min⁻¹). Finally, the system was purged for 0.5 h with He at 200 °C, and the reaction was started.

The reaction was conducted at 200 °C and atmospheric pressure as in the case of conventional Pt-Cu bimetallic catalysts. The reaction mixture consisted of 21000 ppm of 1,2 - dichloroethane, 110000 ppm H₂, and the balance He. The total flow-rate was 41 cc min⁻¹. The reaction was run for 40 or more hours until steady-state performance with respect to activity was obtained. For this investigation steady-state selectivity was defined as a change less than 0.002% in 10 h. After the catalyst reduced at 220 °C was tested in reaction of 1,2-dichloroethane

elimination it was purged at reaction temperature (200 °C) with He (30 cc min⁻¹) for 0.5 h and cooled to 30 °C. Then the gas flow was switched to a mixture containing 500 ppm of C₂H₄, 110,000 ppm of H₂, and a balance of He to obtain a total flow of 41 cc min⁻¹ while the reactor temperature was maintained at 30 °C. The conversion of ethylene to ethane was monitored continuously. After the steady-state selectivity distribution was reached, the temperature was increased at 5 °C min⁻¹ to 200 °C, and conversion level was measured again. Finally, after some time on stream 21000 ppm 1,2-DCE was added to reaction mixture keeping the total flow-rate constant by decreasing the He flow. Then, the ethylene conversion was measured. After testing of the sample initially reduced at 220 °C was finished, the sample was reduced at 500 °C and cycle of kinetics testing procedures starting with hydrodechlorination of 1,2-DCE was repeated for each sample. To reproduce results several trials were performed for each Pt/SiO₂/Si(100) and PtCu1/SiO₂/Si(100) samples.

4.3 RESULTS

4.3.1 XPS Study

X-ray Photoelectron Spectroscopy study showed that neither monometallic Pt nor monometallic Cu/SiO₂/Si(100) model catalysts reduced completely after reduction at 220 °C: both Pt 4f_{7/2} (Figure 23) and Cu 2p_{3/2} (Figure 24) bands are shifted toward higher energy values after reduction at 220 °C in comparison with the same sample reduced at 500 °C. Though, Pt samples do not show any significant amount of Cl left after reduction at 220 °C it does not exclude the possibility of having bulk Cl left and actually it is a well known fact for conventional systems²¹. The position 71.6 eV of Pt 4f_{7/2} binding energy is most probably associated with residual anions (Cl and/or O) left after reduction at 220 °C.

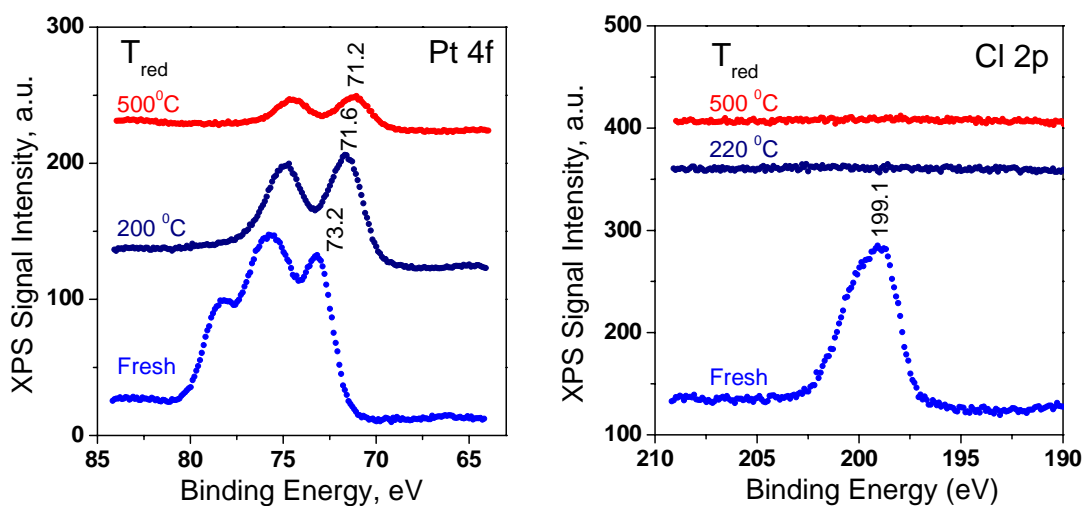


Figure 23. Effect of reduction temperature on reducibility of Pt in Pt/SiO₂/Si(100) model catalyst sample prepared from H₂PtCl₆. “Fresh” – just prepared model catalyst after drying at 130 °C.

While in the case of the Cu/SiO₂/Si(100) model catalyst reduced at 220 °C the presence of residual Cl species is obvious: the band of Cl 2p_{3/2} at 199 eV had still non-zero intensity. Though, following reduction of Cu/SiO₂/Si(100) at 500 °C eliminates band of residual Cl from XPS spectrum completely.

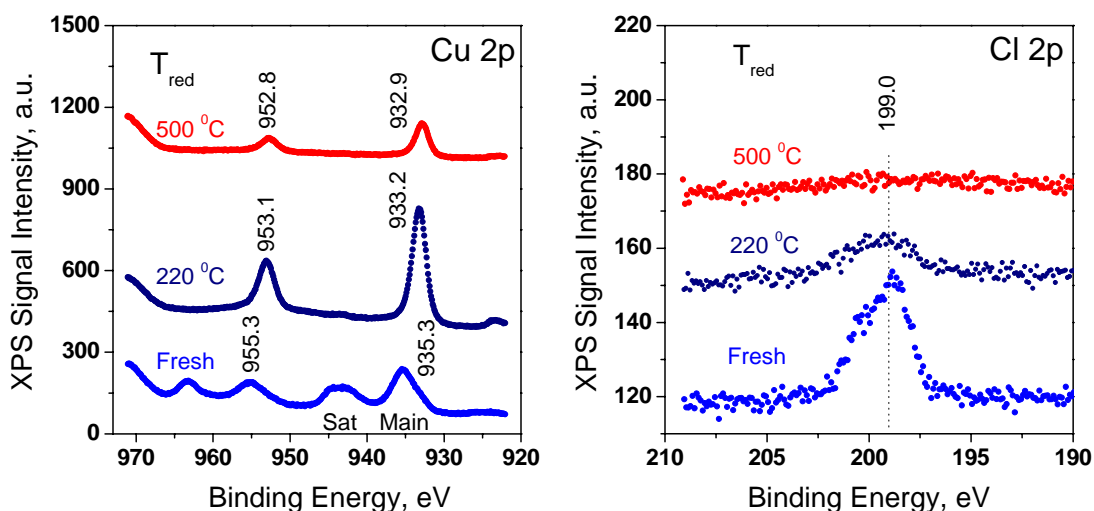


Figure 24. Effect of reduction temperature on reducibility of Cu in Cu/SiO₂/Si(100) model catalyst sample prepared from CuCl₂. “Fresh” – just prepared model catalyst after drying at 130 °C.

The behavior of both Pt and Cu/SiO₂/Si(100) reduced monometallic samples can be easily explained from the standpoint of reactivity of corresponding chlorides toward hydrogen: Pt chlorides are known to be extremely reactive toward H₂ and reduction for them start at temperature of 70-80 °C, while in order to reduce Cu chlorides toward Cu⁰ temperature as high as 280 °C required (see Section 3.2.2).

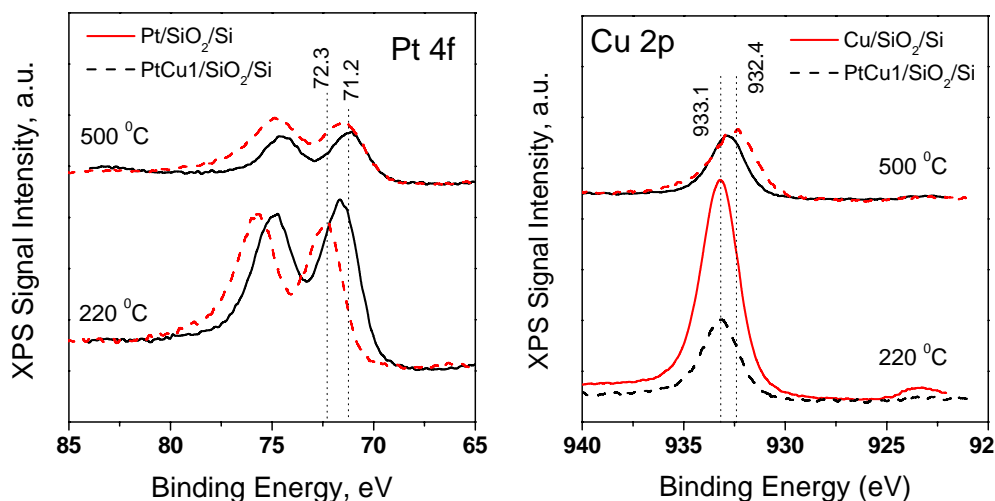


Figure 25. Effect of reduction temperature on reducibility of Pt and Cu in PtCu1/SiO₂/Si(100) model catalyst sample prepared from H₂PtCl₆ and CuCl₂.

The behavior of Pt in the bimetallic PtCu1/SiO₂/Si(100) sample in comparison with monometallic Pt/SiO₂/Si(100) shows that the binding energy of the Pt 4f_{7/2} level is higher than for the bimetallic sample (Figure 25).

Two explanations were proposed to interpret the observed behavior: the presence of residual anions (Cl and O) or/and electronic modification of Pt with Cu and/or Si. The presence of residual anions is the most probable reason of Pt 4f_{7/2} binding energy increase in case of bimetallic samples reduced at 220 °C: no bulk alloy formation was observed for conventional catalyst; residual chlorine and oxygen were observed after reduction at elevated temperatures (Section 3.2.2). In the case of the bimetallic PtCu1/SiO₂/Si(100) model catalyst reduced at 500 °C the shift of the Pt 4f_{7/2} energy toward higher values with band distortion is most probably due to formation of platinum silicides that are characterized by a Pt 4f_{7/2} binding energy of 72.5 eV⁶¹; Pt silicide formation was observed on SiO₂ films supported systems after reduction at 597 °C

⁶². Though, broad structure of Pt 4f_{7/2} band does not exclude the possibility of Pt-Cu alloy formation: expected position for Pt 4f_{7/2} band in Pt-Cu alloy (71.4 eV ⁶³) fell right into the center of observed Pt 4f_{7/2} broad band.

Analysis of the Cu 2p_{3/2} band for Cu/SiO₂/Si(100) and PtCu1/SiO₂/Si(100) allows us to conclude that there was no significant electronic modification of Cu in a bimetallic sample in comparison with monometallic after reduction at 220 °C: the position of the Cu 2p_{3/2} was the same for both samples 933.1 eV (Figure 25). In turn, model Cu/SiO₂/Si(100) and PtCu1/SiO₂/Si(100) catalysts reduced at 500 °C were characterized by a shift of the Cu 2p_{3/2} band toward lower energies. Monometallic Cu/SiO₂/Si(100) sample reduced at 500 °C showed only one band with maximum 932.9 eV (220 °C – 933.1 eV), while bimetallic catalyst showed split-band with maximum at 932.4 and shoulder at 932.9 eV.

The higher energy shift for monometallic and bimetallic model catalysts can easily be explained by presence of residual anions of Cl and O, and shift of Cu 2p_{3/2} to slightly lower energies after reduction of monometallic Cu/SiO₂/Si(100) model catalyst can be explained by removal of Cl and O with complete conversion of copper to Cu⁰ with binding energy of 932.7 eV ^{63, 64}. To explain the presence of 932.4 eV band in the XPS spectrum of the PtCu1/SiO₂/Si(100) model catalyst reduced at 500 °C it is not enough to involve formation of copper silicides (f.g. for η-Cu₃Si the 932.7 eV energy of Cu 2p_{3/2} level was reported ⁶⁴, while Shin et al. ⁶⁵ reported 933.2 eV value for Si/Cu stack annealed at 225 °C). The most probable explanation for 932.4 eV band observation absent in the spectrum of monometallic Cu/SiO₂/Si(100) model catalyst sample is formation of Pt-Cu alloy characterized by 932.3 eV energy ⁶³.

To summarize the results of XPS investigation of model SiO₂/Si(100) catalysts let us mention that complete reduction of either monometallic (Pt and Cu) or bimetallic (Pt-Cu) samples was not observed after hydrogen treatment at 220 °C that is in agreement with data produced for conventional Pt, Cu and PtCu1 silica supported catalysts. Reduction at 500 °C most probably led to partial conversion of metallic Pt and Cu to silicides and formation Pt-Cu alloy (Cu 2p_{3/2} 932.3 eV). Additional evidence is required on behavior of Si 2p_{3/2} band upon reduction temperature variation to prove silicide formation. Besides, in case of bimetallic sample partial electronic modification of Pt with Cu is likely: it is well known that dilution of Pt with Cu leads to only slight electron density transfer from Pt to Cu^{31, 40, 66}. Some authors accept that electronic modification is rather due to intra-atomic charge redistribution between s and d orbitals^{67, 68}. Intra-atomic redistribution of electron density should have non-zero influence on electron binding energy of Pt 4f_{7/2} and Cu 2 p_{3/2}.

4.3.2 AFM Investigation

The objective of AFM investigation was the monitoring of size of Me particles exposed to the surface that reside on the SiO₂ layer. The investigation was carried out in tapping mode right after the reduction step and purging with He. This procedure required transfer of the samples from pretreatment camera to AFM installment with exposure to air at ambient temperature.

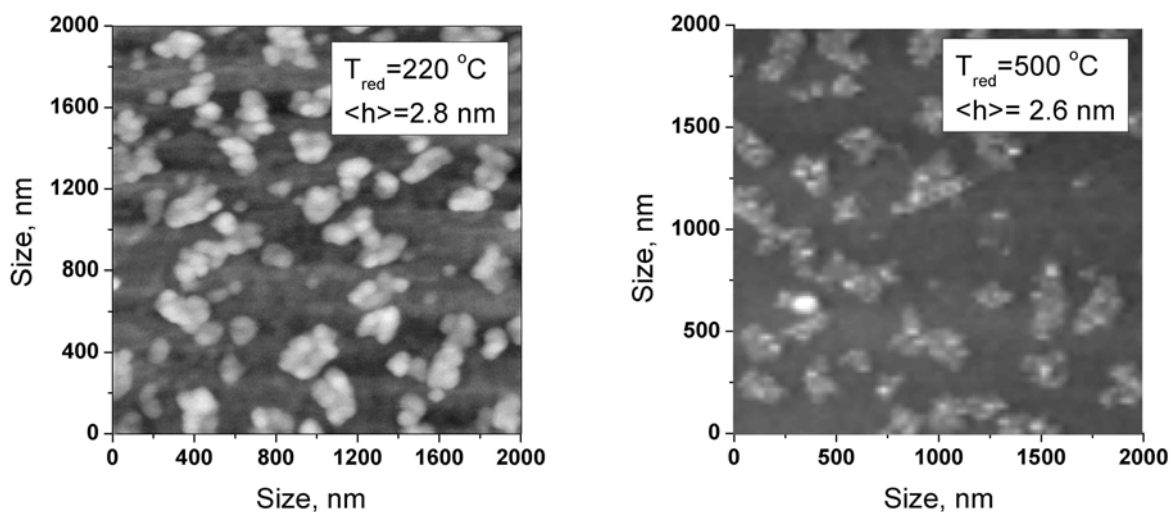


Figure 26. Effect of reduction temperature on average size of Pt particles in monometallic Pt/SiO₂/Si(100) model catalyst. Results of AFM Imaging.

AFM imaging of the surface of Pt/SiO₂/Si(100) model catalyst reduced at 220 °C showed extended Pt particles with lateral dimension up to 500 nm and average of 210 nm (778 Pt layers) (Figure 26). Analysis of height size distribution of Pt particles allowed concluding that average height of Pt particles was on the order of 2.8 nm (10 Pt layers). The following reduction at 500 °C resulted in increase of lateral size of Pt particles with average value of 390 nm due to segregation process (1444 Pt layers). A decrease of the average height of Pt particles was also observed: after reduction at 500 °C the average height of Pt particles was on the order of 2.6 nm (9 Pt layers). Visual observation allows us to conclude significant decrease in metal particles number. That information is not enough to make irrefutable conclusion about decrease of Pt atoms to diffusion into silica layer with formation of platinum silicides. Statistics need to be accumulated from extended area on decrease of number of metallic particles.

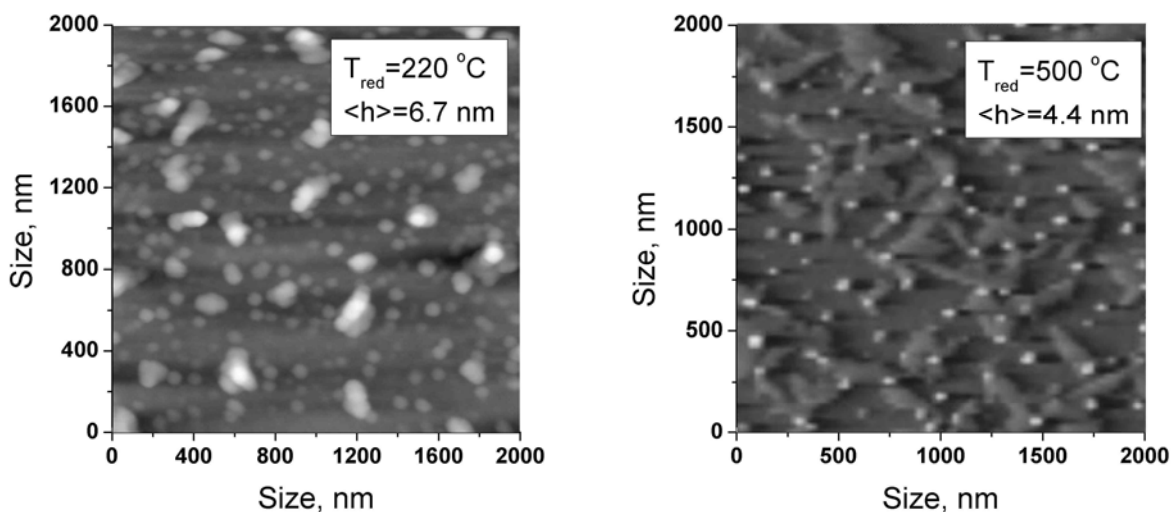


Figure 27. Effect of reduction temperature on average size of Pt particles in monometallic PtCu1/SiO₂/Si(100) model catalyst. Results of AFM Imaging.

Studying of the PtCu1/SiO₂/Si(100) model catalyst reduced at 220 °C with AFM imaging technique showed much smaller metal particles with average lateral dimension of 80 nm (296 Pt layers), while the average height was 6.7 nm (25 Pt layers) (Figure 27). After reduction at 500 °C visual observation of metallic particles on the surface of model catalyst allows us to infer significant decrease of the number of particles with average lateral extension of 50 nm (185 Pt layers). The estimation of average height of metal particles for PtCu1/SiO₂/Si(100) model catalyst after reduction at 500 °C gives value of 4.4 nm (16 Pt layers). Though, as in the case of Pt/SiO₂/Si(100) catalyst this information is not enough to conclude decrease of total amount of Pt and Cu on the surface of SiO₂/Si(100) crystal due to diffusion into the SiO₂ layer and formation of silicides. More thorough statistical processing of results is required to prove that.

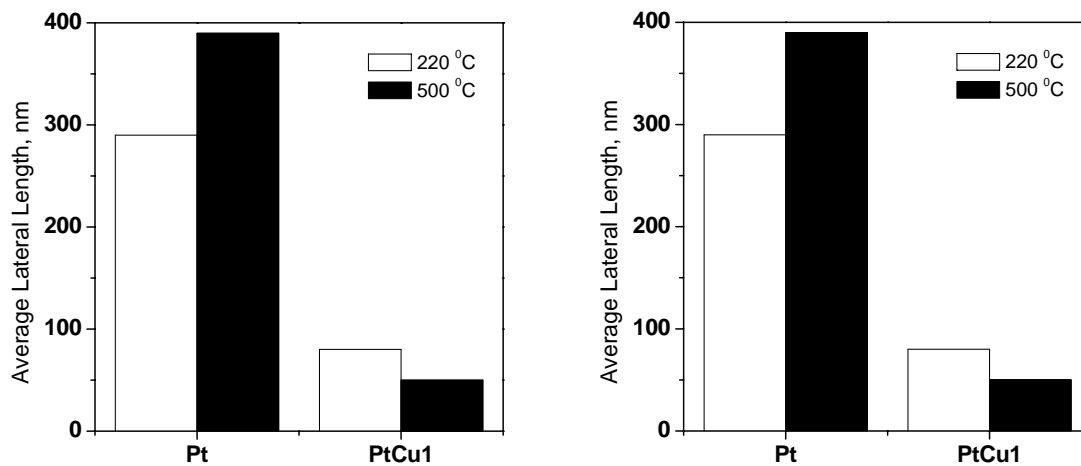


Figure 28. Variation of average height and lateral length as function of reduction temperature for Pt/SiO₂/Si(100) and PtCu1/SiO₂/Si(100) model catalysts.

Figure 28 summarized the results of AFM study for model catalysts samples. In general bimetallic PtCu1/SiO₂/Si(100) showed smaller average lateral length of bimetallic particles, though the average height of them was twice as much as for monometallic Pt/SiO₂/Si(100) sample. The reduction of Pt/SiO₂/Si(100) model catalyst at elevated temperature resulted in slight decrease of average height of the Pt particles, while the average lateral dimension increases almost by 1.5 times. In turn, PtCu1/SiO₂/Si(100) model catalyst showed significant decrease for both average height and lateral length (1.4 and 1.6 times, respectively) of metallic particles after reduction at 500 °C.

4.3.3 Kinetics Study

Reaction of Pt/SiO₂/Si(100) Reduced at 220 °C. When Pt/SiO₂/Si(100) reduced at 220 °C was used as the catalyst for 1,2-DCE hydrogen-assisted dechlorination, two products formed: C₂H₆ and C₂H₄. The selectivity toward C₂H₄ was initially 55% and toward C₂H₆ was initially 45%. With increasing time on stream, the selectivity toward C₂H₄ decreased, and was 33% after 85 h. The decrease in C₂H₄ selectivity correlated with an increase in the C₂H₆ selectivity. During the 85 h time on stream, the conversion increased from 0.005% to 0.01% (Figure 29 A).

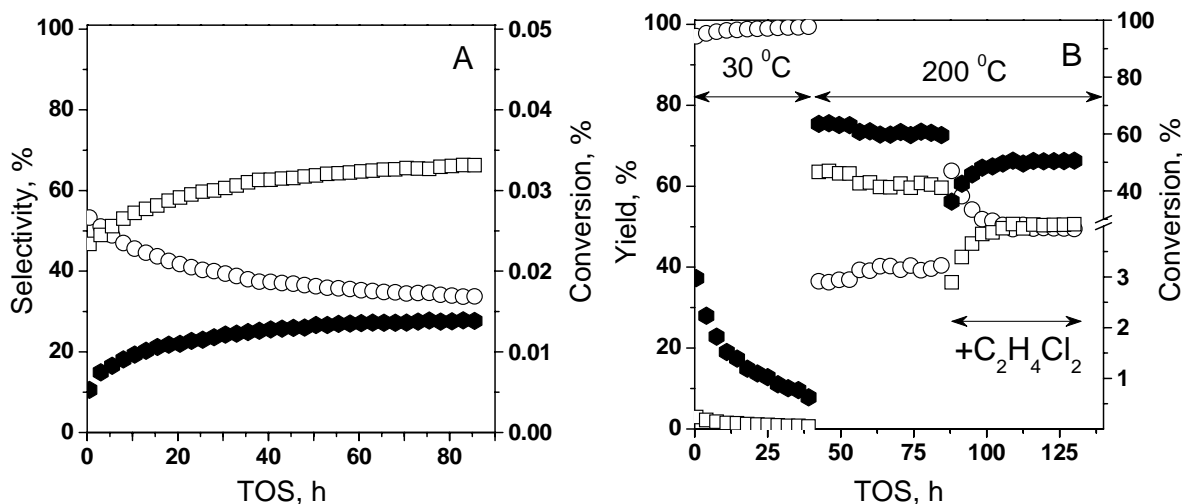


Figure 29. Pt/SiO₂/Si(100) reduced at 220 °C: A. HDCl of 1,2-DCE B. Hydrogenation of C₂H₄. Selectivity toward ethylene (open circle), selectivity toward ethane (open square), conversion (full black hexagons)

The Pt/SiO₂/Si model catalysts reduced at 220 °C also catalyzed ethylene hydrogenation. At 30 °C the C₂H₄ conversion was approximately 4% at the beginning of reaction and the only product was C₂H₆ (Figure 29 B). After 40 h the conversion decreased to 0.5%. Increasing the temperature to 200 °C increased the conversion from 0.5% to 64%. However, the C₂H₄

conversion decreased from 64% to 59% during the 40 h reaction at 200 °C. When 1,2-DCE was added to the reactant stream at the end of the 40 h reaction, there was an immediate decrease in C₂H₄ conversion from 59% to 35% (formation of C₂H₄ from 1,2-DCE was neglected, because the maximum amount that could be formed by this route was two orders of magnitude less than the inlet concentration of C₂H₄). Subsequently, the conversion of C₂H₄ increased from 35% to 51% during 20 h time on stream, and then remained essentially constant thereafter.

Reaction of Pt/SiO₂/Si(100) Reduced at 500 °. When Pt/SiO₂/Si(100) reduced at 500 °C was used as a catalyst for 1,2-DCE hydrogen-assisted dechlorination, the selectivity toward C₂H₄ was 70%, more than 1.5 times higher than when the catalyst was reduced at 220 °C (Figure 30 A). However, the conversion was initially 0.015%, approximately 3 times higher than the samples reduced at 220 °C. The selectivity toward C₂H₄ remained essentially constant at 70% for the whole run.

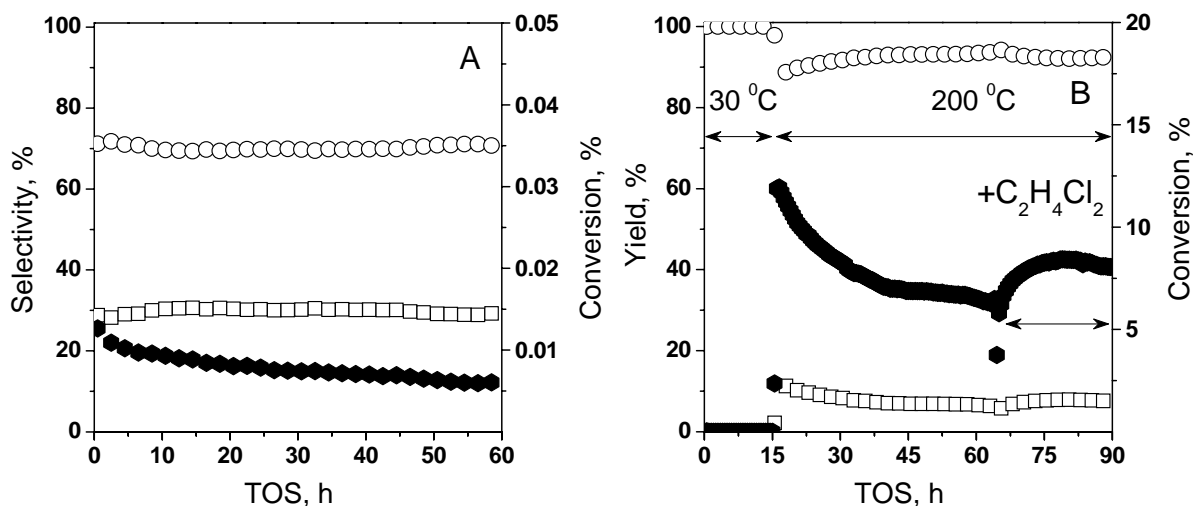


Figure 30. Pt/SiO₂/Si(100) reduced at 500 °C: A. HDCl of 1,2-DCE B. Hydrogenation of C₂H₄. Selectivity toward ethylene (open circle), selectivity toward ethane (open square), conversion (full black hexagons)

The Pt/SiO₂/Si(100) sample reduced at 500 °C was inactive for C₂H₄ hydrogenation at 30 °C. But when the reaction temperature was increased to 200 °C, conversion increased to 12%, a factor of 6 less than for the same sample reduced at 220 °C (Figure 30 B). Though, 50 hours later conversion dropped by 6%. The drop in conversion is approximately the same both for samples reduced at 220 and 500 °C. Immediately after 1,2-DCE was added to reaction mixture, the conversion decreased to 3% and then started to increase. After 15 h the conversion was 8%. The same increase of conversion after addition of 1,2-DCE was observed for the Pt/SiO₂/Si sample reduced at 220 °C, but in this case conversion did not even reach the same level as before 1,2-DCE was added.

Reaction of PtCu1/SiO₂/Si(100) Reduced at 220 °C. The bimetallic PtCu1/SiO₂/Si(100) model catalyst reduced at 220 °C was more selective toward C₂H₄ than the monometallic Pt/SiO₂/Si(100) sample reduced at the same temperature in reaction of hydrogen-assisted dechlorination of 1,2-DCE (Figure 31 A). To be exact, initial selectivity toward C₂H₄ for PtCu1/SiO₂/Si(100) was 94%, while for Pt/SiO₂/Si(100) it was only 55%. During the time on stream selectivity decreased and after 20 hours it reached 89% and was oscillating near this value later on. At the same time conversion was increasing during the whole experiment. At the beginning of reaction it was 0.007% and after 100 hours on stream it reached 0.021%. When PtCu1/SiO₂/Si(100) sample was tested in reaction of C₂H₄ hydrogenation it showed very low activity at 30 °C. At the beginning conversion was 0.5% and after 15 h it decreased to 0.05%. Increase of reaction temperature to 200 °C led to significant increase of conversion. Right after the temperature reached 200 °C conversion was 30% and started steadily to decrease. After 30 hours conversion became equal to 10%, the following drop of conversion during hydrogenation of ethylene was less intense in comparison with first 30 h.

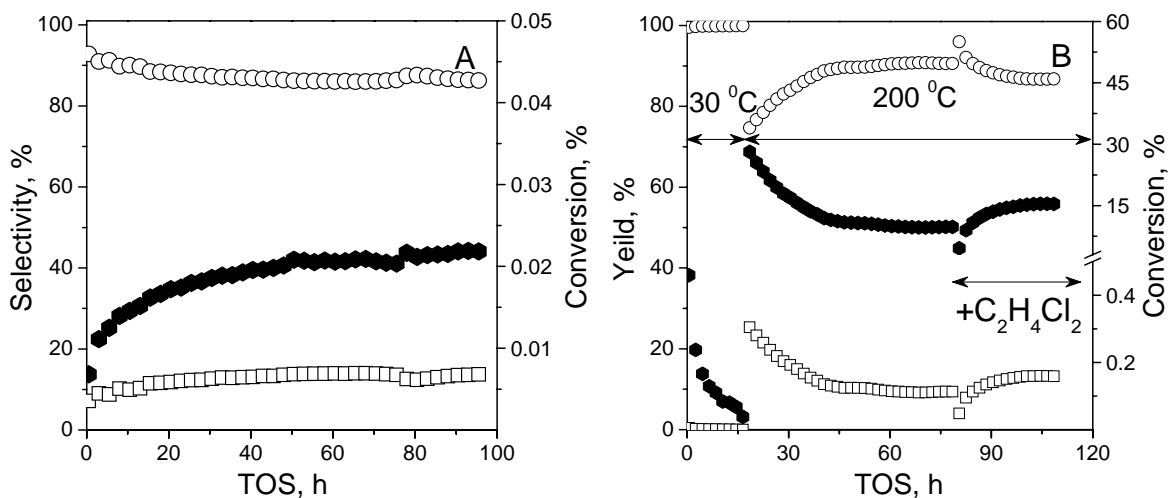


Figure 31. PtCu1/SiO₂/Si(100) reduced at 220 °C: A. HDCl of 1,2-DCE B. Hydrogenation of C₂H₄. Selectivity toward ethylene (open circle), selectivity toward ethane (open square), conversion (full black hexagons)

The following addition of 1,2-DCE led to abrupt decrease of conversion to 4%. As in all previous cases after addition of 1,2-DCE to C₂H₄ conversion was steadily increasing and 20 hours after addition it reached 15%.

Reaction of PtCu1/SiO₂/Si(100) Reduced at 500 °C. When the PtCu1/SiO₂/Si(100) model catalyst was reduced at 500 °C it was 100% selective toward C₂H₄ in the reaction of 1,2-DCE hydrodechlorination, though activity of this sample was much less than after reduction at 220 °C (XFigure 32X). Steady-state activity for this sample was equal 0.005%. No significant change in activity was observed during the time on stream. The PtCu1/SiO₂/Si(100) sample was tested in reaction of hydrogenation of C₂H₄; at 30 °C it showed no activity, at 200 °C conversion was 1.6% at the beginning of reaction and it was decreasing during the time on stream. Addition of 1,2-DCE to reaction mixture of C₂H₄ was omitted whereas hydrogenation activity of sample was extremely low.

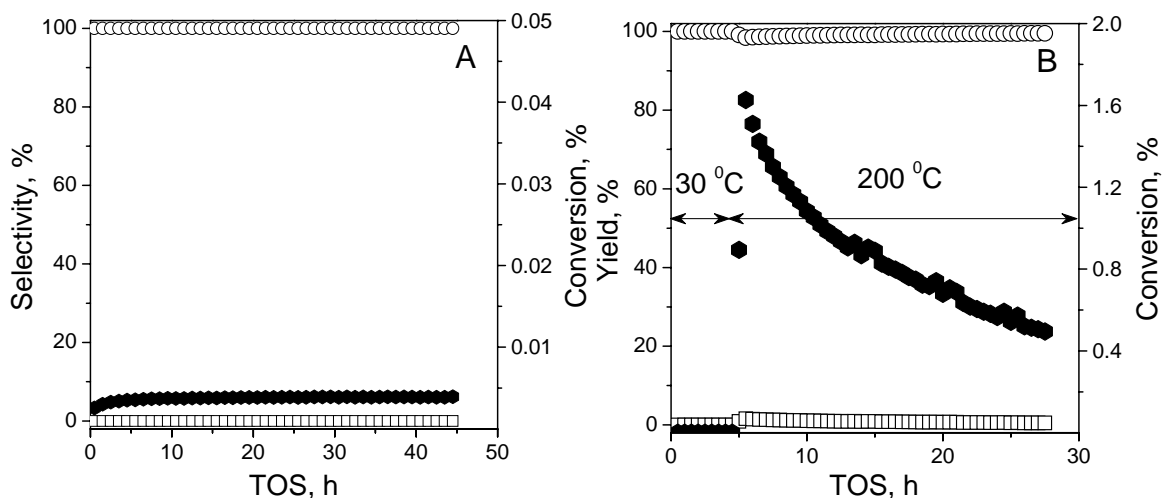


Figure 32. PtCu1/SiO₂/Si(100) reduced at 500 °C: A. HDCl of 1,2-DCE B. Hydrogenation of C₂H₄. Selectivity toward ethylene (open circle), selectivity toward ethane (open square), conversion (full hexagons)

4.4 DISCUSSION

It must be unfortunately accepted that the genuine objective set at the beginning of the study of model SiO₂/Si(100) catalysts with supported metals was not achieved. The objective of this part of the work was to establish a direct correlation between ensemble size effect and selectivity of the reaction of 1,2-DCE hydrodechlorination. The valuable part of this work was getting the direct evidence on ensemble size from SPM techniques and electron imaging techniques. Why did the achievement of the original goals “fail”?

As it follows from kinetics investigation of 1,2-DCE hydrogenation the selectivity performance of model Pt-Cu/SiO₂/Si(100) catalyst was completely different from selectivity performance of the conventional catalyst (Figure 33). The first feature to notice is non-zero C₂H₄

selectivity of Pt/SiO₂/Si(100) catalyst reduced at 220 °C, while conventional Pt/SiO₂ catalyst formed no C₂H₄ at either reduction temperature. Moreover,

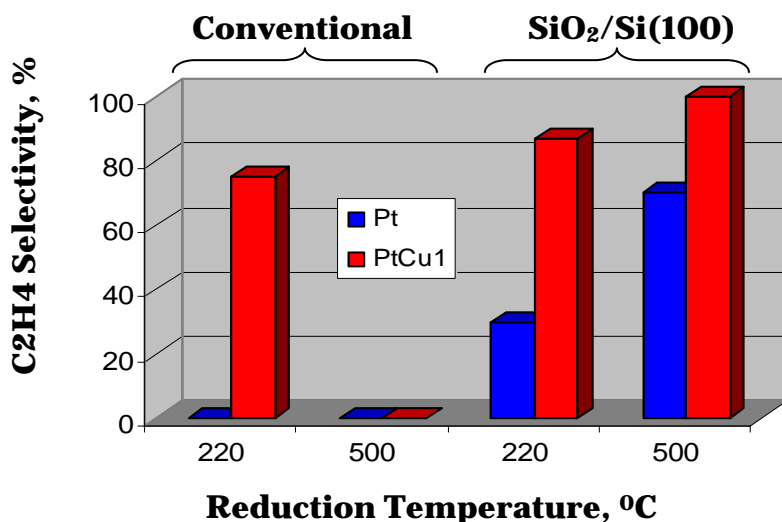


Figure 33. Comparison of initial selectivity performance for conventional and model catalysts reduced at 220 and 500 °C.

reduction of Pt/SiO₂/Si(100) at 500 °C resulted even in more C₂H₄ formation at the expense of C₂H₆. The second point to note is the unusual initial selectivity performance of the PtCu1/SiO₂/Si(100) model catalyst in comparison with the PtCu1/SiO₂ conventional catalyst upon variation of reduction temperature: the conventional PtCu1/SiO₂ after reduction at 500 °C formed less C₂H₄ (essentially 0% Figure 15), than after reduction at 220 °C, while the PtCu1/SiO₂/Si(100) model catalyst produced even more C₂H₄ after reduction at 500 °C in comparison with PtCu1/SiO₂/Si(100) sample reduced at 220 °C (Figure 33).

Such unusual behavior can not be explained by the low conversion level of the reaction: if ethylene is the primary product of 1,2-DCE hydrodechlorination then selectivity toward ethane will depend on the conversion level. To prove that the conventional Pt/SiO₂ sample was diluted with silica (the final Pt loading was adjusted to be 0.03%) and tested in 1,2-DCE

hydrodechlorination reaction at comparable conversion level (0.08%) (Figure 34): no C_2H_4 formation was observed. Moreover, conventional bimetallic catalyst shows 100% selectivity toward C_2H_4 even at high conversion levels. Thus, kinetics reaction factors are not enough to explain the selectivity performance.

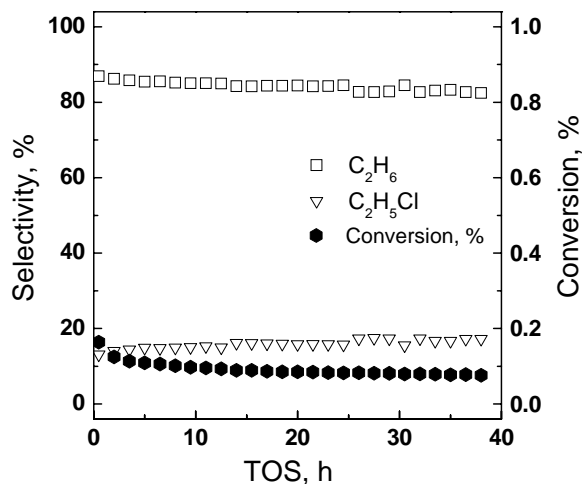


Figure 34. Kinetics testing of Pt/SiO₂ conventional catalyst diluted with SiO₂ in reaction of 1,2-dichloroethane hydrodechlorination.

To provide with explanation such unusual behavior of model PtCu1/SiO₂/Si(100) catalyst in the reaction of 1,2-DCE hydrodechlorination the following hypothesis was proposed: our SiO₂ layer has imperfections in it with silicon (Si)⁶⁹ exposed that participates in reaction of C-Cl bond activation with desorption of ethylene that can be further hydrogenated over extended Pt ensembles. Silicon is known to participate readily in C-Cl bond cleavage even at room temperature and elevated temperature it forms volatile halosilanes^{70, 71}. The desorption of volatile halosilanes can be limited by presence of surface H_{ads} that scavenges Cl_{ads} with HCl formation. In this view the increase of C_2H_4 selectivity for Pt/SiO₂/Si(100) and PtCu1/SiO₂/Si(100) catalyst reduced at 500 °C can be explained by formation of platinum

silicides that is partly supported by XPS data. The logical question that arises is what if we reduce conventional monometallic Pt/SiO₂ catalyst at elevated temperature and form silicides of platinum as reported^{62, 72}, would we have ethylene formation?

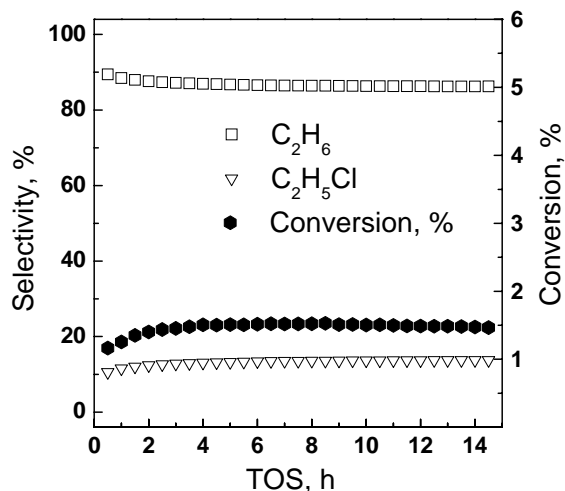


Figure 35. Kinetics testing of Pt/SiO₂ conventional catalyst reduced at 650 °C for 20 h in reaction of 1,2-dichloroethane hydrodechlorination.

To address this issue experiment on 1,2-DCE hydrodechlorination was performed on highly reduced Pt/SiO₂ conventional sample (Figure 35): no ethylene formation was observed. According to literature data^{62, 72} pretreatment used to produce data at Figure 35 leads to partial conversion of Pt to platinum silicides (Pt₃Si and Pt₁₂Si₅). From that data we can conclude that formation of platinum silicides is not minimum requirement for C₂H₄ formation. Most probably even if we have platinum silicide for conventional catalyst the Pt ensemble size is still enough to hydrogenate C₂H₄ formed on exposed silicide surface.

Hippe et al.⁷² report a decrease of observed CO wavenumber from 2086 (reduction 500 °C) to 2048 cm⁻¹ (reduction 650 °C) for 1.6wt% Pt/SiO₂ sample after 10 h treatment in pure H₂.

The singleton frequency for ^{12}CO lays around $2035\text{-}2040\text{ cm}^{-1}$, assuming dipole-dipole coupling magnitude of the $8\text{-}13\text{ cm}^{-1}$. From studying conventional bimetallic catalyst we know that dipole-dipole coupling of that order gave selectivity toward ethylene of $5\text{-}20\%$ (after 5 min of TOS, for samples inclined to reconstruction). Analyzing that information we can conclude that extended ensembles size for Pt/SiO_2 conventional catalyst with partial conversion of Pt to platinum silicides determines selectivity pattern in hydrodechlorination of 1,2-DCE.

High selectivity toward C_2H_4 for model $\text{Pt}/\text{SiO}_2/\text{Si}(100)$ catalyst can be explained by prevailing of Si surface over Pt and almost complete absence of porous structure that makes primary product leave surface with small probability of following adsorption on the surface and reaction. That means that C_2H_4 that forms on Si (and/or Pt_xSi_y) for model catalyst has lower probability to be adsorbed on extended Pt ensembles and hydrogenated to ethane than same probability for conventional catalyst.

4.5 SUMMARY

Studying of 1,2-DCE hydrodechlorination over $\text{Pt}/\text{SiO}_2/\text{Si}(100)$ and $\text{PtCu1}/\text{SiO}_2/\text{Si}(100)$ model catalysts revealed unusual kinetics performance of model systems in comparison with conventional Pt-Cu silica supported systems: model catalyst possesses significantly higher selectivity toward C_2H_4 than conventional catalyst of the same atomic composition. That behavior was rationalized by the following scheme (Figure 36).

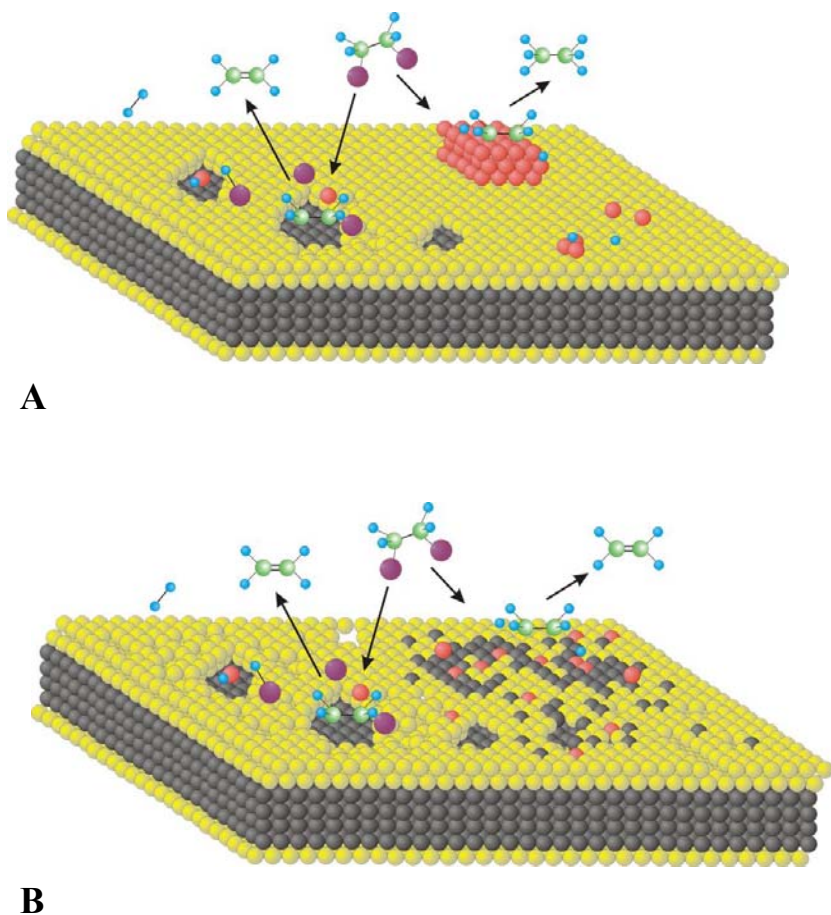
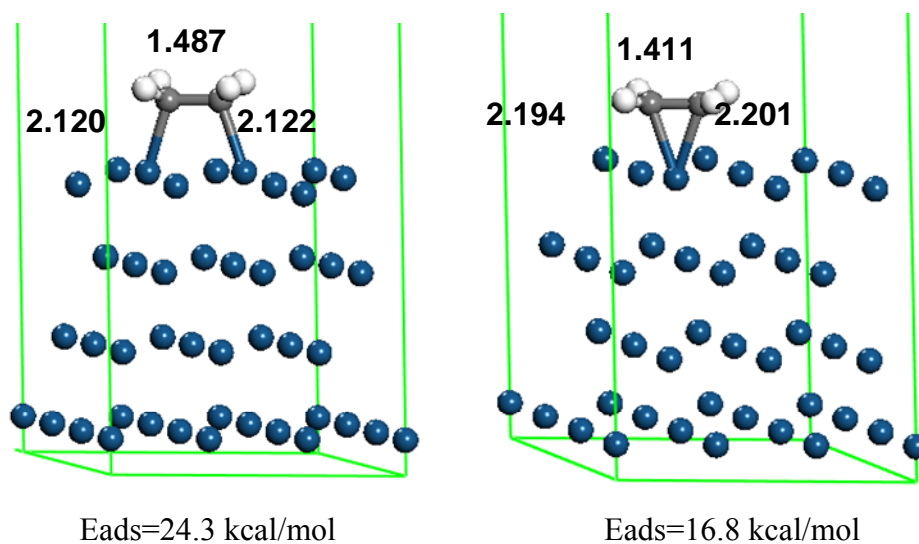


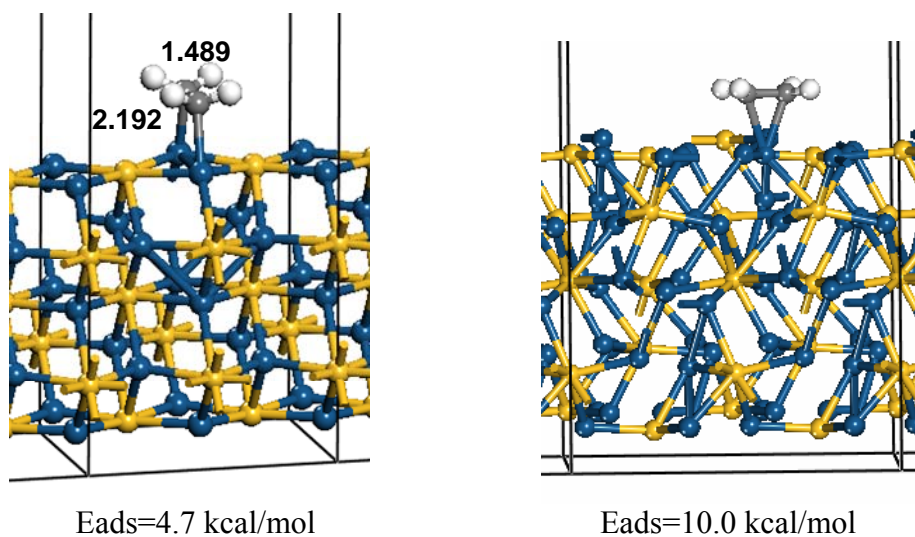
Figure 36. Structure of Pt/SiO₂/Pt(100) model catalyst: silica (SiO₂) (yellow) layer has imperfect structure with exposed silicon (Si) layers (dark grey) and supported Pt particles.

According to our interpretation C₂H₄ forms over exposed silicon patches, while extended Pt particles responsible for formation of ethane from 1,2-DCE and C₂H₄. Complete hydrogenation of C₂H₄ does not occur due to limited porous structure and as consequence small probability of secondary adsorption of primary products. Reduction at elevated temperatures (500 °C) results in increase of defect in SiO₂ layer due to its reduction. In addition Pt (and Cu) partially convert to silicides. Increased silicon surface favors increase of selectivity toward C₂H₄.

Moreover, platinum silicide formation leads to decrease of Pt ensembles and as it was shown theoretically leads to decrease of binding energy of ethylene molecules (Figure 37).



A. C₂H₄ Adsorption on Pt(111) Surface



B. C₂H₄ Adsorption on Pt₃Si(110)

Figure 37. Comparative adsorption of π - and di- σ -bonded C₂H₄ over Pt(111) and Pt₃Si(110) surfaces (periodic slab calculations (VASP) by Dan C. Sorescu)

5.0 STRUCTURAL SENSITIVITY OF C-CL BOND CLEAVAGE. ROLE OF COPPER

5.1 INTRODUCTION

Once the ensemble size effect on selectivity performance was established the prime importance question that arose: what is the influence of ensembles size effect on elementary step realization - C-Cl bond cleavage that is known as rate determining reaction step in hydrodechlorination of 1,2-DCE ⁷³. It was interesting to answer also the question on the role of copper in our bimetallic system, *i.e.* if Cu just dilute the Pt or it participates in C-Cl bond cleavage reaction.

To address the questions designated in the above paragraph, experimental work was performed. In order to narrow experimental implementation of the task the approach involving masking of the Pt surface with carbon deposited was chosen. Carbon was deposited by decomposition of C₂H₄ at elevated temperature. The experimental procedure of C₂H₄ decomposition and following training was designed to get carbon stable to reduction at reaction temperature (200 °C) ⁷⁴⁻⁷⁹ and will be described in the experimental section. To control the ensemble size coverage with carbon was varied by variation of time of C₂H₄ decomposition.

5.2 EXPERIMENTAL PROCEDURE

5.2.1 Catalysts Preparation **

The Pt/SiO₂ was prepared by addition of SiO₂ powder (Aldrich, 99+%, 60-100 mesh, 300 m² g⁻¹, 150 Å) calcined in air at 500 °C for 12 h to [Pt(NH₃)₄](NO₃)₂ (Aldrich, 99%) water solution at constant agitation, after that mixture was allowed to equilibrate overnight. The concentration of the [Pt(NH₃)₄](NO₃)₂ was adjusted to obtain a weight loading of platinum of 3%. After equilibration the impregnated SiO₂ was isolated from the liquid by filtration and was dried at ambient conditions in the air for 72 hours. After 72 hours solid residual was placed into a vacuum envelope and dried again at 100 °C for 12 hours under static vacuum (25 Torr). Then it was transferred to an airtight container and held until needed.

5.2.2 Catalysts Pretreatment

Before carbon deposition the sample was pretreated according to the standard pretreatment policy. First, after the catalyst sample was placed into a specially designed reactor (allowing transfer of catalyst sample from volumetric adsorption system to kinetics system without contact with air) it was heated in He (30 cc min⁻¹) flow from ambient temperature to 130 °C at 10 °C min⁻¹ and then held at 130 °C for 1.5 h. Second, the flow of He was replaced by flow of 5%H₂/Ar (30

** The experimental procedure outlined for catalysts preparation was developed by Professor V. Kovalchuk.

cc min⁻¹) and temperature was raised at 10 °C min⁻¹ to 550 °C. At 550 °C and flowing 5%H₂/Ar mixture the sample was held for 6 h to reduce Pt and stabilize metal particles from further segregation. To remove adsorbed hydrogen from Pt surface the sample was evacuated at 550 °C for 0.5 h and then temperature was lowered still evacuating sample to 35 °C and volumetric adsorption study to determine dispersion was performed. The dispersion value for this step will be referred as fresh catalyst dispersion.

5.2.3 Volumetric Adsorption Study

The volumetric adsorption study was absolutely the same as that described in Section 3.2.3. After dispersion measurement the catalyst was purged with He flow (30 cc min⁻¹) steadily increasing temperature from 35 to 450 °C at 10 °C min⁻¹. The purging procedure was directed to remove adsorbed CO (the control experiment showed recovery of initial dispersion after purging procedure within the mistake of experiment). After purging procedure the catalyst sample was either subjected to carbon deposition procedure or transferred to kinetics system and tested for kinetics performance.

5.2.4 Carbon Deposition

The carbon deposition policy was designed to get stable to reduction at reaction conditions form of carbon at the surface of Pt. The Sample was treated in 30 cc min⁻¹ flow of C₂H₄ for the desired period of time at 450 °C. Then the sample was purged with 30 cc min⁻¹ He flow at the same temperature for 0.5 h to remove gas phase of ethylene. After that the temperature was increased at 10 °C min⁻¹ from 450 to 550 °C and kept for 1 hour at continuous He flow. One hour later, the temperature was decreased at 10 °C min⁻¹ to 220 °C and the sample was reduced in 30

cc min⁻¹ H₂ (5%)/Ar flow for 4 h. After the catalyst sample was evacuated at 220 °C for 1 h temperature was lowered to 35 °C and adsorption of CO to determine dispersion was performed.

5.2.5 Kinetics Study

Kinetics study was performed to evaluate performance of catalytic system as a function of carbon deposited. Before the testing all lines were subjected to cycles (at least 3) of purging with He (0.5 h) and fast evacuation (0.3 atm) to remove any traces of air. The kinetics procedure was close to that described in Section 3.2.5, the only difference was the absence of drying step. Instead of which, the sample was heated from ambient temperature to 200 °C and the reaction started.

The reaction was conducted at 200 °C and atmospheric pressure. The reaction mixture consisted of 7000 ppm of 1,2 - dichloroethane (Fisher Scientific, 99.8+%), 36000 ppm H₂, and the balance He. The total flow-rate was 41 cc min⁻¹. The reaction was run until steady-state performance with respect to selectivity was obtained. For this investigation steady-state selectivity was defined as a change less than 0.2% in 10 h. Every kinetics experiment was performed with a new sample of catalyst.

5.3 RESULTS

Studying HDCl of 1,2-DCE on samples with different dispersion levels due to carbon deposited the dependence of selectivity performance was detected (Figure 38).

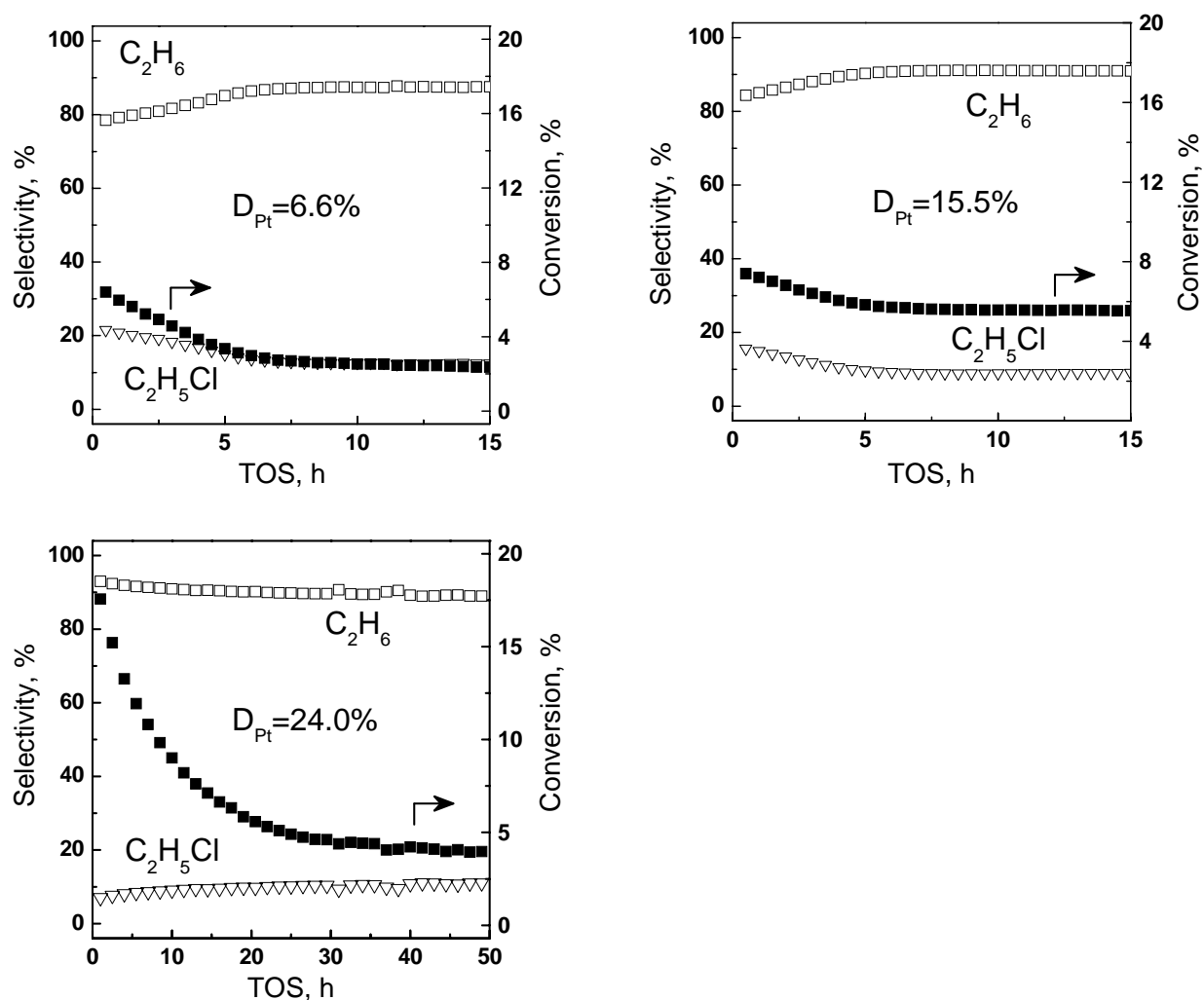


Figure 38. Kinetics performance of C/Pt/SiO₂ catalyst with different dispersion of Pt (24.0% - corresponds to sample with no carbon deposited)

The decrease of dispersion resulted in an insignificant increase of selectivity toward C_2H_5Cl . This phenomenon can not be explained just the variation in the conversion level; by looking at the selectivity pattern of Pt/SiO₂ catalyst with dispersion of 24.0% the reader can notice that while the conversion level decreases, by more than a factor of three (in some runs 8 times: from 40 to 5%) during the 50 hours of time on stream, the selectivity toward C_2H_5Cl increases only by 4%. The selectivity dependence was observed in a wide range of dispersion values (Figure 39). To summarize, the general trend let us say that selectivity toward C_2H_5Cl increased as dispersion of Pt atoms exposed for adsorption decreased. Besides, as one can see from Figure 38 the only products of 1,2-DCE hydrodechlorination were monochloroethane (C_2H_5Cl) and ethane (C_2H_6), no other products were observed in a whole range of platinum dispersion values. This means that ensemble size influences the distribution of original products, but small ensemble size is not enough to produce C_2H_4 on Pt. That supports the idea that Cu is the component of bimetallic Pt-Cu catalyst that is responsible for ethylene (C_2H_4) formation.

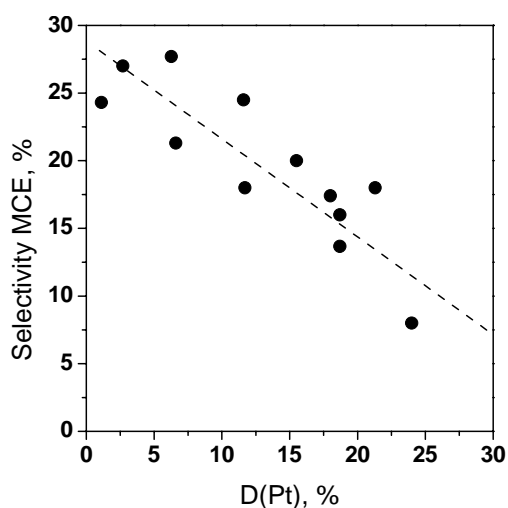


Figure 39. Dependence of selectivity toward monochloroethane (C_2H_5Cl) upon dispersion of Pt in C/Pt/SiO₂ catalyst (dash line is eye-guide).

By recalculation of the turn over frequency (TOF) as function of ensemble size under approximation of cubic Pt particles the following dependence can be tracked (Figure 40).

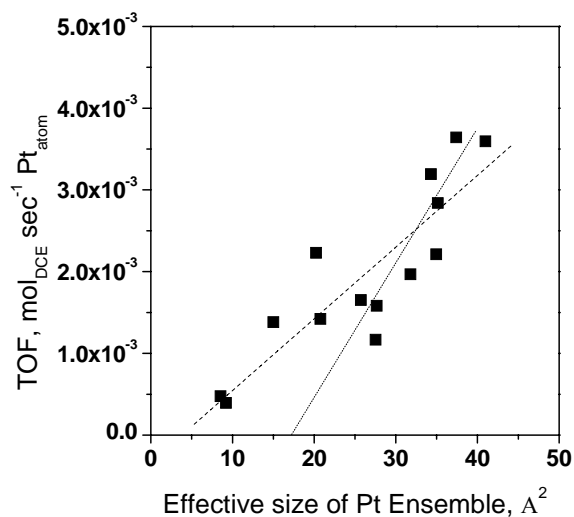


Figure 40. Dependence of turn over frequency (TOF) on effective size of Pt ensemble (dash line – linear fit to experimental data; dot line – a guide for eye).

Cubic approximation was used to simplify the task of evaluation of ensemble size from dispersion measurements data (to get notion of the “real” shape of Pt particles TEM measurements must be done). The fit of the data under a linear approximation gives an idea of the structural sensitivity of C-Cl bond cleavage on Pt ensemble size. From the graph we can see that the minimum ensemble size requirement for C-Cl bond cleavage is around 5 Å.

5.4 DISCUSSION

It is well known that decomposition of pure ethylene on platinum is accompanied by carbonization of the metal surface. The ethylidyne is considered to be the most stable product of interaction between Pt and ethylene at room temperatures⁸⁰. While at elevated temperatures (400 °C) ethylidyne is readily dissociates releasing hydrogen with the formation of carbon species - $[\text{C}\equiv\text{C}]_2^-$ ⁸¹. The structure of carbon deposits and kinetics of ethylene decomposition are functions of the Pt plane and temperature of decomposition. At temperatures close to 500 °C the main form of carbon for Pt monocrystals is chemisorbed, with isolated C atoms; at elevated temperatures this carbon form more dense structures: graphite and diamond like structures. It is widely accepted that carbon deposits do not modify the electronic properties of platinum⁷⁴⁻⁷⁹. The experimental procedure used in this work with first carbon decomposition followed by reduction at 220 °C proves the early findings of Kvon et al.⁷⁶, who showed that carbon that forms on the surface of Pt at elevated temperatures is inert with respect to H_2 at elevated temperatures. Thus, the use of this approach with carbon as an inert Pt site blocker is entirely justified from the chemical point of view.

One of the most important conclusions that follow from Figure 39 and Figure 40 is the structural sensitivity of C-Cl bond cleavage. Technically, the observed increase of selectivity with respect to $\text{C}_2\text{H}_5\text{Cl}$ as a dispersion and as a consequence effective Pt ensemble size decrease can be explained by the following simplified scheme (Figure 41).

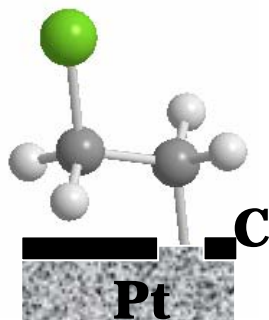


Figure 41. Adsorption of methyl chloride on small Pt ensemble. Dissociation of C-Cl bond in C_2H_4Cl -Pt surface structure depends on presence of Pt atoms in the neighborhood of C-Pt bond.

When 1,2-DCE adsorbs on the surface of Pt the dissociation of first C-Cl bond occurs with formation of methyl chloride radical depicted at the Figure 41. The following fate of the methyl chloride radical can be either reaction with the surface hydrogen species H_{ads} with desorption of monochloroethane (C_2H_5Cl) or dissociation of the second C-Cl bond with formation of di- σ -ethylene. In the second case, the probability of the process depends more strongly on the size of the Pt ensemble with the bounded methyl chloride radical. In order to dissociate second C-Cl two extra Pt atoms are required: the first Pt atom to bind Cl atom and the second Pt atom to form an additional C-Pt bond. Taking into the account the formation of di- σ -ethylene and one adsorbed Cl atom one may require at least 4 Pt atoms to run the reaction of complete hydrogenation of to ethane (forth Pt atom to bind H_{ads}). Or taking into the account methyl chloride radical and chlorine atom one may require 3 Pt atoms to run the reaction of partial hydrogenation of 1,2-DCE to monochloroethane (C_2H_5Cl).

A linear fit of our experimental data shows Pt ensemble size requirement of 5 Å to run reaction 1,2-DCE hydrogenation effectively. On an atomic scale it corresponds roughly to 2 Pt atoms. Though, as one can see from the Figure 40 the data spread is so wide that data for higher

Pt ensemble size give ensemble size requirement of 16 Å that corresponds to 6 Pt atoms. Without any reserve it can be concluded that C-Cl bond splitting reaction is structurally sensitive, but determination of the minimum ensemble size requirement needs more thorough investigation of the dependence of the TOF on the effective size of the Pt ensembles.

5.5 SUMMARY

Investigation of C-Cl bond cleavage structural sensitivity in reaction of hydrodechlorination of 1,2-DCE showed that of C-Cl bond cleavage efficiency depends on the size of the Pt ensembles: according to TOF dependence on effective ensemble size in cubic approximation of Pt particles the minimum requirement for effective C-Cl bond cleavage is in the range of 2-6 Pt atoms. As a proof to this conclusion, the dependence of the selectivity of 1,2-DCE hydrodechlorination shows an increase of monochloroethane (C₂H₅Cl) in the effluent flow as the effective Pt ensemble size decreases. That experimental observation was rationalized in terms of reduced probability of dissociation of a second C-Cl bond on small Pt ensembles.

Experimental findings give more support to early kinetics simulations⁷³ that state that formation of ethylene occurs exclusively over Ag (or in our case Cu) surface. To be exact, no formation of C₂H₄ was observed at any dispersion values. As a consequence, small ensemble size of Pt is not the only requirement for production of C₂H₄ from 1,2-DCE by hydrogenation.

6.0 EXECUTIVE CONCLUSIONS

The experimental work performed in course of the current study of ensemble size effect in catalysis of hydrodechlorination reaction of 1,2-DCE on Pt-Cu bimetallic silica supported catalyst allowed to draw out several important conclusions.

First, it was shown that selectivity performance of reaction of 1,2-DCE hydrodechlorination depends strongly of Pt ensemble size. The correlation between initial selectivity toward ethylene (Table 2) and ^{12}CO dipole-dipole coupling that is proportional to the size of Pt ensembles (Figure 12) tells us that the larger the size of Pt ensembles the lower selectivity toward ethylene.

Second, for the first time decrease of selectivity toward C_2H_4 after reduction of bimetallic catalysts at elevated temperature was observed. Though, elevated temperature reduction leads to formation of extended Pt-Cu alloy (FTIR), but at the same time dipole-dipole coupling increase is evidence of segregation of Pt at the surface of bimetallic particles. Segregation of Pt at the surface of bimetallic particles leads to increase of Pt ensembles.

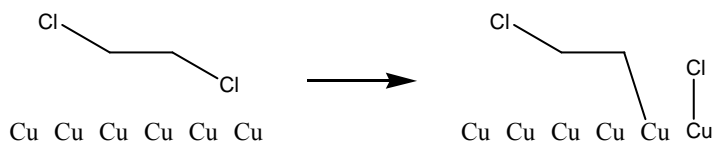
Third, investigation of Pt-Cu/SiO₂/Si(100) model catalyst emphasize that alloying phenomena is more general and silicon can play a role of copper. Silicon by reacting with Pt forms platinum silicides (XPS), thus decreasing the size of Pt ensembles. In platinum silicides Si plays the role of Cu, *i.e.* Si is responsible for formation of ethylene from 1,2-dichloroethane. Preliminary

theoretical calculations show that π - and di- σ -bonded ethylene of platinum silicides has reduced binding energy in comparison with monometallic platinum surface.

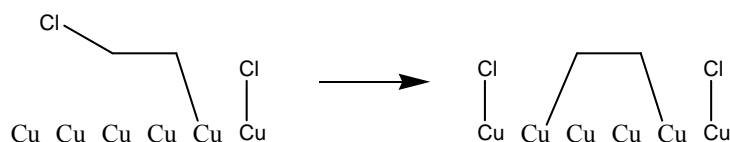
Forth, investigation of ensemble-size effect by selective poisoning of Pt surface with carbon deposited revealed exceptional role of copper in formation of ethylene from 1,2-dichloroethane. That conclusion is in agreement with early kinetics simulations that showed that for bimetallic Pd-Ag catalyst silver is a component that provide sites for C-Cl bond splitting with formation of ethylene from 1,2-dichloroethane⁷³.

And finally, as it was shown in Section 5.0 on example of reaction of 1,2-dichloroethane hydrodechlorination the C-Cl bond splitting is structural sensitive reaction with minimum ensemble size requirement of the 2-6 Pt atoms. Decrease of Pt ensemble size by blockage of platinum surface with carbon leads to decrease of turn over frequency and increase of selectivity toward monochloroethane (C_2H_5Cl).

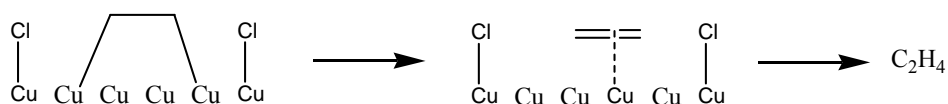
Based on conclusions of current work the following mechanism of 1,2-dichloroethane elimination on highly selective catalyst can be proposed. The C-Cl bond activation occurs at the Cu surface:



Formation of methyl chloride radical at the surface of Cu is accompanied by spontaneous β -chloride elimination reaction with formation of di- σ -bonded ethylene (see Appendix B):

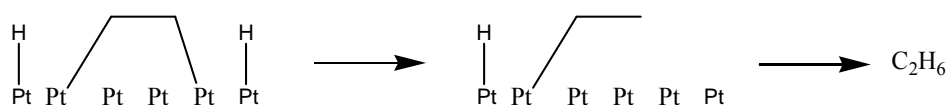


In turn, the di- σ -bonded ethylene is not stable structure at the surface of Cu and it transforms to π -bonded ethylene and later desorbs into the gas phase:

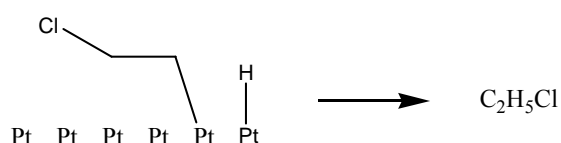


The chlorine atom left on the surface after ethylene adsorption can be easily scavenged by adsorbed hydrogen H_{ads} .

Platinum plays only role a hydrogen activator in highly selective HDCl catalyst, i.e. it provides centers for H_2 dissociation and formation of H_{ads} . It was reported that H_2 molecule can be easily activated to H_{ads} on isolated Pt atoms⁸². In case of unselective catalyst with enlarged Pt ensembles mechanism of 1,2-DCE hydrodechlorination is the same up to the step of di- σ -bonded ethylene formation, but unlike Cu surface Pt surface catalyses hydrogenation of di- σ -bonded ethylene to ethane:



besides, on the step of first C-Cl bond hydrogenolysis methyl chloride radical has higher probability to be hydrogenated than to convert to di- σ -bonded ethylene by β -chloride elimination:



7.0 RECOMMENDATIONS FOR FUTURE WORK

The presented work gives answers for several very important questions. Though, there is still a field for further thorough investigation of related phenomena.

One of the questions the author would like to answer is the nature of active centers in the working catalysts. This question is of prime importance for explanation of action of bimetallic Pt-Cu catalysts in reaction of interest. Currently, all authors consider the mechanism of 1,2-dichloroethane hydrodechlorination from the position of metallic particles with Me in zero oxidation state. Relevancy of such approach is rather questionable despite the excess of H₂ in reaction mixture, as soon as mixture enriched also by chlorine containing compounds: C₂H₄Cl₂, C₂H₅Cl and HCl. This issue is especially related to oxidation state of Cu that is known can be easily reduced at reaction temperature from Cu²⁺ to Cu⁺ chloride (180-200 °C), while temperature of 280 °C is required to convert Cu⁺ to Cu⁰ ²². Answering this question will allow to get more insight into the chemistry of the process.

The work on model catalyst can be significantly improved by studying the influence of silicides formation on selectivity. Theoretical investigation of bonding of reaction products to Pt and Pt_xSi_y surfaces must be studied in more detail to show the change of reactive character with respect to pure Pt surface.

Besides, the work on influence of ensemble size effect on C-Cl bond splitting can be done with more simple hydrochlorocarbons (such as CH₃Cl). That approach will allow to establish more accurately the ensemble size requirement for C-Cl bond splitting.

The question of studying the trends for hydrodechlorination of monochloroethane over Pt-Cu bimetallic systems deserves special attention to fulfill the picture of mechanism of reaction. As preliminary experimental data has shown (Appendix B) hydrodechlorination of monochloroethane over bimetallic catalyst leads to formation of ethylene.

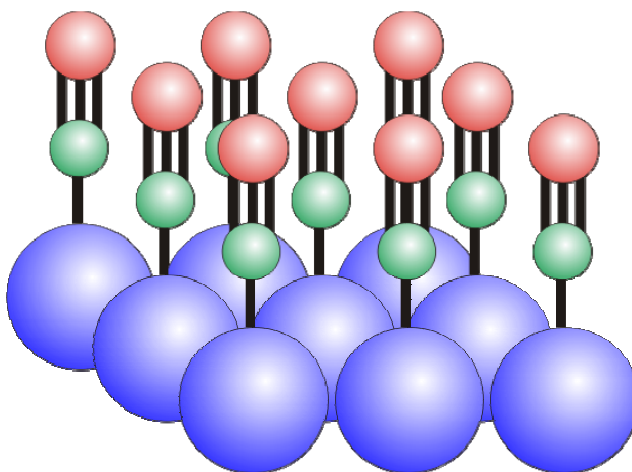
The work on getting the direct evidence of ensemble size influence on selectivity of the reaction of 1,2-dichloroethane hydrodechlorination can be studied by using metal single crystals or film systems. Both systems even more favorable than model catalyst used in this study: kinetically they have no diffusion limitations and they extremely convenient to study by surface sensitive techniques (SPM (AFM, STM) and spectroscopy techniques). The only difficulty that experimentalist will encounter with is low catalytic activity due undeveloped surface area of undispersed systems.

APPENDIX A

THEORY OF DIPOLE-DIPOLE COUPLING AND ITS APPLICATION.

Dipole-dipole coupling is widely used in chemistry as a tool for detection of intermolecular interaction. In course of work and communication with other students author noticed that many students do not understand this phenomenon in such a depth to apply it for their own investigation. With hope that this work will be a basis for future students in studying bimetallic catalytic systems author included some useful information on dipole-dipole coupling phenomenon.

To start, the dipole-dipole coupling between CO molecules over the surface of metals is purely physical phenomenon. Essentially it is coupling of permanent electric dipoles (0.112 D) of CO molecules with each other. As reader understands, absolutely perfect surface of metal favors parallel orientation of CO molecules:



In such geometry dipole-dipole interaction is proportional to number (Θ) of carbon monoxide molecules of the same isotopic composition in the neighborhood of each other:

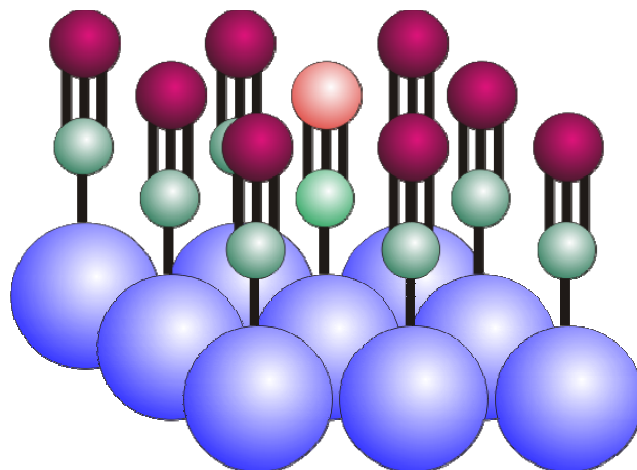
$$v = v_{\text{singleton}} \sqrt{1 + \frac{\alpha_v U_0 \theta}{1 + \alpha_e U_0 \theta}}$$

where α_v and α_e electronic and vibrational polarization of carbon monoxide molecule. And U is a function of the surface:

$$U_0 = \sum_m \left(\frac{1}{(x_n^2 + y_m^2)^{3/2}} + \left[\frac{1}{(x_n^2 + y_m^2 + 4d^2)^{3/2}} - \frac{12d^2}{(x_n^2 + y_m^2 + 4d^2)^{5/2}} \right] \right)$$

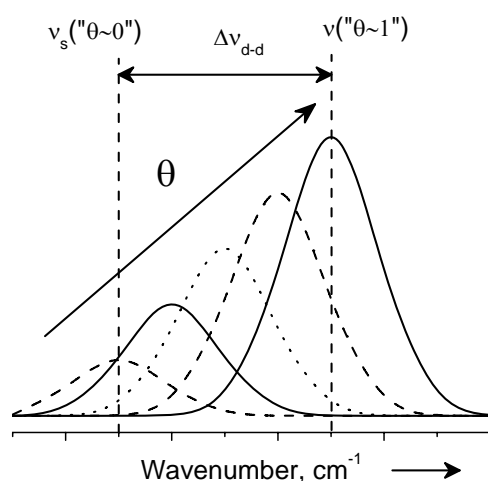
called sometimes the lattice sum. Where x and y are essentially parameters of the lattice describe the distance between dipoles on the surface. While d is the distance of dipole to its image plane^{††}. First term in the sum makes the most significant input into dipole-dipole coupling. As one can understand the U_0 term is a function of lattice structure or crystal plane. Technically direct determination of U_0 function for supported systems used in presented study is not possible, unless enough statistic information on the preferential crystal ordination is received with some additional technique (electron microscopy).

As it was mentioned above dipole-dipole coupling is possible only in the case of molecules of the same isotopic composition. Essentially this statement is incorrect, as soon as even molecules of different isotopic composition (i.e. ^{12}CO and ^{13}CO) possess permanent dipole moment of the same magnitude. More correctly say that in case of molecule of



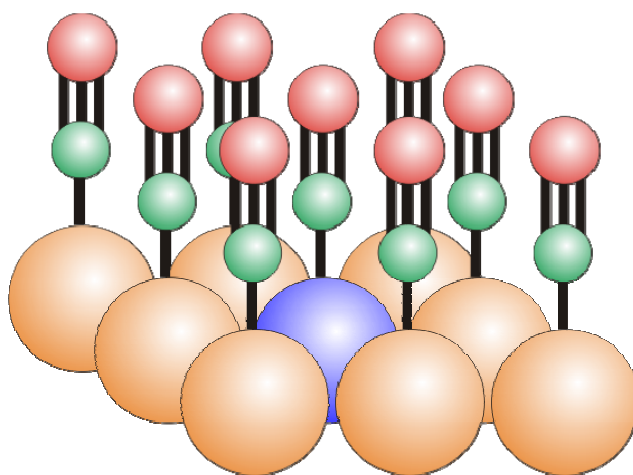
^{††} Dipole image is essentially “virtual” dipole moment in the bulk of the metal induced by permanent dipole adsorbed at the surface of the metal.

different isotopic composition dipoles oscillate with different frequency, thus breaking collective vibration mode. Essentially if ^{12}CO molecule is adsorbed in the neighborhood of $^{13}\text{C}^{18}\text{O}$ molecules one is able to detect frequency of singleton (uncoupled vibration). It is extremely important characteristic that is usually related as a frequency at zero coverage. Singleton frequency is used for determination of electronic modification of the surface as well as for dipole-dipole coupling evaluation as show below:



Dipole-dipole coupling is defined as difference between singleton frequency and frequency for coupled system. While electronic modification values can be deduced by knowing the frequency of singleton for electronically unperturbed system.

And to conclude, by introduction of hetero-atoms (such as Cu) into the original surface (Pt) ones again beaks the lateral symmetry in term of interaction due to difference of CO frequency adsorbed on hetero-

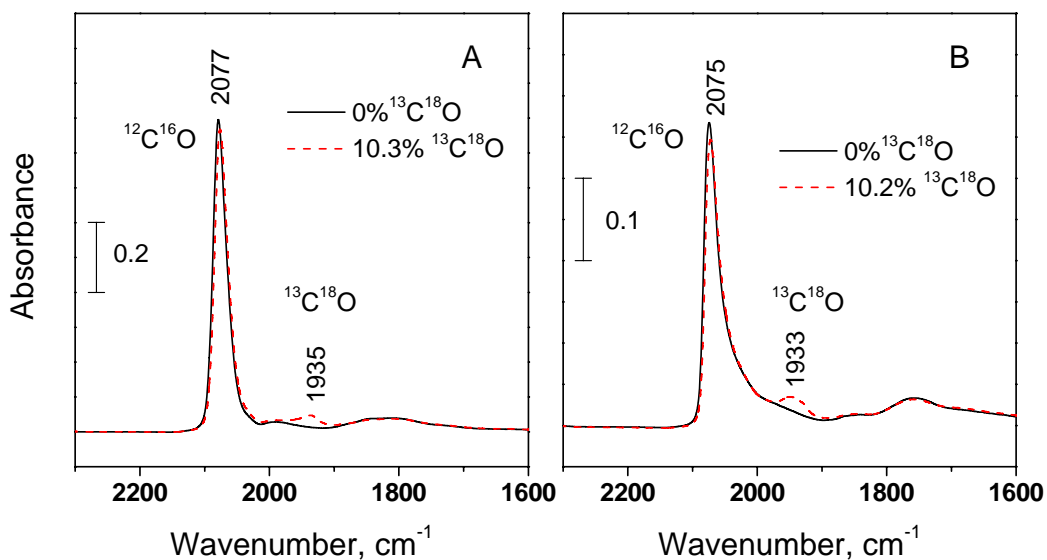


atoms (Cu) from frequency of CO adsorbed on atoms of original surface (Pt). In some instance hetero-atoms are unable to bind CO effectively. But in both cases dilution of original surface with some admixtures lead to decrease of dipole-dipole coupling of CO associated with original surface.

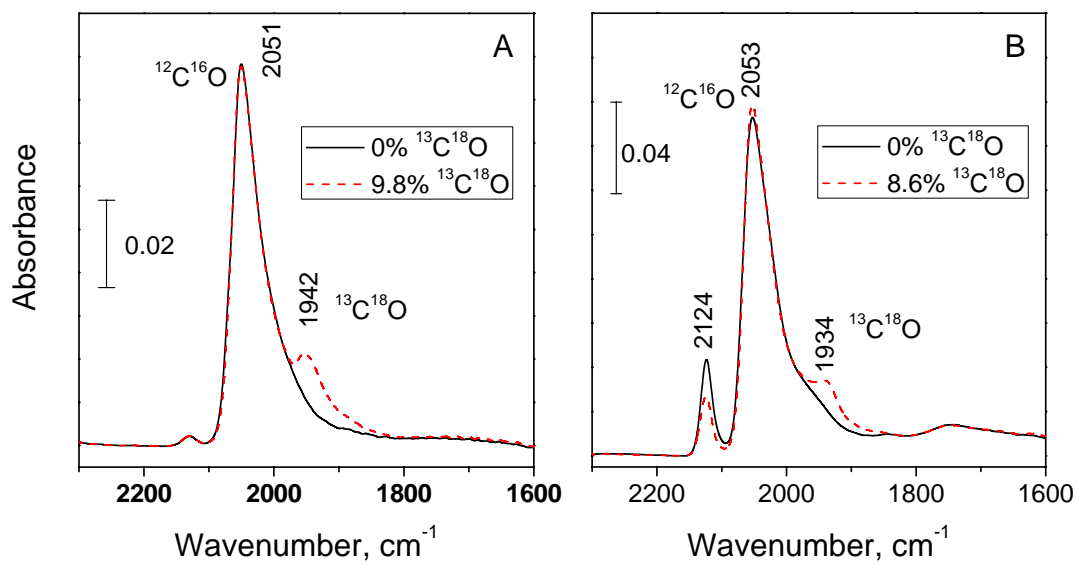
APPENDIX B

EXPERIMENTAL RESULTS OF THE DIPOLE-DIPOLE COUPLING DETERMINATION.

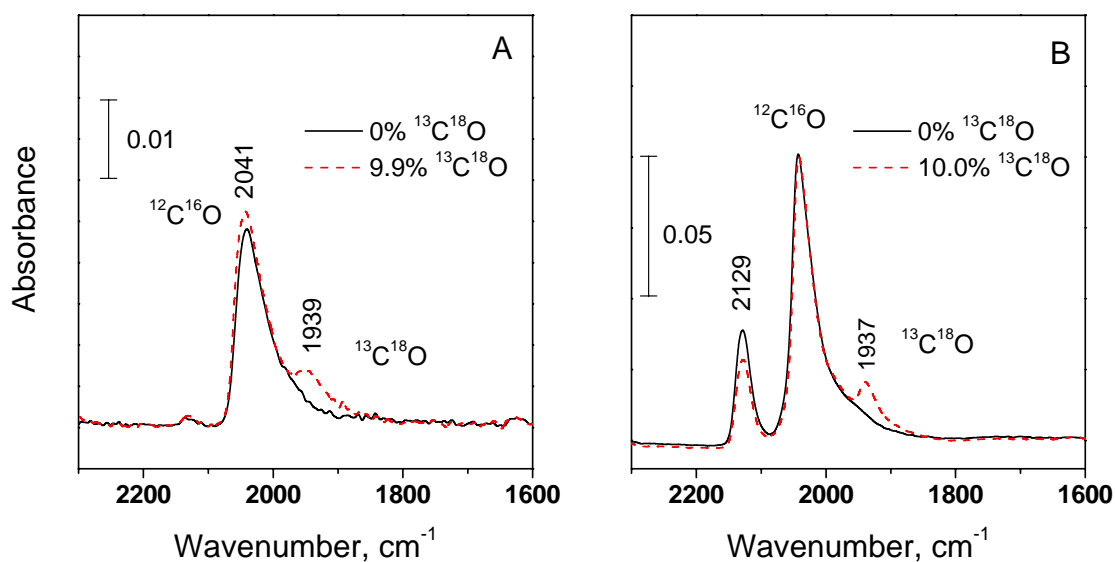
Here some experimental data on determination of dipole-dipole coupling and singleton frequencies will be presented for selected samples in order to give reader a notion of experimental approach. Essentially observed frequency of $^{13}\text{C}^{18}\text{O}$ were considered as a singleton frequencies for the purpose of current work. And singletons of ^{12}CO were obtained by addition of 100 cm^{-1} (based on normal isotopic shift for gas phase) to frequencies of $^{13}\text{C}^{18}\text{O}$.



Adsorption of $^{12}\text{C}^{16}\text{O}/^{13}\text{C}^{18}\text{O}$ over Pt/SiO₂ monometallic sample reduced at 220 °C (A) and 500 °C (B).



Adsorption of ¹²C¹⁶O/¹³C¹⁸O over PtCu₁/SiO₂ bimetallic sample reduced at 220 °C (A) and 500 °C (B).

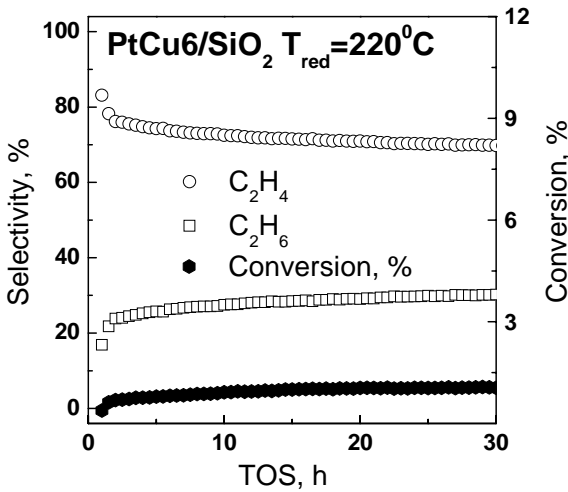
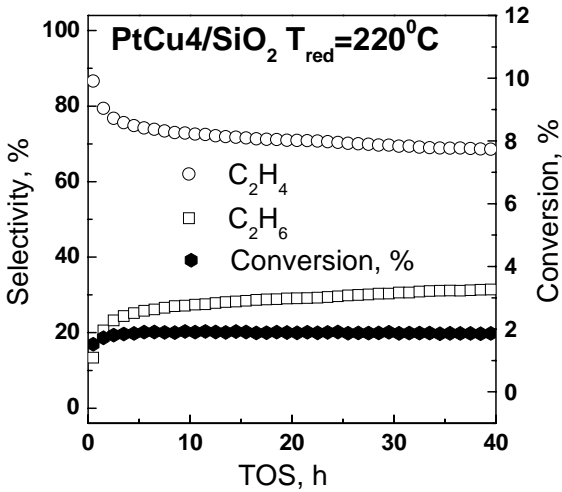
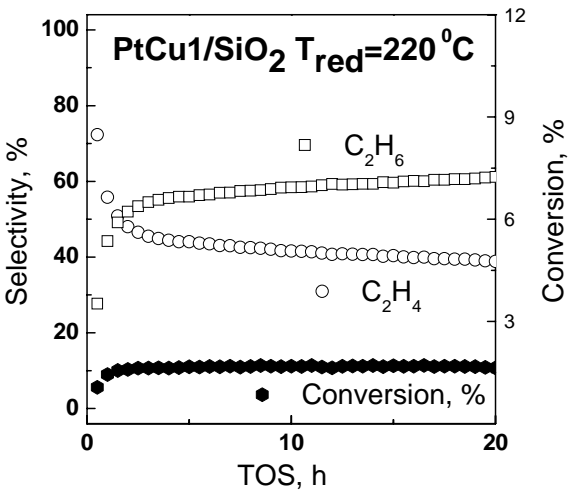
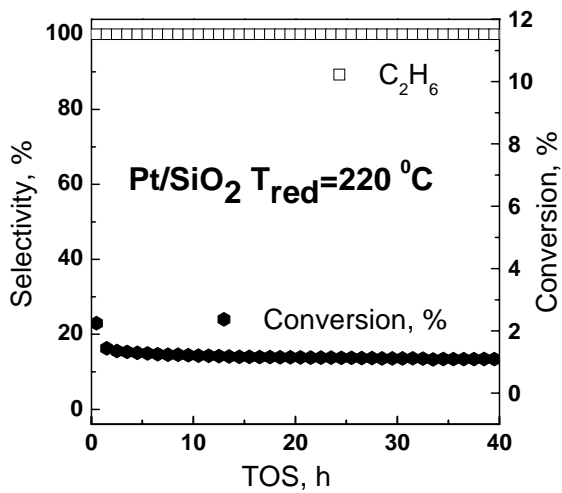


Adsorption of ¹²C¹⁶O/¹³C¹⁸O over PtCu₆/SiO₂ monometallic sample reduced at 220 °C (A) and 500 °C (B).

APPENDIX C

MONOCHLOROETHANE HYDRODECHLORINATION OVER PLATINUM-COPPER BIMETALLIC CATALYSTS.

Recent experimental findings of monochloroethane hydrodechlorination showed that Pt silica supported catalyst produced no ethylene as in the case of 1,2-dichloroethane hydrodechlorination reaction, while bimetallic catalyst were selective toward ethylene. Experimental conditions used in this study are absolutely the same as those used for 1,2-dichloroethane hydrodechlorination: 7000 ppm C₂H₅Cl, 35000 ppm H₂, He balance, 41 cc min⁻¹ total flow, 200 °C.



BIBLIOGRAPHY

1. Konya, Z.; Kukovecz, A., Special Issue on Catalytic Dehalogenation. *Applied Catalysis, A: General, Special Issue on Catalytic Dehalogenation* **2004**, 271, (1-2), 1-2.
2. EPA *Petroleum refinery MACT standard guidance*; US Environmental Protection Agency, Research Triangle Park, NC, USA.: 2000; pp i-xi, 1-179.
3. Kroschwitz, J.; Editor, *Kirk-Othmer Concise Encyclopedia of Chemical Technology, 4th Edition*. 1999; p 2196 pp.
4. US EPA FINAL RULE LISTING CERTAIN INDUSTRIAL WASTEWATER SLUDGES GENERATED BY CHLORINATED ALIPHATIC CHEMICAL MANUFACTURING FACILITIES, AS RCRA HAZARDOUS WASTECODES K174 & K175: INDUSTRY PROFILE AND ESTIMATION OF REGULATORY COSTS. *Economics Background Document (29 Sept 2000)* **2002**.
5. Hall, R. E.; Lee, C. W.; Hassel, G. R.; Ryan, J. V. *Experimental investigation of PIC formation in CFC incineration*; Energy and Environ. Res. Corp., Irvine, CA, USA.: 1991; p 10 pp.
6. Niessen, W. R.; Sarofim, A. F., Emission and control of air pollutants from the incineration of municipal solid waste. *Proc. Int. Clean Air Congr., 2nd* **1971**, 595-609.
7. Kim, Y.-J.; Osako, M., Investigation on the humification of municipal solid waste incineration residue and its effect on the leaching behavior of dioxins. *Waste Management (Amsterdam, Netherlands)* **2004**, 24, (8), 815-823.
8. Cominetta, P., Incineration of highly toxic liquors and chemical residues. *Environmental Pollution Management* **1972**, 2, (4), 133-7.
9. Cisneros, M. D.; Holbrook, M. T.; Ito, L. N. Hydrodechlorination process and catalysts for the conversion of chlorinated alkanes into less-chlorinated alkanes. 94-113056677501, 19940822., 1995.
10. Schoedel, R.; Weber, K.; Birke, P.; Neumann, U.; Grundmann, H. Hydrodechlorination of chlorinated hydrocarbons with Pd/aluminosilicate catalysts. 94-44263904426390, 19940726., 1995.
11. Ito, L. N.; Harley, A. D.; Holbrook, M. T.; Smith, D. D.; Murchison, C. B.; Cisneros, M. D. Catalytic conversion of 1,2-dichloropropane to propylene. 93-US76589407819, 19930813., 1994.

12. Ito, L. N.; Harley, A. D.; Holbrook, M. T.; Smith, D. D.; Murchison, C. B.; Cisneros, M. D. Process for catalytic dechlorination 2-chloropropene to propylene with hydrogen. 93-US76069407817, 19930813., 1994.
13. Ito, L. N.; Murchison, C. B.; Holbrook, M. T.; Harley, A. D.; Smith, D. D. Processes for converting chlorinated alkenes to useful, less chlorinated alkenes via copper-platinum-catalyzed hydrodechlorination. 94-2278065476979, 1995.
14. Wu, X.; Letuchy, Y. A.; Eyman, D. P., Catalytic hydrodechlorination of CCl₄ over silica-supported PdCl₂-containing molten salt catalysis: the promotional effects of CoCl₂ and CuCl₂. *Journal of Catalysis* **1996**, 161, (1), 164-177.
15. Vadlamannati, L. S.; Kovalchuk, V. I.; d'Itri, J. L., Dechlorination of 1,2-dichloroethane catalyzed by Pt-Cu/C: unraveling the role of each metal. *Catalysis Letters* **1999**, 58, (4), 173-178.
16. Early, K. O.; Rhodes, W. D.; Kovalchuk, V. I.; d'Itri, J. L., Hydrogen-assisted 1,2,3-trichloropropane dechlorination on supported Pt-Sn catalysts. *Applied Catalysis B-Environmental* **2000**, 26, (4), 257-263.
17. Heinrichs, B.; Noville, F.; Schoebrechts, J.-P.; Pirard, J.-P., Palladium-silver sol-gel catalysts for selective hydrodechlorination of 1,2-dichloroethane into ethylene II. Surface composition of alloy particles. *Journal of Catalysis* **2000**, 192, (1), 108-118.
18. Rhodes, W. D.; Lazar, K.; Kovalchuk, V. I.; d'Itri, J. L., Hydrogen-Assisted 1,2-Dichloroethane Dechlorination Catalyzed by Pt-Sn/SiO₂: Effect of the Pt/Sn Atomic Ratio. *Journal of Catalysis* **2002**, 211, (1), 173-182.
19. Luebke, D. R. Exploration of the structure and activity of bimetallic catalysts for the dechlorination of chlorocarbons. 2002.
20. Anderson, J. H., Jr.; Conn, P. J.; Brandenberger, S. G., Hydrogen chemisorption and surface composition of silica-supported platinum-copper alloys. *Journal of Catalysis* **1970**, 16, (3), 326-31.
21. Anderson, J. R., *Structure of Metallic Catalysts*. 1975; p 478 pp.
22. Rouco, A. J., TPR study of Al₂O₃- and SiO₂-supported CuCl₂ catalysts. *Applied Catalysis, A: General* **1994**, 117, (2), 139-49.
23. Rouco, A. J., *Low-temperature ethylene oxyhydrochlorination: effects of supports and promoters on the mobilities of active species in CuCl₂ catalysts*. 1995; Vol. 157, p 380-7.
24. Hammaker, R. M.; Francis, S. A.; Eischens, R. P., Infrared study of intermolecular interactions for carbon monoxide chemisorbed on platinum. *Spectrochimica Acta* **1965**, 21, (7), 1295-309.

25. Bond, G. C.; Namijo, S. N.; Wakeman, J. S., Thermal analysis of catalyst precursors. 2. Influence of support and metal precursor on the reducibility of copper catalysts. *Journal of Molecular Catalysis* **1991**, 64, (3), 305-19.
26. Vadlamannati, L. S.; Luebke, D. R.; Kovalchuk, V. I.; d'Itri, J. L., Olefins from chlorocarbons: reactions of 1,2-dichloroethane catalyzed by Pt-Cu. *Studies in Surface Science and Catalysis* **2000**, 130A, (International Congress on Catalysis, 2000, Pt. A), 233-238.
27. Borovkov, V. Y.; Luebke, D. R.; Kovalchuk, V. I.; D'Itri, J. L., Hydrogen-Assisted 1,2-Dichloroethane Dechlorination Catalyzed by Pt-Cu/SiO₂: Evidence for Different Functions of Pt and Cu Sites. *Journal of Physical Chemistry B* **2003**, 107, (23), 5568-5574.
28. Bourane, A.; Dulaurent, O.; Bianchi, D., Heats of Adsorption of Linear and Multibound Adsorbed CO Species on a Pt/Al₂O₃ Catalyst Using in Situ Infrared Spectroscopy under Adsorption Equilibrium. *Journal of Catalysis* **2000**, 196, (1), 115-125.
29. Bourane, A.; Dulaurent, O.; Bianchi, D., Comparison of the Coverage of the Linear CO Species on Pt/Al₂O₃ Measured under Adsorption Equilibrium Conditions by Using FTIR and Mass Spectroscopy. *Journal of Catalysis* **2000**, 195, (2), 406-411.
30. Bourane, A.; Dulaurent, O.; Chandes, K.; Bianchi, D., Heats of adsorption of the linear CO species on a Pt/Al₂O₃ catalyst using FTIR spectroscopy. Comparison between TPD and adsorption equilibrium procedures. *Applied Catalysis, A: General* **2001**, 214, (2), 193-202.
31. Sokolova, N. A.; Barkova, A. P.; Furman, D. B.; Borovkov, V. Y.; Kazansky, V. B., IR-spectroscopic study of the state of Cu and Pt in copper-platinum-alumina catalysts for paraffin dehydrogenation subjected to different reductive and oxidative treatments. *Kinetics and Catalysis (Translation of Kinetika i Kataliz)* **1995**, 36, (3), 434-40.
32. Lambert, S.; Ferauche, F.; Brasseur, A.; Pirard, J.-P.; Heinrichs, B., Pd-Ag/SiO₂ and Pd-Cu/SiO₂ cogelled xerogel catalysts for selective hydrodechlorination of 1,2-dichloroethane into ethylene. *Catalysis Today* **2005**, 100, (3-4), 283.
33. Toolenaar, F. J. C. M.; Stoop, F.; Ponec, V., On electronic and geometric effects of alloying. An infrared spectroscopic investigation of the adsorption of carbon monoxide on platinum-copper alloys. *J. Catal.* **1983**, 82, (1), 1-12.
34. Stoop, F.; Toolenaar, J. C. M.; Ponec, V., Geometric and ligand effects in the IR spectra of carbon monoxide adsorbed on a platinum-copper alloy. *Journal of the Chemical Society, Chemical Communications* **1981**, (20), 1024-5.
35. Toolenaar, F. J. C. M.; Reinalda, D.; Ponec, V., Adsorption of carbon monoxide on platinum-copper alloys. On the possible role of atomic and collective properties of metals in chemisorption: observations by infrared spectroscopy. *Journal of Catalysis* **1980**, 64, (1), 110-15.

36. Chandler, B. D.; Pignolet, L. H., DRIFTS studies of carbon monoxide coverage on highly dispersed bimetallic Pt-Cu and Pt-Au catalysts. *Catalysis Today* **2001**, 65, (1), 39-50.
37. Dandekar, A.; Vannice, M. A., Determination of the dispersion and surface oxidation states of supported Cu catalysts. *Journal of Catalysis* **1998**, 178, (2), 621-639.
38. Hadjiivanov, K. I.; Kantcheva, M. M.; Klissurski, D. G., IR study of CO adsorption on Cu-ZSM-5 and CuO/SiO₂ catalysts: σ and π components of the Cu+-CO bond. *Journal of the Chemical Society, Faraday Transactions* **1996**, 92, (22), 4595-4600.
39. Dulaurent, O.; Courtois, X.; Perrichon, V.; Bianchi, D., Heats of Adsorption of CO on a Cu/Al₂O₃ Catalyst Using FTIR Spectroscopy at High Temperatures and under Adsorption Equilibrium Conditions. *Journal of Physical Chemistry B* **2000**, 104, (25), 6001-6011.
40. Rodriguez, J. A.; Kuhn, M., Electronic and Chemical Properties of Ag/Pt(111) and Cu/Pt(111) Surfaces: Importance of Changes in the d Electron Populations. *Journal of Physical Chemistry* **1994**, 98, (44), 11251-5.
41. Santra, A. K.; Rao, C. N. R., Interaction of Carbon Monoxide with Bimetallic Overlayers. *Journal of Physical Chemistry* **1994**, 98, (23), 5962-5.
42. Hadjiivanov, K.; Venkov, T.; Knozinger, H., FTIR spectroscopic study of CO adsorption on Cu/SiO₂: formation of new types of copper carbonyls. *Catalysis Letters* **2001**, 75, (1-2), 55-59.
43. Maeland, A. J.; Gibb, T. R. P., Jr., X-ray diffraction observations of the Pd-H₂ system through the critical region. *Journal of Physical Chemistry* **1961**, 65, 1270-2.
44. Lyakishev, N. P., *Diagrams of State of Bimetallic Systems (in Russian)*. Mashinostroenie: Moscow, 1997; Vol. 2.
45. Tyson, W. R.; Miller, W. A., Surface free energies of solid metals: estimation from liquid surface tension measurements. *Surface Science* **1977**, 62, (1), 267-76.
46. Van Langeveld, A. D.; Ponec, V., The surface composition of platinum-copper alloys; experimental observations and theory of surface segregation. *Applications of Surface Science (1977-1985)* **1983**, 16, (3-4), 405-23.
47. Van Langeveld, A. D.; Ponec, V., Surface segregation in platinum-copper alloys. *Surface Science* **1983**, 126, (1-3), 702-7.
48. Lide, D. R., *CRC Handbook of Chemistry and Physics, 83rd Edition*. 2002; p 2664 pp.
49. Nikol'skii, B. P.; Editors; et al., *Spravochnik Khimika, Tom 2: Osnovnye Svoistva Neorganicheskikh i Organicheskikh Soedinenii (Handbook for Chemists, Vol. 2: Fundamental Properties of Inorganic and Organic Compounds)*. 2nd ed. 1965; p 1168 pp.

50. Norton, P. R.; Davies, J. A.; Jackman, T. E., Absolute coverage and isosteric heat of adsorption of deuterium on platinum(111) studied by nuclear microanalysis. *Surface Science* **1982**, 121, (1), 103-10.
51. Spiewak, B. E.; Dumesic, J. A., Microcalorimetric measurements of differential heats of adsorption on reactive catalyst surfaces. *Thermochimica Acta* **1997**, 290, (1), 43-53.
52. Passos, F. B.; Schmal, M.; Vannice, M. A., Effect of In and Sn on the adsorption behavior and hydrogenolysis activity of Pt/Al₂O₃ catalysts. *Journal of Catalysis* **1996**, 160, (1), 106-117.
53. Liao, T. H.; Sun, Q., Chemisorption of hydrogen on stepped surfaces of Ni and Cu. *Physica Status Solidi B: Basic Research* **1997**, 200, (2), 491-498.
54. Wilmer, H.; Genger, T.; Hinrichsen, O., The interaction of hydrogen with alumina-supported copper catalysts: a temperature-programmed adsorption/temperature-programmed desorption/isotopic exchange reaction study. *Journal of Catalysis* **2003**, 215, (2), 188-198.
55. Rodriguez, J.; Truong, C.; Goodman, D., Infrared Vibrational Studies of CO Adsorption on Cu/Pt(111) and CuPt(111) Surfaces. *Journal of Chemical Physics* **1992**, 96, (10), 7814-7825.
56. de Menorval, L.-C.; Chaqroune, A.; Coq, B.; Figuerast, F., Characterization of mono- and bi-metallic platinum catalysts using CO FTIR spectroscopy. Size effects and topological segregation. *Journal of the Chemical Society, Faraday Transactions* **1997**, 93, (20), 3715-3720.
57. Luebke, D. R.; Vadlamannati, L. S.; Kovalchuk, V. I.; d'Itri, J. L., Hydrodechlorination of 1,2-dichloroethane catalyzed by Pt-Cu/C: effect of catalyst pretreatment. *Applied Catalysis, B: Environmental* **2002**, 35, (3), 211-217.
58. de Jong, A. M. Surface Spectroscopy of Model Catalysts. Schuit Institute of Catalysis, Technical University of Eindhoven, Eindhoven, 1994.
59. Gunter, P. L. J.; Niemantsverdriet, J. W.; Ribeiro, F. H.; Somorjai, G. A., Surface science approach to modeling supported catalysts. *Catalysis Reviews - Science and Engineering* **1997**, 39, (1 & 2), 77-168.
60. van Hardeveld, R. M.; Gunter, P. L. J.; van Ijzendoorn, L. J.; Wieldraaijer, W.; Kuipers, E. W.; Niemantsverdriet, J. W., Deposition of inorganic salts from solution on flat substrates by spin-coating: theory, quantification and application to model catalysts. *Applied Surface Science* **1995**, 84, (4), 339-46.
61. Larrieu, G.; Dubois, E.; Wallart, X.; Baie, X.; Katcki, J., Formation of platinum-based silicide contacts: kinetics, stoichiometry, and current drive capabilities. *Journal of Applied Physics* **2003**, 94, (12), 7801-7810.

62. Lamber, R.; Jaeger, N. I., On the reaction of platinum with silica substrates: observation of the platinum silicide (Pt₃Si) phase with copper-gold (Cu₃Au) superstructure. *Journal of Applied Physics* **1991**, 70, (1), 457-61.
63. Wang, W.; Tian, X.; Chen, K.; Cao, G., Synthesis and characterization of Pt-Cu bimetallic alloy nanoparticles by reverse micelles method. *Colloids and Surfaces, A: Physicochemical and Engineering Aspects* **2006**, 273, (1-3), 35-42.
64. Banholzer, W. F.; Burrell, M. C., XPS, Auger study of copper silicide (Cu₃Si) and its reaction with oxygen. *Surface Science* **1986**, 176, (1-2), 125-33.
65. Shin, D.-W.; Wang, S. X.; Marshall, A. F.; Kimura, W.; Dong, C.; Augustsson, A.; Guo, J., Growth and characterization of copper nanoclusters embedded in SiC matrix. *Thin Solid Films* **2004**, 473, (2), 267-271.
66. Schneider, U.; Castro, G. R.; Wandelt, K., Adsorption on ordered copper-platinum (Cu₃Pt)(111): site selectivity. *Surface Science* **1993**, 287-288, (Pt. A), 146-50.
67. Cho, E. J.; Oh, S. J., Unoccupied states and the charge transfer in Cu-Pt alloys studied by bremsstrahlung isochromat spectroscopy and x-ray photoelectron spectroscopy. *Journal of the Korean Physical Society* **1997**, 31, (2), 323-328.
68. Nahm, T.-U.; Kim, J.-Y.; Oh, S. J.; Chung, S. M.; Park, J. H.; Allen, J. W.; Jeong, K.; Kim, S., Photoemission study of electronic structures of disordered Ni-Pt and Cu-Pt alloys. *Physical Review B: Condensed Matter* **1996**, 54, (11), 7807-7815.
69. Van den Oetelaar, L. C. A.; Partridge, A.; Toussaint, S. L. G.; Flipse, C. F. J.; Brongersma, H. H., A Surface Science Study of Model Catalysts. 2. Metal-Support Interactions in Cu/SiO₂ Model Catalysts. *Journal of Physical Chemistry B* **1998**, 102, (47), 9541-9549.
70. Cheng, C. C.; Lucas, S. R.; Gutleben, H.; Choyke, W. J.; Yates, J. T., Atomic Hydrogen-Driven Halogen Extraction From Si(100) - Eley-Rideal Surface Kinetics. *Journal Of The American Chemical Society* **1992**, 114, (4), 1249-1252.
71. He, Z. H.; Yang, X.; Zhou, X. J.; Leung, K. T., Room-temperature chemisorption of chloroethylenes on Si(111)7 x 7: formation of surface vinyl, vinylidene and their chlorinated derivatives. *Surface Science* **2003**, 547, (1-2), L840-L846.
72. Hippe, C.; Lamber, R.; SchulzEkloff, G.; Schubert, U., Influence of the strong metal-support interaction on the CO chemisorption at a Pt/SiO₂ catalyst. *Catalysis Letters* **1997**, 43, (3-4), 195-199.
73. Heinrichs, B.; Schoebrechts, J.-P.; Pirard, J.-P., Palladium-Silver Sol-Gel Catalysts for Selective Hydrodechlorination of 1,2-Dichloroethane into Ethylene. *Journal of Catalysis* **2001**, 200, (2), 309-320.

74. Kvon, R. I.; Koscheev, S. V.; Boronin, A. I., XPS study of carbon species at the surface of platinum single crystal planes. *Journal Of Molecular Catalysis A-Chemical* **2000**, 158, (1), 297-300.
75. Kvon, R. I.; Ivanov, E. A.; Boronin, A. I., Carbon states and kinetics of carbon deposition from ethylene at Pt(110) surface. *Reaction Kinetics And Catalysis Letters* **1998**, 65, (2), 381-388.
76. Kvon, R. I.; Boronin, A. I., High-temperature carbon states at Pt(1 1 0) surface and their reactivity towards H-2 and O-2. *Catalysis Today* **1998**, 42, (3), 353-355.
77. Kvon, R. I.; Ivanov, E. A.; Ochshepkov, D. Y.; Boronin, A. I., Kinetics of carbon deposition from ethylene on Pt(110) surface. *Reaction Kinetics And Catalysis Letters* **1997**, 62, (2), 299-304.
78. Kvon, R. I.; Boronin, A. I.; Shaikhutdinov, S. K.; Buyanov, R. A., XPS and STM study of carbon deposits at the surface of platinum (110). *Applied Surface Science* **1997**, 120, (3-4), 239-242.
79. Shaikhutdinov, S. K.; Boronin, A. I.; Kvon, R. I., Carbon on the Pt(110) surface: A scanning tunneling microscopy study. *Surface Science* **1997**, 382, (1-3), 187-192.
80. Kesmodel, L. L.; Dubois, L. H.; Somorjai, G. A., Dynamical LEED study of acetylene and ethylene chemisorption on platinum(111): evidence for the ethylidyne group. *Chemical Physics Letters* **1978**, 56, (2), 267-71.
81. Yagasaki, E.; Backman, A. L.; Masel, R. I., The adsorption and decomposition of ethylene on platinum(210), (1 * 1)platinum(110), and (2 * 1)platinum(110). *Journal of Vacuum Science & Technology, A: Vacuum, Surfaces, and Films* **1990**, 8, (3, Pt. 2), 2610-5.
82. Linke, R.; Schneider, U.; Busse, H.; Becker, C.; Schroeder, U.; Castro, G. R.; Wandelt, K., Interaction of hydrogen with Cu₃Pt(111): dissociation via isolated platinum atoms. *Surface Science* **1994**, 307-309, (1-3), 407-11.